The role of Stp1, a secreted effector, in the biotrophic interaction of *Ustilago maydis* and its host plant maize

Dissertation

zur
Erlangung des Doktorgrades
der Naturwissenschaften
(Dr. rer. nat.)

Dem Fachbereich Biologie
der Philipps-Universität Marburg
vorgelegt von

Liang Liang
aus Hebei/P. R. China

Marburg/Lahn, 2012

Die Untersuchungen zur vorliegenden Arbeit wurden von Anfang January 2009 bis June 2012 unter der Betreuung von Frau Prof. Dr. Regine Kahmann in Marburg am Max-Planck-Institut für terrestrische Mikrobiologie in der Abteilung Organismische Interaktionen durchgeführt.

Vom Fachbereich Biologie
der Philipps-Universität Marburg als Dissertation
angenommen am: 28.12.2012

Erstgutachter: Frau Prof. Dr. Regine Kahmann
Zweitgutachter: Herr Prof. Dr. Michael Bölker

Tag der mündlichen Prüfung: 08.02.2013

Declaration

I hereby declare that the dissertation entitled "**The role of Stp1, a secreted effector, in the biotrophic interaction of *Ustilago maydis* and its host plant maize**" submitted to the Department of Biology, Philipps-Universität Marburg, is the original and independent work carried out by me under the guidance of the PhD committee, and the dissertation is not formed previously on the basis of any award of Degree, Diploma or other similar titles.

Marburg, Oct 2012

Liang Liang

Contents

Abbreviations

Δ	Deletion
A	Adenine
aa	amino acid
AD	activiation domain
Ade	L-Adenine hemi-sulfate salt
Amp	Ampicillin
BD	DNA binding domain
CBX	Carboxin
cDNA	complementary DNA
CP	cysteine protease
C-terminal	Carboxyl-terminal
C-terminus	Carboxyl-terminus
CV	colume volume
DAPI	4',6-diamidino-2-phenylindole
dH2O	distilled water
DMSO	Dimethyl sulphoxide
dpi	days post infection
EDTA	Ethylene Diamine Tetraacetic Acid
ETI	effector-triggered immunity
GO	gene ontology
GST	glutatione S-transferase
h	hour
HA	Hemagglutinin
His	Histidine/L-Histidine HCl monohydrate
hpi	hours post infection
HR	hypersensitive response
IP	Immuno-precipitation
IPTG	isopropyl β-D-1-thiogalactopyranoside
Kan	Kanamycin
kDa	kilodalton
LC-MS	Liquid chromatography mass spectrometry
Leu	L-Leucine
M	Molar
mA	milliampere
min	Minute
ml	milliliter
mM	Millimolar
NB	nucleotide binding
NLS	nuclear localization signal
N-terminal	amino-terminal
N-terminus	amino-terminus
OD600	Optical density at 600 nm
P/MAMPs	Pathogen/microbe associated molecular patterns
PEG	Polyethylene glycol
PI	Propidium Iodide
PPRs	pattern recognition receptors
PTI	PAMP-triggered immunity
Rif	Rifampicin
rpm	revolutions per minute
RT-PCR	Real time PCR or reverse transcription PCR
S	second
SDS-PAGE	Sodium dodecyl sulfate polyacrylamide gel electrophoresis
Sip	Stp1 interacting protein
stp1	stop after penetration
Try	L-Tryptophan
V	Voltage
w/v	weight/volume
WGA	wheat germ agglutinin
Y2H	yeast two-hybrid
µl	microliter

Summary

Secreted effectors play crucial roles during the establishment of the biotrophic interaction between *Ustilago maydis* and maize. In a previous study (Schipper, 2009) it had been demonstrated that a deletion of the *stp1* effector gene resulted in a complete loss of virulence symptoms in maize infection and that such mutants elicited a hypersensitive response. This distinguishes *stp1* from most other secreted effectors that are either dispensable for pathogenicity or have only a minor effect on virulence. This study focuses on the functional analysis of Stp1.

A mutational analysis showed that the conserved N- and C-terminal domains of Stp1 can be separately expressed but are both required for Stp1 protein function. The long central variable domain was demonstrated to be dispensable yet may promote fungal growth in vascular bundles. *stp1* homologs from closely related smut fungi of *U. maydis* could replace *stp1* in *U. maydis*, indicating a conserved function. $Stp1_{\Delta 136\text{-}432}$ lacking the central domain could be purified to homogeneity and was stable, while the isolated C-terminal domain, $Stp1_{433\text{-}515,}$ was unstable after purification. This could suggest that N- and C-terminal domains of Stp1 stabilize each other. Stp1-HA expressed by *U. maydis* was detected in the nucleus of plant cells by immunolocalization suggesting that Stp1 may suppress plant defense responses by affecting the transcription of respective genes.

Both cytoplasmic and apoplastic maize proteins were identified as interaction partners of Stp1 by yeast two-hybrid assays using $Stp1_{\Delta 136\text{-}432}$ as bait, suggesting that Stp1 may be an effector with both apoplastic and cytoplasmic functions The C-terminus of Stp1 as well as $Stp1_{\Delta 136\text{-}432}$ could inhibit the activity of a maize extracellular cysteine protease, Sip3, which was identified as one of the apoplastic interaction partners. The interactions between Stp1 and the cytoplasmic interactors Sip9, a cell number regulator 8, Sip16, a CCR4-NOT transcription complex subunit, Sip19, a serine/threonine-protein kinase and Sip21, a VIP2 protein were verified with full-length cDNA but await to be confirmed by other techniques. RNA-Seq analysis demonstrated that several early defense response genes are not induced by *stp1* mutants expressing the N-terminus of Stp1 while *stp1* mutants expressing the C-terminus of Stp1 triggered even stronger plant defense responses than *stp1* mutants during colonization. This suggests that N- and C-terminal domains of Stp1 have distinct functions.

Zusammenfassung

Bei der Etablierung der biotrophen Interaktion zwischen *Ustilago maydis* und Mais spielen sekretierte Effektoren eine entscheidende Rolle. In einer vorausgegangenen Studie (Schipper, 2009) konnte gezeigt werden, dass die Deletion des *stp1* Effektor-Gens zu einem vollständigen Verlust der Virulenz führt und dass entsprechende Mutanten eine hypersensitive Reaktion auslösen. Diesbezüglich unterscheidet sich *stp1* von den meisten anderen untersuchten Effektoren, die entweder keinen oder nur einen geringen Beitrag zur Virulenz des Pilzes leisten. Diese vorliegende Arbeit befasst sich mit der funktionellen Analyse von Stp1.

Mutationsanalysen zeigten, dass die konservierten N- und C-terminalen Domänen von Stp1 zwar als separate Polypeptide exprimiert werden können, aber die Gegenwart beider Domänen nötig ist, um die Stp1 Funktion zu komplementieren. Es wurde nachgewiesen, dass die zentrale variable Domäne von Stp1 keine essentielle Funktion übernimmt, allerdings könnte diese Domäne für die Proliferation des Pilzes entlang der Leitbündel eine Rolle spielen. *stp1* Homologe aus mit *U. maydis* nahe verwandten Brandpilzen waren in der Lage, die Funktion von *stp1* in *U. maydis* zu komplementieren, was für eine konservierte Funktion spricht. Eine Stp1 Version, bei der die zentrale Domäne deletiert wurde ($Stp1_{\Delta 136-432}$), konnte bis zur Homogenität aufgereinigt werden und erwiess sich als stabil, während die isolierte C-terminale Domäne, $Stp1_{433-515,}$ nach der Aufreinigung instabil war. Diese Beobachtung könnte darauf hinweisen, dass sich die N- und C-terminalen Domänen von Stp1 gegenseitig stabilisieren. Durch Immunlokalisierung konnte ein Stp1-HA Fusionsprotein im Zellkern von Pflanzenzellen detektiert werden, die mit dem Stamm SG200stp1-HA infiziert waren. Demzufolge könnte Stp1 auf die Transkription von Genen Einfluss nehmen und dadurch die pflanzliche Abwehrreaktion unterdrücken.

In einem Hefe-zwei-Hybrid-System, bei dem Stp1 als Köder benutzt wurde, konnten sowohl apoplastische als auch cytoplasmatische Mais Proteine als Stp1-Interaktoren identifiziert werden. Dies könnte bedeuten, dass Stp1 ein Effektorprotein mit dualer Funktion zum einen im Apoplasten und zum anderen im pflanzlichen Zytoplasma ist. Sowohl die gereinigte C-terminale als auch die N-terminale Domäne von Stp1war in der Lage, die Aktivität der extrazellulären Mais Cystein-Protease Sip3 zu inhibieren, die zuvor

als ein apoplastischer Interaktionspartner von Stp1 identifiziert werden konnte. Die Interaktion zwischen Stp1 und den cytoplasmatischen Interaktoren Sip9 (cell number regulator 8), Sip16(CCR4-NOT Transkriptionskomplex Untereinheit), Sip19 (Serine/Threonin- Kinase) und demVIP2 Protein Sip21 konnten nach Expression der jeweiligen Gene in voller Länge verifiziert werden, müssen aber zukünftig noch durch weitere Methoden bestätigt werden. RNA-Seq Analysen des Transkriptoms infizierter Mais Blätter zeigten, dass einige der frühen pflanzlichen Abwehrgene, die nach Infektion mit einem *stp1*-Deletions Stamm induziert werden, Hingegen führte die Infektion mit einem *stp1*-Deletions Stamm komplementiert durch den Stp1 C-Terminus sogar zu einer stärkeren Abwehrreaktion als sie nach Infektion mit dem *stp1*- Deletionsstamm beobachtet wurde. Dies weist darauf hin, dass die N- und C-terminale Domänen von Stp1 unterschiedliche Funktionen erfüllen könnten.

1. Introduction

1.1 The *Ustilago maydis*/Zea mays pathosystem

The *Ustilago maydis*–maize pathosystem has emerged as the current model for plant pathogenic basidiomycetes and as one of the models for biotrophic interaction (Brefort *et al.*, 2009).

1.1.1 Maize, an economic important model organism for fundamental research

Maize (*Zea mays*), the domesticated variant of mesoamerican teosinte is subjected to cultivation and selection since 4,200 years B.C. (Benz, 2001). In 2010, 844 million tonnes of maize was produced worldwide, more than rice (672 million tonnes) and wheat (651 million tonnes) (Food and Agriculture Organization of the United Nations, 2010). Beyond its major agricultural and economic contributions, maize is an important model organism for fundamental research in the inheritance and functions of genes, the physical linkage of genes to chromosomes, the mechanistic relation between cytological crossovers and recombination, the origin of the nucleolus, the properties of telomeres, epigenetic silencing, imprinting, and transposition (Schnable *et al.*, 2009, Bennetzen, 2009). An improved draft nucleotide sequence of the 2.3 gigabase genome of maize is published in 2009 and ever since it is undergoing continuous update (Schnable et al., 2009). In the latest release, 39,656 genes (63,540 transcripts) in the filtered gene set are annotated (http://www.maizesequence.org) which will significantly promote fundamental research on maize and related grasses.

1.1.2 *Ustilago maydis* as a model organism

All aerial parts of maize can be infected by the facultatively biotrophic fungus, *Ustilago maydis*. The infection leads to disease symptoms like chlorosis, ligular swellings and tumors (Kamper et al., 2006). *U. maydis*, which is pathogenic only on corn and its close relative teosinte, belongs to the basidiomycetes, a group of fungi that includes the common mushroom and many plant pathogens such as the smuts and rusts (Banuett, 1992). Several features make this microorganism a model for a number of important cellular processes such as signalling, dimorphism, DNA recombination and repair, plant microbe interactions etc (Bolker, 2001, Kamper et al., 2006, Holliday, 2004). *U. maydis* can be grown in defined media. The fungus is haploid, grows by budding and forms compact colonies on plates that

can be replica plated (Dean *et al.*, 2012). *U. maydis* can induce prominent disease symptoms (tumors) on all aerial parts of maize within less than a week (Brefort et al., 2009). In addition, solopathogenic, haploid strains are instrumental for the study of pathogenesis (Bölker, 1995). A number of molecular tools are available such as a PCR based gene replacement strategy, inducible promoter systems and fluorescent protein based localization techniques (Kamper, 2004, Basse & Steinberg, 2004, Doehlemann *et al.*, 2009). One of the major breakthroughs for the *U. maydis* research community was the public release of the genome sequence combined with a solid manual annotation that resulted in high-quality data currently curated in the database MUMDB at MIPS (Vollmeister *et al.*, 2012, Kamper et al., 2006).

1.1.3 Life cycle of *U. maydis*

The dimorphic fungus, *U. maydis*, exhibits three distinct morphological forms in its life cycle. Haploid cells, which are nonpathogenic, are saprophytic and grow in a yeast-like unicellular form (sporidium) that divides by budding (Fig. 1A) (Perez-Martin *et al.*, 2006). Fusion of two compatible haploid cells, which harbor different alleles of *a* and *b* mating types loci, is required to generate the filamentous dikaryon which is strictly dependent on the host plant for sustained growth (Fig. 1B) (Bolker, 2001, Kahmann, 2000). The dikaryotic hyphae show tip-directed growth and cytoplasm accumulates in the tip cell compartment, whereas, older parts of the hyphae become vacuolated and are sealed off by regularly spaced septa (Brefort et al., 2009). The pathogenic dikaryotic differentiating appresoria are able to penetrate plant cells (Fig. 1C). During penetration, the host plasma membrane invaginates and tightly surrounds the intracellular hyphae (Brefort et al., 2009). An interaction zone develops between plant and fungal membranes that is characterized by fungal deposits produced by exocytosis (Kamper et al., 2006). After penetration, the hyphae first proliferate intracellularly (Fig. 1D) and then at later stages accumulate in mesophyll tissue and are found mostly in apoplastic cavities that arise in the developing tumors (Doehlemann et al., 2009). Massive proliferation is followed by nuclear fusion and fragmentation of the hyphae, a process that releases individual cells that will produce the diploid spore (teliospore, Fig. 1 E and F) (Perez-Martin et al., 2006). Fungal proliferation is associated with development of the prominent disease symptoms of *U. maydis*, tumors (Fig. 1 G).

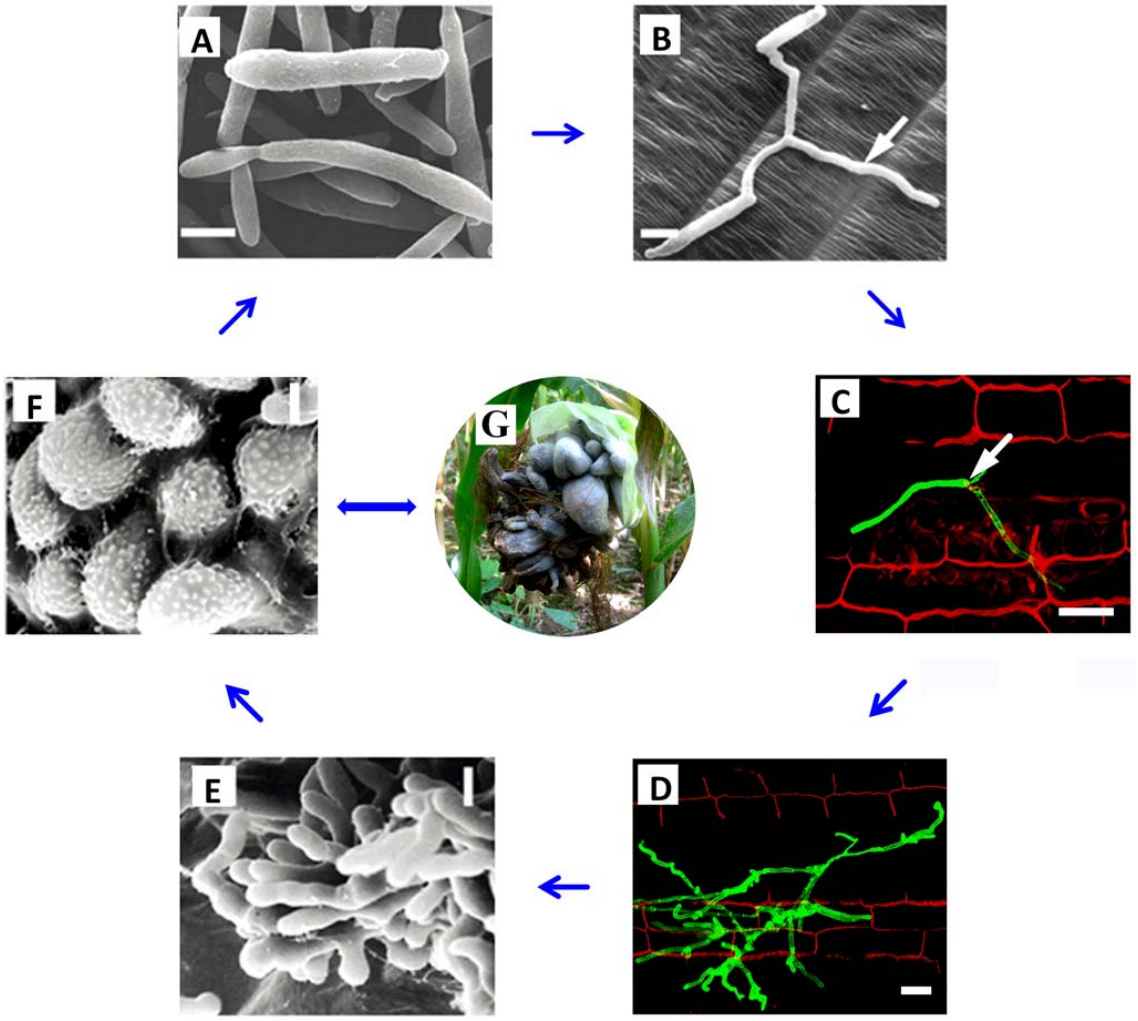

Fig.1. Life cycle of *U. maydis*. A: Scanning electron microscopy (SEM) image of haploid sporidia. B: SEM image of mated sporidia on plant epidermis; arrow denotes dikaryotic filament. C: Confocal image of hyphae after penetration stained with WGA-AF488 and propidium iodide (WGA/PI), the arrow denotes appresorium. D: Confocal image of hyphae proliferating on planta stained with WGA/PI. E: SEM image of sporogenous hyphae and early stages of spore development. F: SEM image of ornamented teliospores. G, Tumors formed on the ear of maize. Scale bars in A, B E and F, 5 µm. Scale bars in C and D, 20 µM. Figure A, B E and F were modified from Kamper et al. (2006).

1.2 Plant defense response and R proteins

Although plants are under continuous attack by pathogens, most encounters result in plant resistance and disease being the exception (Takken & Joosten, 2000). Passive protection against pathogens that are not specialized to attack is provided by cell walls, wax layers and preformed chemical barriers (Jones & Dangl, 2006). In case a pathogen overcomes these obstacles, plants have evolved three different strategies of defense namely, PAMP-triggered immunity, effector-triggered immunity and systematic acquired resistance.

1.2.1 PAMP-triggered immunity

Pathogen/microbe associated molecular patterns (PAMPs, also called MAMPs) are recognized by receptor-like proteins or kinases (RLP/Ks) termed pattern recognition receptors (PRRs) (Dodds & Rathjen, 2010). PAMPs are typically essential components of whole classes of pathogens, such as bacterial flagellin or fungal chitin. Plants also respond to endogenous molecules released by pathogen invasion, such as cell wall or cuticular fragments called danger-associated molecular patterns (DAMPs). Stimulation of PRRs leads to PAMP-triggered immunity (PTI) including rapid ion fluxes across the plasma membrane, MAP kinase activation, production of reactive-oxygen species, rapid changes in gene expression and cell wall reinforcement (Zipfel, 2008). Successful pathogens have evolved strategies to infect host plants, either by evading recognition or by suppressing the subsequent signalling steps. In many cases, suppression of PTI involves secretion of virulence molecules by the pathogens called effectors (Jones & Dangl, 2006).

1.2.2 Effector-triggered immunity

The second strategy of the perception of a pathogen is based on resistance (R) genes in plants whose products confer recognition of cognate secreted virulence determinants from the pathogen referred to as ‘effectors’ (Avr proteins). This recognition induces effector-triggered immunity (ETI) which often culminates in a hypersensitive response (HR). This gene-for-gene hypothesis was introduced by Flor in the 1940s, and dozens of R-Avr gene combinations have since been characterized (Jones & Dangl, 2006, van der Hoorn & Kamoun, 2008). Recognition events during ETI are mostly mediated by a class of receptor proteins that contain nucleotide binding (NB) domains and leucine-rich repeat (LRR). NB-LRR proteins can recognize pathogen effectors either directly by physical association or indirectly through and accessory protein that is a pathogen virulence target or a structure mimic of one (Dodds & Rathjen, 2010). Three conceptual models have been proposed to describe the mechanism of indirect recognition. The ‘guard’ model postulates that NB-LRR proteins guard an accessory protein (or guardee) that is targeted and modified by pathogen effectors (Jones & Dangl, 2006). The ‘decoy’ model proposes that duplication of the effector target gene or independent evolution of a target mimic could relax evolutionary constraints and allow the accessory protein to participate solely in effector perception (van der Hoorn & Kamoun, 2008). The ‘bait-and-switch’ model envisages a two-step

recognition event. First, an effector interacts with the accessory 'bait' protein associated with an NB-LRR, and then a subsequent recognition event occurs between the effector and NB-LRR protein to trigger signalling (Collier & Moffett, 2009).

1.2.3 Systemic acquired resistance

Plants are also protected by a mechanism called systemic acquired resistance (SAR), which occurs at sites distant from primary and secondary immune responses and protects plants from subsequent pathogen attacks (de Wit, 2007). SAR is effective against a broad range of pathogens and is dependent on different plant hormones including salicylic acid (SA), jasmonic acid (JA), ethylene (ET), abscisic acid (ABA) or combinations thereof. SA and SA derivatives are important for resistance to biotrophic pathogens that require living plant cells for reproduction, while JA and JA conjugates cooperate with ET to regulate resistance to necrotrophic pathogens that kill plant cells as they reproduce (Panstruga *et al.*, 2009). The SA and JA defense pathways are mutually antagonistic, and bacterial pathogens have evolved to exploit this fact to overcome SA-mediated defense responses (Kunkel & Brooks, 2002).

1.3 Secreted effectors in host-pathogen interactions

The deployment of secreted effectors is postulated to be the key to host infection (Rafiqi *et al.*, 2012). Research on effectors secreted by pathogens including bacteria, oomycetes and fungi during host invision has dominated the field of molecular plant–microbe interactions over recent years (de Jonge *et al.*, 2011). In a successful infection, pathogen effectors facilitate suppression of the plant immune system and orchestrate the reprogramming of the infected tissue so that it becomes a source of nutrients that are required by the pathogen to support its growth and development (Koeck *et al.*, 2011). Identification of bacterial effector proteins has provided unparalleled insights into the evolution of bacterial pathogenesis and host mimicry employed by bacterial proteins to interfere with host signaling and signal transduction processes (Whisson *et al.*, 2007). Important progress in the study of oomycete effectors has been made leading to the identification of large repertoires of effectors with characteristic RXLR and other motifs required for host cell uptake, elucidation of the 3D structures of RXLR effectors, novel insights into how

cytoplasmic effectors subvert host cells etc. (Bozkurt *et al.*, 2012). However, the functions of fungal effector proteins are only beginning to be revealed.

1.3.1 Translocation and function of bacteria effectors

Plant pathogenic bacteria require a type III secretion system (TTSS) to translocate effector proteins into host cells to promote disease by altering the normal physiology of the plant in favour of the pathogen (Abramovitch & Martin, 2005). The type III secretion system in pathogenic bacteria consisits of 15–20 Hrp (hypersensitive response and pathogenicity) proteins building a secretion apparatus that is involved in the secretion and translocation of effector proteins to the plant cell (Cornelis & Van Gijsegem, 2000). The cloning of the first bacterial avirulence gene, avrA, from *Pseudomonas syringae* pv. glycinea marked the beginning of the molecular analysis of bacterial effectors and has paved the way for determining of the role of bacterial effectors in pathogen virulence and the triggering of plant innate immunity (Staskawicz, 2009).

Key modules of PAMP-triggered immunity signaling pathways are frequently targeted by type III effectors (Feng & Zhou, 2012). The kinase domain of FLS2, EFR, and CERK1 constitutively interacts with BIK1, constituting a preformed immune receptor complex. The perception of flg22 and elf18 by FLS2 and EFR recruits another receptor- like kinase called BAK1 to activate the immune receptor complexes, leading to the phosphorylation of BIK1 and activation of downstream signaling. AvrPto and AvrPtoB directly target Arabidopsis and tomato PAMP receptors FLS2, EFR, and CERK1 to block PTI. In addition, MAPK cascades are similarly targeted by multiple *P. syringae* effectors such as HopAI1 and HopF2 which inactivate MPKs and MKKs respectively. A significant portion of type III effectors act by eliminating their host target proteins (Feng & Zhou, 2012). For example, AvrPphB and AvrRpt2, the cysteine proteases, recognize and cleave BIK1 and RIN4 respectively. HopZ1 and HopM1 induce the degradation of their target proteins, GmHID1 and MIN7 which participates in vesicle formation that is associated with plant defense (Hann & Rathjen, 2010). Type III effectors can also physically impede the function of their target proteins (Feng & Zhou, 2012). For example, AvrPto and AvrPtoB interact with BAK1 and inhibit the kinase activity of their targets (Shan *et al.*, 2008). Post-translational modification of host proteins is another common strategy employed by type III effectors

(Feng & Zhou, 2012). For example, HopU1 ADP-ribosylates GRP7 on Arg47 and Arg49 to abolish its RNA-binding activity and PTI function in plants. AvrAC and HopAI1 inhibit the PTI signal transduction pathway by blocking phosphorylation of MPKs and BIK1. Furthermore, multiple effector proteins have been shown to manipulate the JA pathway in concert, such as AvrB, AvrRpt2, AvrPphB, HopPtoK, and AvrPphEpto (Chisholm *et al.*, 2006). Type III effectors can also target nucleic acids and regulate transcription of the host plant. For example, XopD represses the expression of several defense-related genes in tomato plants (Feng & Zhou, 2012) and AvrBs3 effector family of *X. campestris* alters plant nuclear gene transcription, likely as a mean to down-regulate host defense (Chisholm et al., 2006, Bonas & Van den Ackervaken, 1997).

The function of effectors is redundant and interchangeable. The redundancy of effectors is illustrated by the combinatorial deletion of the 28 effectors of *P. syringae* pv. tomato DC3000 which are collectively essential but individually dispensable for the ability of the bacteria to defeat defenses, grow, and produce symptoms in plants (Kvitko *et al.*, 2009). Functional redundancy of effectors is achieved by targeting common host components through different molecular strategies (Hann *et al.*, 2010). Two effectors that illustrate effector redundancy and interchangeability are the unrelated AvrPto and AvrPtoB proteins of *P. syringae* pv tomato DC3000 (Pto DC3000) which both target the flagellin receptor complex (Hann et al., 2010).

1.3.2 Translocation and function of oomycetes effectors

Oomycetes, are filamentous eukaryotes that are more closely related to brown algae than fungi, cause some of the most devastating plant diseases such as late blight of potato and sudden oak death. The identification of a common motif, RXLR, in oomycete AVR proteins sparked excitement and speculation regarding translocation of effectors from these fungus-like pathogens (Rehmany *et al.*, 2005, Whisson et al., 2007). In plants, effectors can be translocated into the host cell (cytoplasmic effectors) or targeted to the apoplast (apoplastic effectors) (Bozkurt et al., 2012). Two large classes of cytoplasmic effectors, RXLR and crinkler (CRN) proteins could be reliably predicted by the occurrence of the conserved motifs in an N-terminal region that follows the signal peptide (Bozkurt et al., 2012). In a noted yet controversial paper, Kale *et al*. proposed that binding of oomycete and

fungal pathogen effectors to PI3P via the RXLR domain is required for host cell entry via lipid raft-mediated endocytosis (Kale *et al.*, 2010). However, this model has not been universally accepted due to lack of reproducibility of the PI3P binding experiments and the discovery that a conserved C-terminal domain, rather than the RXLR domain, of AVR3a is required for binding to phosphatidylinositol monophosphates (PIPs) in vitro. Additionally, recognition of PI3P in endoplasmic reticulum by the host-targeting signal of secreted effectors of *Plasmodium falciparum* can facilitate export of the effector proteins from the intracellular pathogen into the surrounding erythrocyte (Bhattacharjee *et al.*, 2012). Therefore, the mechanisms of RXLR effectors entry into plant cells remain unclear and under debate (Bozkurt et al., 2012).

Many apoplastic effectors act as enzyme inhibitors, e.g. chitinases, glucanases and proteases. For example, glucanase inhibitor proteins (GIPs) which are secreted by *Phytophthora sojae*, specifically inhibit the endoglucanase activity of their plant host (Rose *et al.*, 2002). *P. infestans* deploys Kazal-like and cystatin protease inhibitors to target secreted host serine and cysteine proteases, respectively (Tian *et al.*, 2007, Tian *et al.*, 2004, Bozkurt et al., 2012). Recently, the *P. infestans* RXLR effector AVRblb2 has been shown to localize to plasma membrane and prevent secretion of a plant immune protease at the haustorial interface (Bozkurt *et al.*, 2011). A second type of apoplastic effectors interferes with adhesion, and possibly signalling, between host cell wall and plasma membrane. For example, IPI-O of *P. infestans* can mediate disruption of plasma membrane-cell wall contacts and interfere with cell-wall-associated defences (Stassen & Van den Ackerveken, 2011). A third type of apoplastic effectors are toxins that are produced by most necrotrophic or hemibiotrophic oomycetes. These include two families of toxic proteins, PcF/SCR proteins and NEP1 like proteins (NLPs) (Stassen & Van den Ackerveken, 2011).

1.3.3 Identification and function of fungal effectors

Most fungal avirulence genes encode virulence factors that are small secreted cysteine-rich proteins with no homology to known proteins in the databases (Stergiopoulos & de Wit, 2009, Chisholm et al., 2006). Fungal effectors are also grouped into extracellular effectors that are secreted into the apoplast or xylem of their host plants and cytoplasmic effectors

that are translocated into host cells (Stergiopoulos & de Wit, 2009). Two rust cytoplasmic effectors, RTP1 of *Uromyces fabae* and AvrP123 of *M. lini*, accumulate in the host nucleus and may have a role in manipulating host gene expression during infection (Kemen *et al.*, 2005, Rafiqi et al., 2012). Two apoplastic effector proteins, Avr2 and Avr4, have been characterized from the leaf-mold fungus *Cladosporium fulvum* (Chisholm et al., 2006). Avr2 inhibits tomato Rcr3 cysteine protease required for Cf-2-dependent disease resistance (Rooney *et al.*, 2005). Avr4 contains a chitin binding domain that binds chitin and is thought to shield the fungal cell wall from plant chitinases (van den Burg *et al.*, 2003).

The sequencing of *U. maydis* genome identified 554 secreted proteins, among these 386 could not be ascribed a function including 272 that are either specific to *U. maydis* or contain no recognisable domains (Kamper et al., 2006, Ellis *et al.*, 2009). Of all the genes encoding secreted proteins, 12 clusters of genes were found, which comprise 3-26 genes and are scattered all over the genome. Deletion of individual clusters resulted in phenotypes ranging from complete lack of symptoms to hypervirulence (Kamper et al., 2006). Recently, a secreted chorismate mutase of *U. maydis*-Cmu1 was shown to be taken up by plant cells and changes the metabolic status of host cells through metabolic priming (Djamei *et al.*, 2011). This is one of the few cases where effector function could be suggested by amino acid sequence features (Rafiqi et al., 2012). Two extracellular effectors of *U. maydis*, Pep1 and Pit2 are required for virulence of this fungus (Doehlemann *et al.*, 2011, Hemetsberger *et al.*, 2012). Pep1 is shown to inhibit the peroxidase driven oxidative burst and thereby suppress the early immune responses of maize. Although advances in effectors identification have been made, the functional characterization of huge numbers of novel effector proteins is significantly lags behind.

1.4 Co-evolution of plants and their microbial pathogens

Microbes have been interacting with plants for hundreds of millions of years. During co-evolution of plants and their microbial pathogens, the plant and microorganism have competing interests, which lead to an evolutionary ‘arms race’ in which the interaction constantly selects for genetic changes in both pathogen and plant populations (Takken & Rep, 2010). Genetic changes that enhance fitness, e.g. the ability to avoid host detection or regain pathogen recognition ability, will be maintained in the population. The quantitative

output of the plant immune system as well as the evolutionary relationship between PTI and ETI was illustrated as a four phased 'zigzag' model (Fig. 2) (Jones & Dangl, 2006, Dubery *et al.*, 2012). In Phase 1, P/MAMPs are recognized by PRRs, resulting in PTI that can stop further colonization. In Phase 2, successful pathogens deploy effectors that contribute to pathogen virulence. Effectors can interfere with PTI. This results in effector-triggered susceptibility (ETS). In phase 3, a given effector is 'specifically recognized by one of the NB-LRR proteins, resulting in effector-triggered immunity (ETI). In Phase 4, natural selection drives pathogens to avoid ETI by shedding or diversifying the recognized effector gene, or by acquiring effectors that suppress ETI. Thereafter, natural selection results in the evolution of new R specificities so that ETI can be triggered again. Like all models, the 'Zig-Zag' model could not explain every aspect of the host–pathogen molecular interactions. This model has its limitations and fails to incorporate aspects of damage-associated molecular patterns, necrotrophy and symbiosis, physical and temporal scales, order of events and quantitative aspects of defenses (Pritchard & Birch, 2011).

1.5 Stp1 plays crucial role in the establishment of biotrophic interaction between *U. maydis* and maize

Um02475 termed *stp1* (**st**op after **p**enetration **1**) is one of the genes encoding secreted effectors which is identified from the genomic sequencing and bioinformatic analysis of *U. maydis* (Kamper et al., 2006, Schipper, 2009). *stp1* is the rightmost gene in the three gene cluster 5B, the deletion of which results in a complete loss of virulence symptoms in maize infections (Kamper et al., 2006). Deletion analysis revealed that only *stp1* is responsible for the loss of virulence phenotype of a cluster 5B deletion mutant (Schipper, 2009). Homologs of *stp1* are found only in closely related smut fungi and bioinformatic analysis gave no hints to functional domains.

Fungal growth of *stp1* deletion mutant arrest directly after penetration of the first epidermal cell and tumors were never found. Diaminobenzidine staining of infected leaves revealed that H_2O_2 and phenolic compounds accumulate around penetration sites of *stp1* deletion mutants which indicated that a hypersensitive response was triggered. Microarray analysis also illustrated the difference between SG200 and SG200Δstp1 in plant responses at transcriptomic level. The strong plant defense response elicited by *stp1* deletion mutants

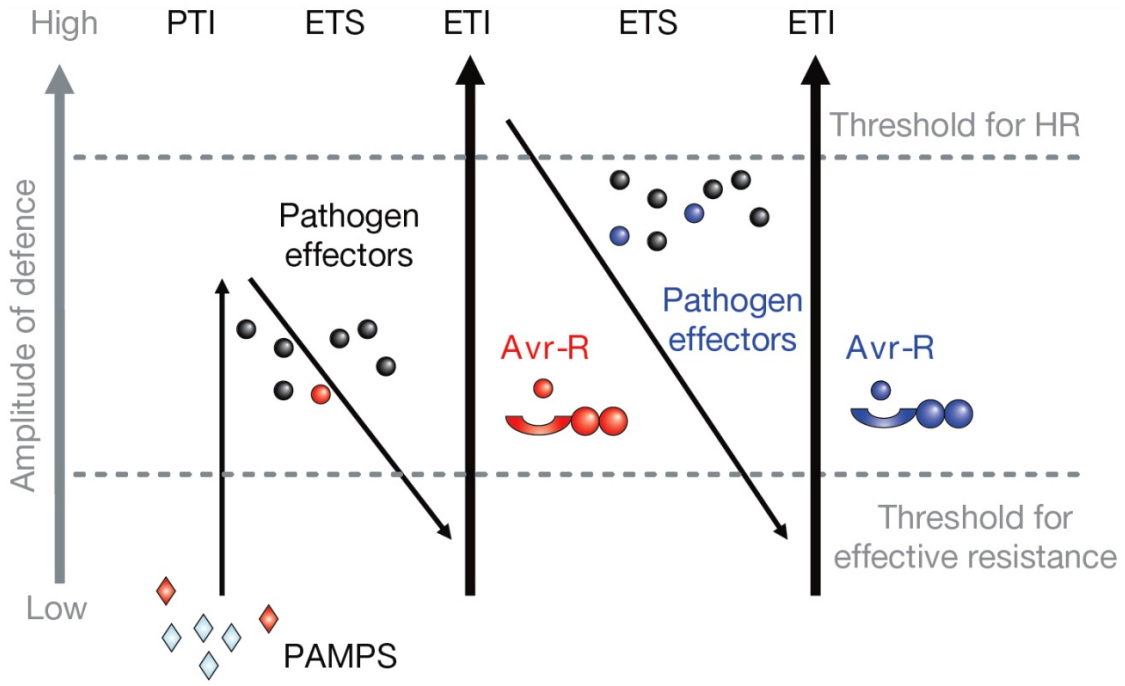

Fig.2. A zigzag model illustrates the quantitative output of the plant immune system (Jones & Dangl, 2006). In this scheme, the ultimate amplitude of disease resistance or susceptibility is proportional to [PTI–ETS+ETI]. In phase 1, plants detect MAMPs/PAMPs (red diamonds) via PRRs to trigger PAMP-triggered immunity (PTI). In phase 2, successful pathogens deliver effectors that interfere with PTI, or otherwise enable pathogen nutrition and dispersal, resulting in effector-triggered susceptibility (ETS). In phase 3, one effector (indicated in red) is recognized by an NB-LRR protein, activating effector-triggered immunity (ETI), an amplified version of PTI that often passes a threshold for induction of hypersensitive cell death (HR). In phase 4, pathogen isolates are selected that have lost the red effector, and perhaps gained new effectors through horizontal gene flow (in blue)—these can help pathogens to suppress ETI. Selection favours new plant NB-LRR alleles that can recognize one of the newly acquired effectors, resulting again in ETI.

suggested that Stp1 was able to suppress plant defense reactions directly or indirectly. Functional domain analyses of Stp1 revealed that the central glycine-rich domain of Stp1 was dispensible for protein function while the N- and C-terminal conserved domains were essential during biotrophic growth. Confocal microscopy observation indicated that Stp1-mCherry fusion proteins localized to the apoplastic interaction zone of infected plant cells. After transient expression in *Nicotiana benthamiana*, Stp1 lacking the signal peptide specifically localized to sub-compartments of the nucleus (Schipper, 2009).

Five intracellular plant proteins were identified to interact with Stp1 in a yeast-two hybrid screen (Schipper, 2009). Moreover, one of the interactors, Sip12, co-localized with Stp1 lacking the signal peptide after expression in *N. benthamiana* (Schipper, 2009). These

results suggested that Stp1 might be translocated into the plant cell where it could be involved in regulation of plant defense responses.

1.6 Aims of this study

The focus of this study is functional analysis of Stp1, a secreted effector that is crucial for the establishment of biotrophic interaction between *U. maydis* and its host plant maize. The main emphasis in this study is (1) identification of interactors of Stp1 through yeast two-hybrid assay and analysis of the mechanism of the interaction to uncover the function of Stp1; (2) determination whether Stp1 is an apoplastic or cytoplasmic effector; (3) heterologous expression & purification of Stp1 and structural analysis of Stp1 to reveal functional information residing in the structure; (4) functional domain analysis of Stp1.

2. Results

2.1 Functional domain analysis of Stp1

2.1.1 The variable domains of Stp1 are dispensable

An amino acid sequence alignment of Stp1 orthologs shows that N- and C-termini of Stp1 are conserved among different smut fungi while the central glycine-rich domain is highly divergent (Fig. 3). Previous experiments have already shown that Stp1 without part of the glycine-rich region ($Stp1_{\Delta 136\text{-}338}$) could complement SG200Δstp1 (Schipper, 2009). To analyze whether the whole glycine-rich domain is dispensable or not, I generated a plasmid p123pstp1-$stp1_{\Delta 136\text{-}432}$ which contained a *stp1* allele that retained only the coding region for 107 amino acids of the N-terminus and for 83 amino acids of the C-terminus (Fig. 4). This plasmid was inserted into the *ip* locus (Loubradou *et al.*, 2001) of SG200Δstp1 to produce SG200Δstp1-$stp1_{\Delta 136\text{-}432}$. Plant infection assays with three independently generated strains showed that $Stp1_{\Delta 136\text{-}432}$ could fully complement SG200Δstp1 (Fig. 5). This result shows that $Stp1_{\Delta 136\text{-}432}$ retains its function even though 58 % of the protein is deleted and illustrates that the glycine-rich central domain of Stp1 is dispensable.

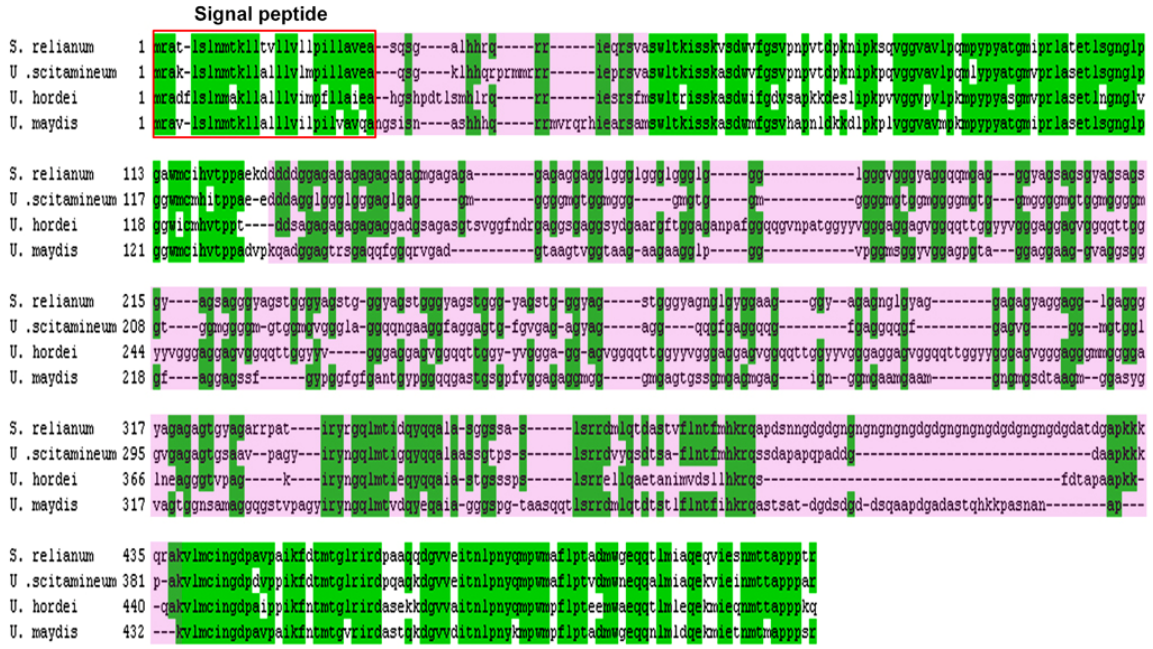

Fig. 3. Stp1 orthologs exist in related smut fungi. *S. relianum*: *Sporisorium reilianum* (Schirawski *et al.*, 2010), *U. scitamineum*: *Ustilago scitamineum* (R. Kahmann, unpublished), *U. hordei*: *Ustilago hordei* (Laurie *et al.*, 2012), *U. maydis*: *Ustilago maydis* (Kamper et al., 2006). Green color denotes conserved amino acids. Pink color denotes variable domains.

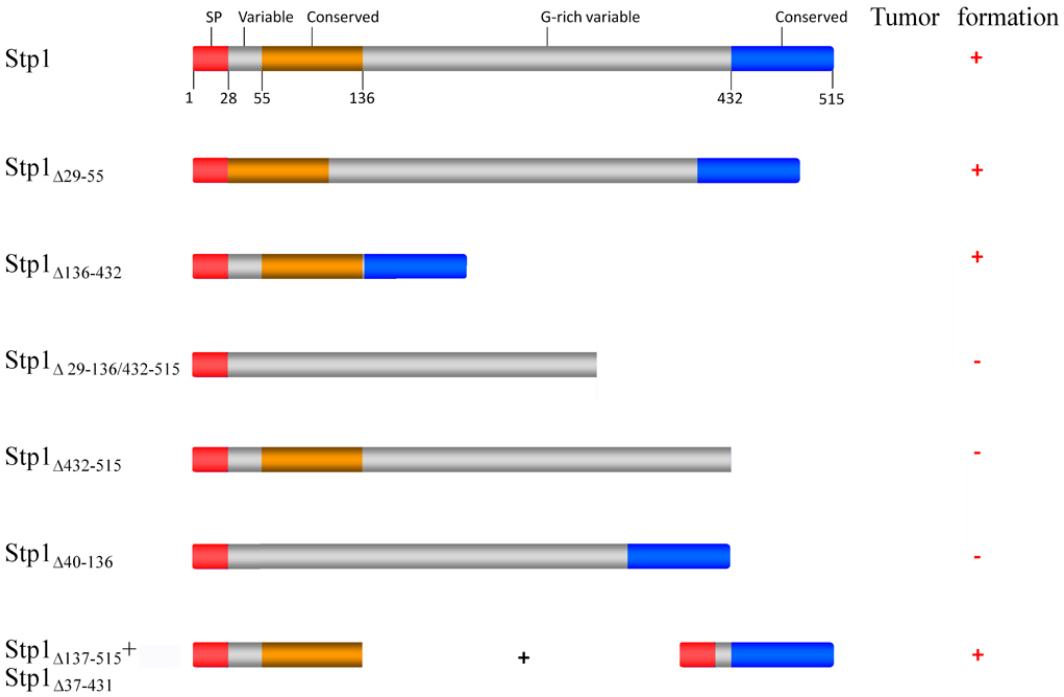

Fig. 4. Domain structure of Stp1 and Stp1 mutant proteins. To test tumor formation, Stp1 derivatives were integrated into the *ip* locus of G200Δstp1 and the respective strains were used to infect maize plants. $Stp1_{\Delta 432\text{-}515}$ and $Stp1_{\Delta 40\text{-}136}$ were constructed by Kerstin Schipper (Schipper, 2009). Red (SP): signal peptide, grey: variable domains of Stp1, orange: N-terminus of Stp1, blue: C-terminus of Stp1.

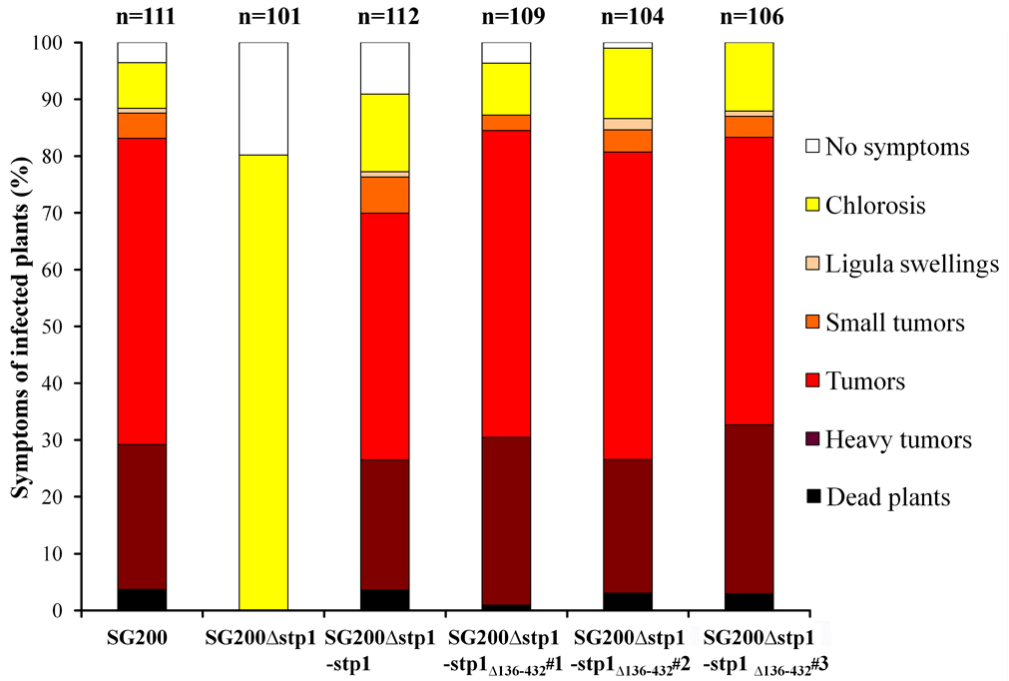

Fig. 5. $Stp1_{\Delta 136\text{-}432}$ complements SG200Δstp1. Strains tested for virulence in seedling infection are indicated. For each strain, three independent infections were performed and averaged. The total number of maize plants infected is given above each column. Symptoms were scored 12 days after infection following the scheme developed by Kamper *et al* (2006) indicated on the right.

To rule out the possibility that the central domain of Stp1 might have a minor function, a plasmid p123pstp1-Stp1$_{\Delta 29\text{-}136/432\text{-}515}$ in which the variable glycine-rich domain was fused with the signal peptide was constructed (Fig. 4) and inserted into the *ip* locus of SG200Δstp1 to generate SG200Δstp1-stp1$_{\Delta 29\text{-}136/432\text{-}515}$. No disease symptoms were detected on plants infected with SG200Δstp1-stp1$_{\Delta 29\text{-}136/432\text{-}515}$ (Fig. 6). To detect partial complementation, SG200Δstp1-stp1$_{\Delta 29\text{-}136/432\text{-}515}$ infected maize leaves were stained with WGA-AF 488 / propidium iodide (WGA/PI) and observed by confocal microscopy. Similar to the *stp1* deletion mutant, growth of SG200Δstp1-stp1$_{\Delta 29\text{-}136/432\text{-}515}$ stopped after penetration. Occasionally, some hyphae of SG200Δstp1-stp1$_{\Delta 29\text{-}136/432\text{-}515}$ were proliferating in vascular bundles (Fig. 7 A and D). The hyphae of SG200Δstp1 were also observed in vascular bundles in rare cases (Fig. 7 B and E). But, SG200Δstp1-stp1$_{\Delta 29\text{-}136/432\text{-}515}$ which proliferate along the vascular bundles in a continuous way grew better than SG200Δstp1 and triggered less plant defense responses than SG200Δstp1 (Fig. 7). This could indicate that the expression of the glycine-rich domain of *stp1* could have a weak effect on

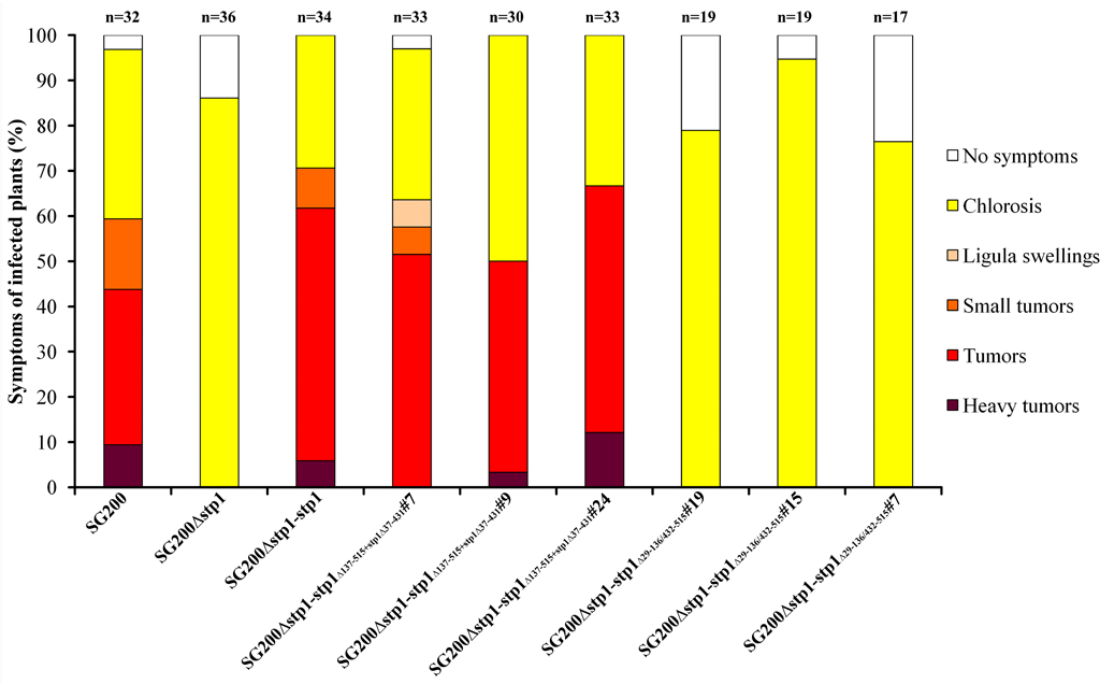

Fig. 6. N- and C-termini of Stp1 can be expressed separately while the strains expressing glycine-rich domain of Stp1 cannot restore tumor formation. Strains tested for virulence in seedling infection are indicated. The total number of maize plants infected is given above each column. Symptoms were scored 12 days after infection following the scheme developed by Kamper *et al* (2006) indicated on the right.

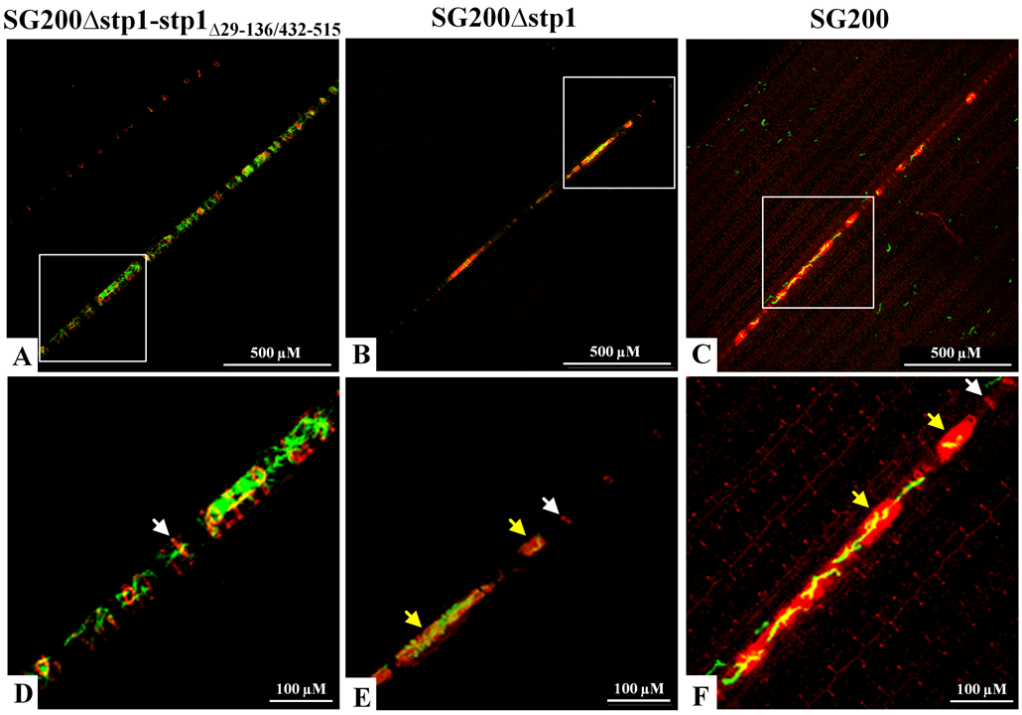

Fig. 7. SG200Δstp1-stp1$_{\Delta 29\text{-}136/432\text{-}515}$ proliferation in vascular bundles. A, B and C: Maize plants infected with indicated strains. D, E and F: Enlargement of the areae in the white rectangular of A, B and C. Maize leaves infected with indicated strains were collected one day after infection, stained with WGA/PI as described in methods and observed using confocal microscopy. The pictures are the overlay of WGA and PI channels. The Fungal hyphae are shown in green. The plant cell wall, vascular bundle and the autofluorescence indicating plant defense responses are shown in red. Yellow colored areae are the overlap of the signals of fungal hyphae and plant defense responses. The white arrows denote the red ring of vascular bundles. The yellow arrows denote the plant defense responses.

biotrophic development. However, in very rare case, the hyphae of SG200 could also be observed in vascular bundle (Fig. 7 C and F). Therefore, further studies are needed to substantiate this point quantitatively.

Furthermore, the complementation of SG200Δstp1 by N-terminus truncated Stp1 indicated that the segment spanning amino acids 29-55 of Stp1 is dispensable (Fig. 4) (Schipper, 2009). To further analyze the functional regions close to the C-terminus, the plasmids p123pstp1-stp1$_{\Delta 433\text{-}454}$, p123pstp1-stp1$_{\Delta 455\text{-}476}$, p123pstp1-stp1$_{\Delta 477\text{-}494}$ and p123pstp1-stp1$_{\Delta 495\text{-}515}$ incorporating C-terminus truncated *stp1* genes were constructed and kindly provided by K. schipper. All plasmids were inserted into SG200Δstp1 to produce SG200Δstp1-stp1$_{\Delta 433\text{-}454}$, SG200Δstp1-stp1$_{\Delta 455\text{-}476}$, SG200Δstp1-stp1$_{\Delta 477\text{-}494}$ and SG200Δstp1-stp1$_{\Delta 495\text{-}515}$. Of these strains, only SG200Δstp1-stp1$_{\Delta 455\text{-}476}$ was able to cause

disease in preliminary test, which demonstrated that the Stp1 segment between amino acids 455 and 476 was dispensable (Fig. 8). The infection will be repeated to substantiate this result.

2.1.2 N- and C-termini of Stp1 could be separately expressed

To elucidate whether the two domains of Stp1 can be expressed as separate proteins, a plasmid p123pstp1-stp1$_{\Delta 137\text{-}515}$+pstp1-stp1$_{\Delta 37\text{-}431}$ that specifies two gene fragments encoding N- and C-terminus of Stp1, both fused with the *stp1* promoter and signal peptide was constructed and kindly provided by M. Daume and K. Schipper (Fig. 4). This plasmid was inserted into the *ip* locus of SG200Δstp1 to produce SG200Δstp1-stp1$_{\Delta 137\text{-}515}$+stp1$_{\Delta 37\text{-}431}$. The plant infection assays of this strain demonstrated that separately expressed N- and C-termini of Stp1 were functional (Fig. 6).

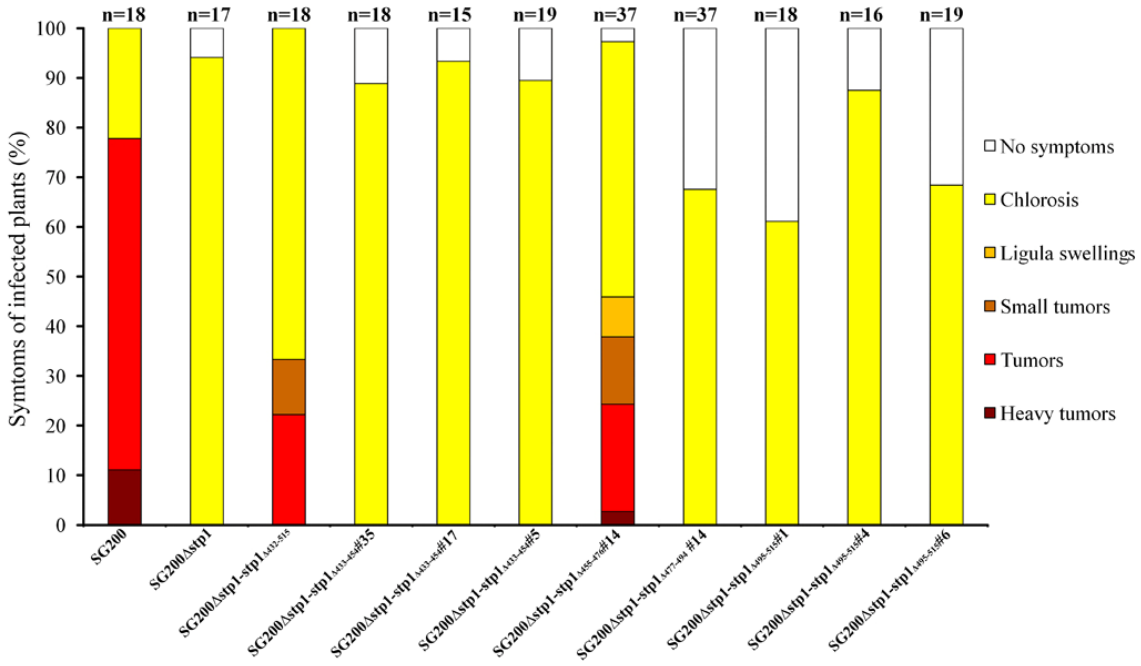

Fig. 8. Stp1 segment between amino acids 455 and 476 is dispensable. Strains tested for virulence in seedling infection are indicated. The total number of maize plants infected is given above each column. Symptoms were scored 12 days after infection following the scheme developed by Kamper *et al* (2006) indicated on the right.

No tumors were formed on plants infected with SG200Δstp1-stp1$_{\Delta 432\text{-}515}$ or SG200Δstp1-stp1$_{\Delta 40\text{-}136}$ (Fig. 4) in which either N- or C-termini of Stp1 are deleted (Schipper, 2009). This had indicated that both N- and C-terminus of Stp1 are needed for its function

(Schipper, 2009). To investigate whether expression of only the N- or the C-terminal domain of Stp1 is sufficient to allow partial colonization, maize leaves infected with respective strains were stained with WGA/PI and observed using confocal microscopy. The results showed that SG200Δstp1 stopped after penetration while SG200 profusely colonized the tissue (Fig. 9 panel A). Meanwhile, colonization of SG200Δstp1-stp1$_{\Delta 432\text{-}515}$ and SG200Δstp1-stp1$_{\Delta 40\text{-}136}$ also stopped after penetration (Fig. 9 panel A). Besides the representative growth of indicated *U. maydis* strains in panel A (Fig. 9), some hyphae of SG200Δstp1 could proliferate on plant surface which could not reflect colonization (Fig. 9 panel B). Additionally, SG200Δstp1, SG200Δstp1-stp1$_{\Delta 432\text{-}515}$ and SG200Δstp1-stp1$_{\Delta 40\text{-}136}$ were detected in deeper tissue layers (Fig. 9 panel B). However, it is difficult to determine whether the deeper growth reached mesophyll cells or it ceased in epidermal cells. So far, no obvious differences between SG200Δstp1, SG200Δstp1-stp1$_{\Delta 432\text{-}515}$ and SG200Δstp1-stp1$_{\Delta 40\text{-}136}$ were observed.

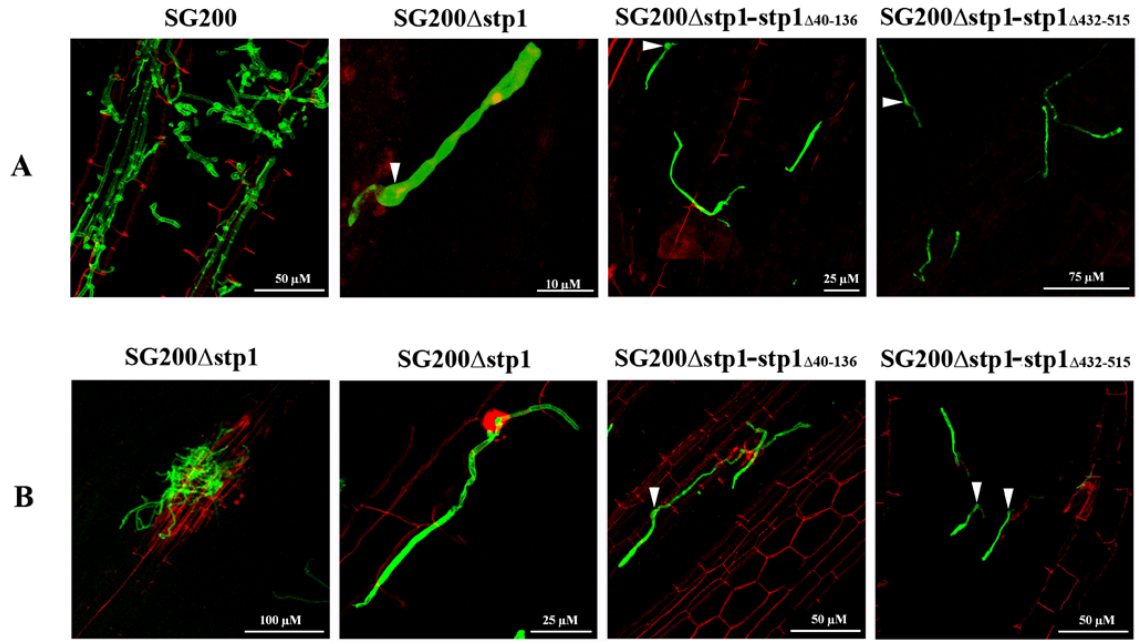

Fig. 9. Early biotrophic development of SG200Δstp1:stp1$_{\Delta 432\text{-}515}$ and SG200Δstp1:stp1$_{\Delta 40\text{-}136}$. The maize leaves infected with indicated *U. maydis* strains were collected three days after infection, stained with WGA/PI as described in methods and observed using confocal microscopy. The first figure in panel B showed surface growth of SG200Δstp1. The pictures shown are the overlay of WGA and PI channels. The fungal hyphae are shown in green. The plant cell walls as well as the autofluorescence indicating plant defense responses are shown in red. The white arrows denote appresoria.

To further visualize leaf colonization, Chlorazol black E was used for staining. SG200 proliferates in both epidermal tissue and mesophyll tissue (Fig. 10 A, E). Most hyphae of

SG200Δstp1 as well as SG200Δstp1-stp1$_{\Delta 432\text{-}515}$ and SG200Δstp1-stp1$_{\Delta 40\text{-}136}$ stopped growing immediately after penetration as shown in Fig. 9. Rarely, hyphae of SG200Δstp1-stp1$_{\Delta 432\text{-}515}$ and SG200Δstp1-stp1$_{\Delta 40\text{-}136}$ could penetrate epidermal cells and grow into mesophyll cells (Fig. 10 G, H). However growth inside mesophyll cells could also be rarely observed in SG200Δstp1 infected plants (Fig. 10 F). The finding that neither the N- nor the C-terminus of Stp1 can partially rescue the growth arrest of the *stp1* mutant indicated that both N- and C-terminus of Stp1 were playing crucial functional roles. Further studies need to be performed to determine if there are differences between SG200Δstp1, SG200Δstp1-stp1$_{\Delta 432\text{-}515}$ and SG200Δstp1-stp1$_{\Delta 40\text{-}136}$ in terms of the ratio of fungal hyphae penetrated into mesophyll cells or the length of fungal hyphae.

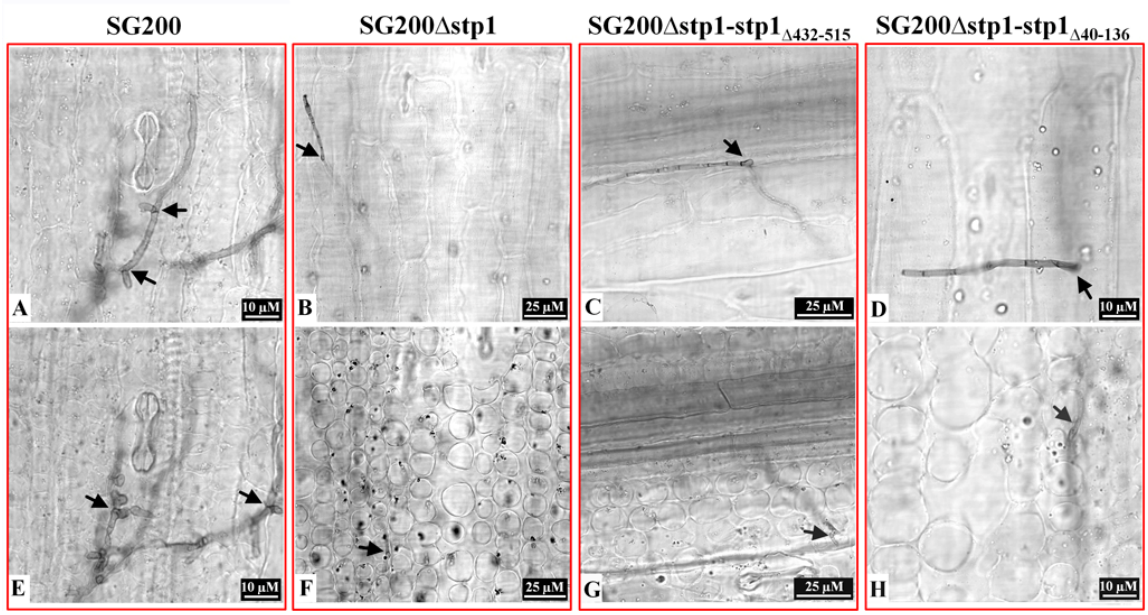

Fig. 10. Plant colonization by SG200Δstp1-stp1$_{\Delta 432\text{-}515}$ and SG200Δstp1-stp1$_{\Delta 40\text{-}136}$. The maize leaves infected with indicated *U. maydis* strains were collected two days after infection, stained with chlorazol black E as described in methods and observed using confocal microscopy at bright field. Two figures in the same red rectangular denote two different cross sections of the same sample. The black arrows in B, C and D denote appresoria, in F G and H denote the fungal hyphae in mesophyll and in A and E denote branching of fungal hyphae in both epidermal and mesophyll.

2.1.3 Stp1 related proteins in other smut fungi can replace Stp1 of *U. maydis*

N- and C-termini of Stp1 are conserved among different smut fungi while the middle central glycine-rich domain is highly divergent (Fig. 3). To determine whether these orthologs can substitute for Stp1 in *U. maydis*, we generated the plasmids p123pstp1- Uh-stp1 and p123pstp1-Us-stp1 in which *stp1* orthologs from *U. hordei* and *U. scitamineum*

were fused with the promoter and signal peptide of *stp1* from *U. maydis* respectively. The plasmids were inserted into SG200Δstp1 to produce SG200Δstp1-Uh-stp1 and SG200Δstp1-Us-stp1. The plant infection assays (Fig. 11) demonstrated that both stp1 orthologs from *U. hordei* and *U. scitaminem* could complement SG200Δstp1 (Fig. 11) which indicated that the function of Stp1 orthologs was conserved.

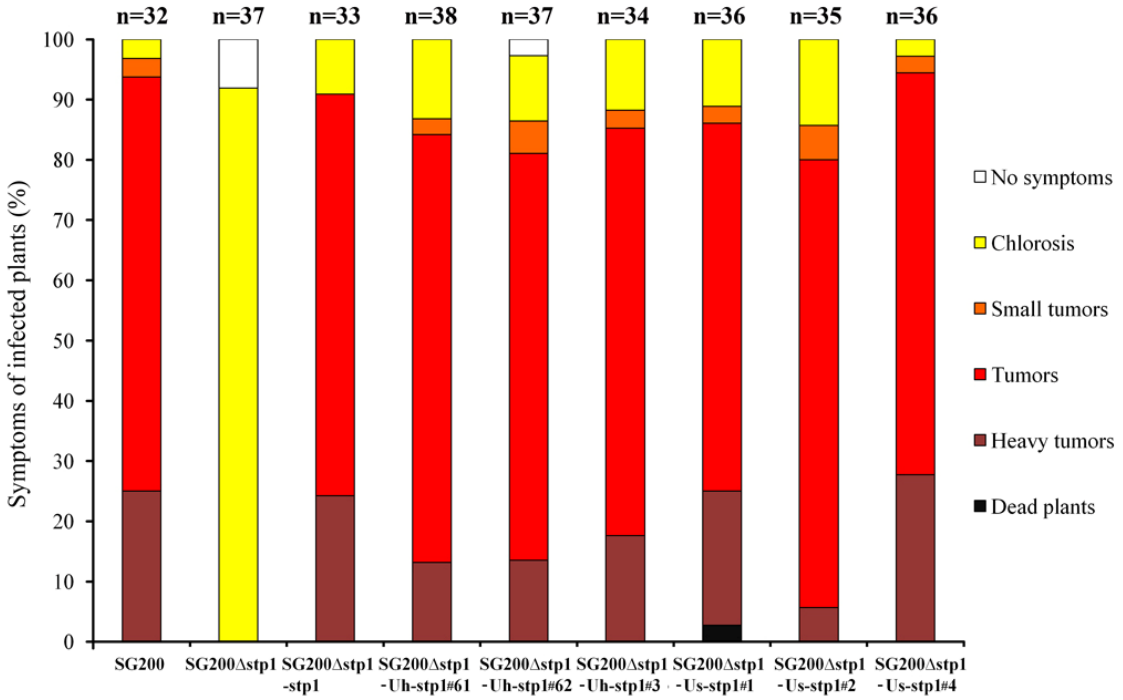

Fig. 11. *stp1* orthologs from other smut fungi can replace *stp1* of *U. maydis*. Strains tested for virulence in seedling infection are indicated. The total number of maize plants infected is given above each column. Symptoms were scored 12 days after infection following the scheme developed by Kamper *et al* (2006) indicated on the right.

2.1.4 The putative functional domains show low similarity with known functional domains in the databases are not valid

BLAST analysis indicated that the C-terminus of Stp1 showed low similarity with the NAD^+-binding domain of NmrA (nitrogen metabolism repression regulator NmrA) family proteins (Nunez-Corcuera *et al.*, 2008). Therefore, the plasmids P123pstp1-stp1$_{\Delta 136\text{-}432T452V}$ and P123pstp1-stp1$_{T452V}$ in which the threonine 452 was replaced by valine were constructed to test if they could complement SG200Δstp1. Both plasmids were introduced into SG200Δstp1 respectively to produce SG200Δstp1-stp1$_{\Delta 136\text{-}432T452V}$ and SG200Δstp1-stp1$_{T452V}$. Plant infection assays showed that both SG200Δstp1-stp1$_{\Delta 136\text{-}432T452V}$ and

SG200Δstp1-stp1$_{T452V}$ could cause disease on maize plants (Fig. 12), which indicated that the presumed NAD$^+$-binding function of Stp1 might not be relevant for its function.

The very C-terminal domain of the Tin2 effector plays an important functional role (S. Tanaka, personal communication). To test whether the very C-terminus of Stp1 was essential or not, the plasmids p123pstp1-stp1$_{PPAA}$ and p123pstp1-stp1$_{SRAA}$, in which the C-terminal PP and SR were replaced by AA respectively, were generated. Both plasmids were introduced into SG200Δstp1 to produce SG200Δstp1-stp1$_{PPAA}$ and SG200Δstp1-stp1$_{SRAA}$. Plant infection assays revealed that both SG200Δstp1-stp1$_{PPAA}$ and SG200Δstp1-stp1$_{SRAA}$ could cause disease on maize plants (Fig. 13), which indicated that the very C-terminus of Stp1 was not crucial for its function.

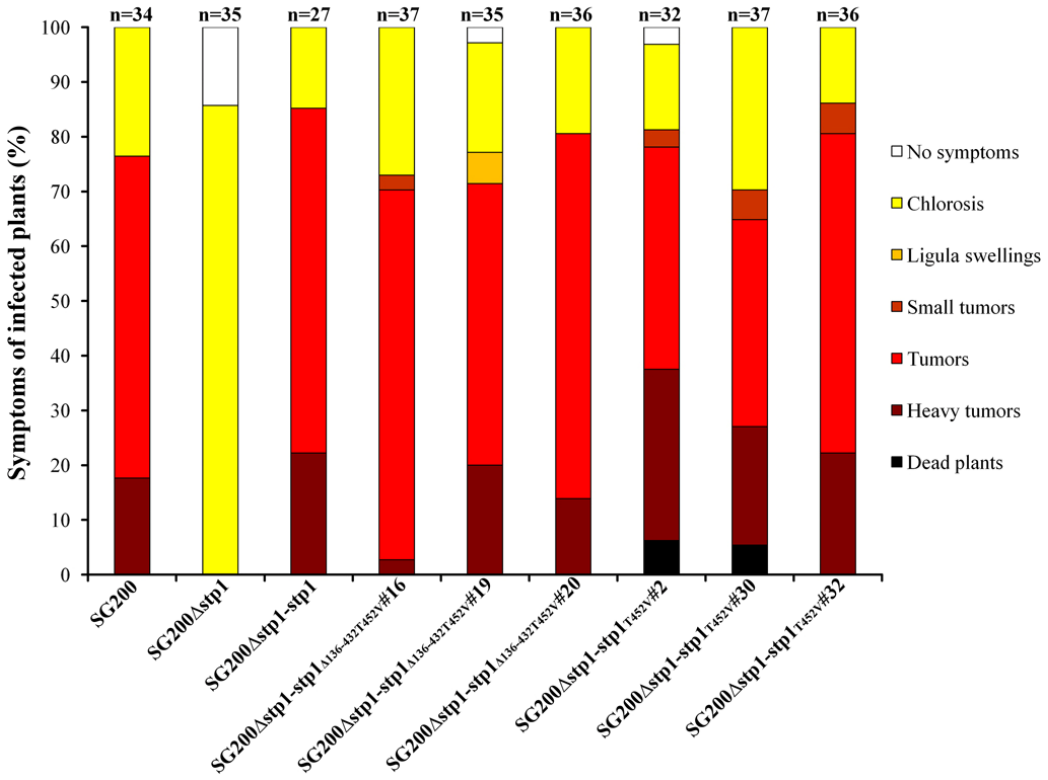

Fig. 12. The putative NAD$^+$-binding domain of Stp1 is not relevant for its function. Strains tested for virulence in seedling infection are indicated. The total number of maize plants infected is given above each column. Symptoms were scored 12 days after infection following the scheme developed by Kamper *et al* (2006) indicated on the right.

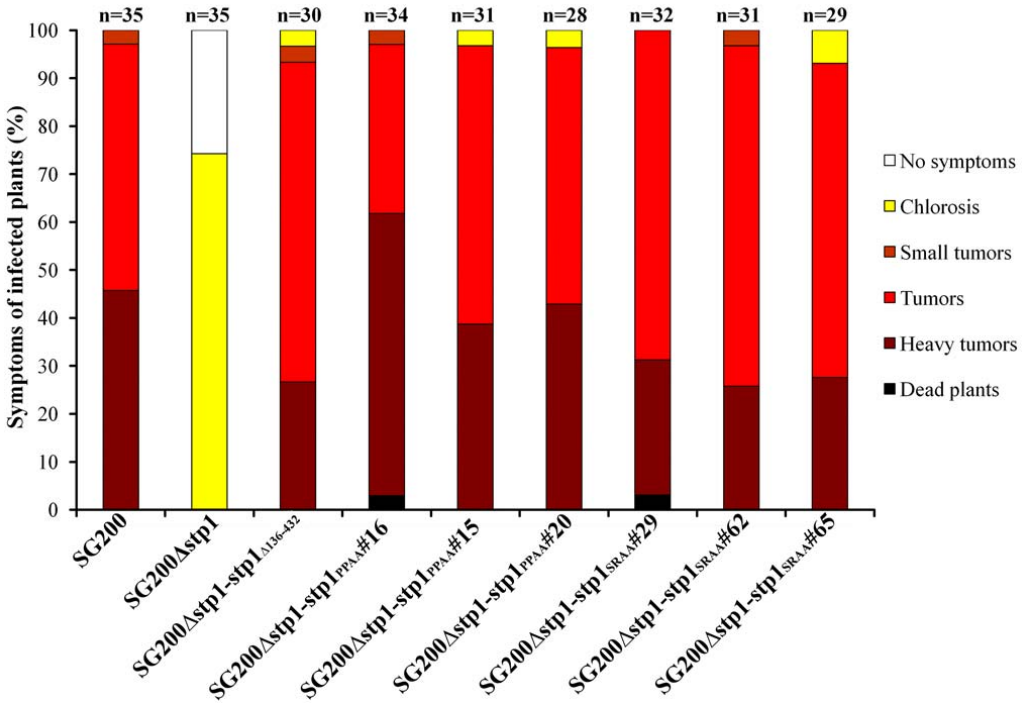

Fig. 13. The very C-terminus of Stp1 is not critical for its funcion. Strains tested for virulence in seedling infection are indicated. The total number of maize plants infected is given above each column. Symptoms were scored 12 days after infection following the scheme developed by Kamper *et al* (2006) indicated on the right.

2.2 Interactors of Stp1 and Stp1$_{\Delta 136\text{-}432}$ are both cytoplasmic and apoplastic maize proteins

To answer what host protein (s) is being targeted leading to enhanced virulence, one of the most common way is to identify host proteins that physically interact with an effector. Among several methods exist, the most frequently utilized is yeast two-hybrid system (Munkvold & Martin, 2009). To screen for interactors of Stp1, yeast two-hybrid assays had been firstly performed using full-length Stp1 as bait (Schipper, 2009) and then redone using Stp1$_{\Delta 136\text{-}432}$ as bait in this study.

2.2.1 Interactors identified by full-length Stp1 are not likely to be functionally relevant

Employing full-length Stp1 as bait, five putative interaction partners of Stp1 (Sip2-adenylate kinase Adk1, Sip10-homolog to myrosinase precursor, Sip12-RING-E3 ubiquitin ligase, homolog to Vip2, Sip29-potential transcription factor and Sip31-GroEL chaperone)

had been identified through Y2H assays (Schipper, 2009). Meanwhile, deletion analysis showed that the long glycine-rich domain in the middle of Stp1 was dispensable. To determine whether the putative interactors were interacting specifically with the functional N- or C- terminal domains, I have first tested the interaction between $Stp1_{\Delta 136\text{-}338}$ and the putative interaction partners-Sip12 and Sip29. The respective prey plasmids were kindly provided by K. Schipper and the interactions were tested by yeast re-transformation. The results showed that the truncated $Stp1_{\Delta 136\text{-}338}$ was interacting with full-length Stp1 and weakly with Sip12 (Fig. 14). However, $Stp1_{\Delta 136\text{-}338}$ was not interacting with Sip29 (Fig. 14). To test the interactions between $Stp1_{\Delta 136\text{-}432}$ and Sip10, Sip12, Sip29 and Sip31, pGBK-$stp1_{\Delta 136\text{-}432}$ was generated and the corresponding plasmids kindly provided by K. Schipper were co-transformed into AH109. The results showed that $Stp1_{\Delta 136\text{-}432}$ was interacting with full-length Stp1, but it was not interacting with any of the putative interaction partners of the full-length Stp1 (Fig. 14). In the expression assays using Western blotting, the expression of AD-Sip12 (AD, activation domains of GAL4) and AD-Sip29 were not detected (Fig. 14). Full-length *sip12* and *sip29* will be cloned and the interactions will be retested. The Y2H assays indicated that the interaction between Stp1 and Sip10, Sip12, Sip29 and Sip31 was not likely to be functionally relevant. Therefore, Y2H assays were redone employing $Stp1_{\Delta 136\text{-}432}$ as bait.

2.2.2 Interactors of $Stp1_{\Delta 136\text{-}432}$ are both cytoplasmic and apoplastic maize proteins

pGBK-$stp1_{\Delta 136\text{-}432}$ and a prey cDNA library of *U. maydis* infected maize leaves (two days and five days post infection) were subsequently co-transformed into AH109. Duplicates were eliminated by sorting after PCR amplification and digestion by *Hae*III.

After screening of the library, twelve distinct interaction partners of $Stp1_{\Delta 136\text{-}432}$ were identified and verified by re-transformation (Table. 1). Bioinformatic analysis by Signal P (http://www.cbs.dtu.dk/services/SignalP/) and TargetP (http://www.cbs.dtu.dk/services/TargetP/) showed Sip1 and Sip3 were predicted to be secreted maize proteins while the others were predicted to be cytoplasmic proteins (Table 1). Interestingly, although the interactors identified by full-length Stp1 are not interacting with $Stp1_{\Delta 136\text{-}432}$, all putative interactors identified using $Stp1_{\Delta 136\text{-}432}$ as bait were interacting

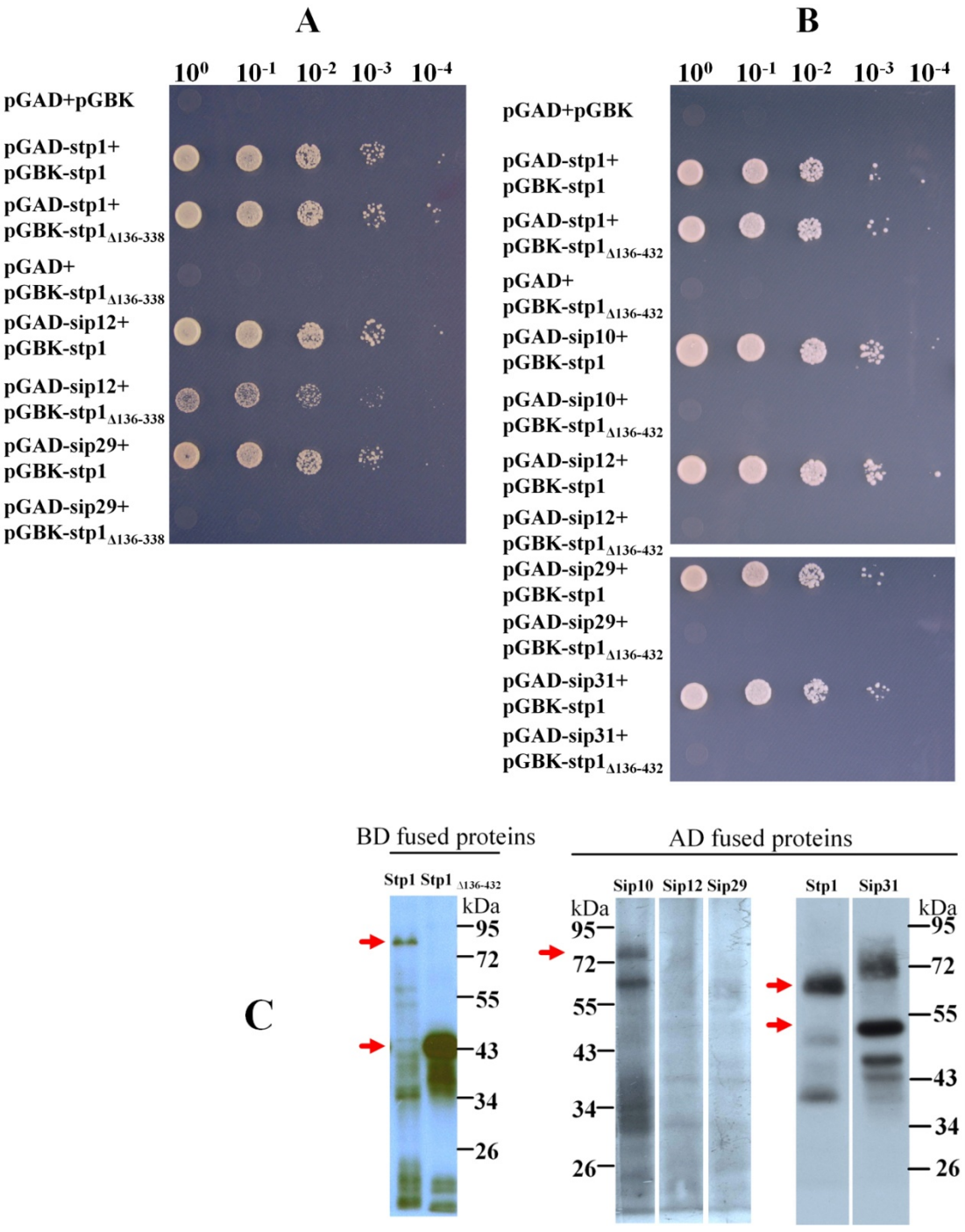

Fig. 14. Sip10, Sip12, Sip29 and Sip31 are not interacting with Stp1$_{\Delta 136-432}$ in Y2H assays. A, Interactions between Sip12, Sip29 and Stp$_{\Delta 136-338}$. B, Interactions between Sip10, Sip12, Sip29, Sip31 and Stp$_{\Delta 136-432}$. The re-transformation and growth assay were performed as described in methods. C, Expression of indicated proteins in yeast was detected by Western blotting. DNA binding domains (BD) were detected using c-Myc antibody and activation domains (AD) were detected using HA antibody. The red arrows denote the signals of indicated proteins (BD-Stp1: 68.5 kDa, BD-Stp$_{\Delta 136-432}$: 42 kDa, AD-Sip10: 72.7 kDa, AD-Sip12: 54.8 kDa, AD-Sip29: 123.1 kDa, AD-Sip31: 42 kDa, AD-Stp1: 68.5 kDa).

Table. 1. Y2H interaction partners of Stp1 and Stp1$_{\Delta 136-432}$ are both apoplastic and cytoplasmic maize proteins.

	Interaction partners	Signal peptide	Frequency	Interaction with Stp1$_{\Delta 136-432}$	Interaction with Stp1
Sip1	Putative beta-galactosidase BG1	Yes	1	N	N
Sip2	Putative Adenylate kinase	No	8	N	+
Sip3▲	Putative cysteine protease 1	Yes	1	+	+
Sip4	Putative chaperone protein dnaJ	No	156	+	N
Sip5	Putative DAG protein	No	1	+	N
Sip6▲	Putative Rhamnogalacturonate lyase	No	379	-	+
Sip7	Hypothetical protein	No	54*	+	+
Sip8▲	Putative thiamine biosynthesis protein thiC	No		-	+
Sip9▲	Putative SAT5 (cell number regulator 8)	No	138	+	+
Sip10	Putative myrosinase precursor	No	15	-	+
Sip11	Putative Transducin family protein	No	2	+	N
Sip12	Putative VIP2 (E3 ubiquitin ligase)	No	45	N	+
Sip14▲	Putative VIP2 (E3 ubiquitin ligase)	No	1	-	+
Sip16▲	Putative CCR4-NOT transcription complex subunit	No	1	+	+
Sip17	Putative iron-sulfur protein2	No	2	N	N
Sip19▲	Putative Serine/threonine-protein kinase MHK	No	2	+	+
Sip20	Putative FPA RNA binding	No	3	N	N
Sip21▲	Putative VIP2	No	1	+	+
Sip29	Putative transcription factor	No	37	-	+
Sip31	Putative GroEL chaperone	No	3	-	+

N: not tested yet, *: Both the size of PCR products and the pattern of *Hae*III digestion fragments of Sip7 and Sip8 are identical. Therefore, their frequency could not be separated. ▲: interaction was tested with full-length cDNA clones of the respective genes. Previously identified interaction partners (Schipper, 2009) are indicated in red fonts

with full-length Stp1 (Fig. 14 and Table. 1) which indicated that the glycine-rich domain of Stp1 was binding unspecifically with many different proteins.

In many cases, the putative interactors isolated from the library contained only a fragment of the full-length gene. Therefore, before further analysis, I chose eight putative interactors (Sip3, Sip6, Sip8, Sip9, Sip14, Sip16, Sip19 and sip21) for the interaction studies depicted in Table 1, which could conceivably be involved in plant defense reaction or plant development regulation. Full-length genes of them were cloned from cDNA of *U. maydis* infected maize leaves. These genes were then inserted into pGADT7 vector to generate pGAD-sip3, pGAD-sip6, pGAD-sip8, pGAD-sip9, pGAD-sip14, pGAD-sip16, pGAD-

sip19 and pGAD-sip21. Their interactions with Stp1 and $Stp1_{\Delta 136-432}$ were then tested by co-transformation. The results showed that Sip6, Sip8 and Sip14 were not interacting with $Stp1_{\Delta 136-432}$ anymore (Fig. 15). 50.2 % isolates from Y2H screening is Sip6, the putative rhamnogalacturonate lyase, and most of the isolates is C-terminus of rhamnogalacturonate lyase. This indicates that one important source of false positives is the gene fragments. Sip14 and Sip21 are both putative VIP2 proteins which is a component of transcription complex units. The difference between these two proteins is that in Sip21 the N-terminal Ringfinger domain is missing which indicated that the interaction between Sip21 and Stp1 was not likely correlated with the Ringfinger domain.

2.2.3 N- and C-termini of Stp1 may play separate functions

To learn via which domain Stp1 was binding to the interactors, pGBK-$stp1_{29-135}$ and pGBK-$stp1_{433-515}$ were generated. The interactions between the full-length maize proteins and separate N- or C-terminus of Stp1 were also tested by co-transformation. The results showed that Sip6 was only weakly interacting with N-terminus of Stp1 while the other interactors were interacting strongly with N-terminus (Fig. 15). Sip21 was interacting weakly with the C-terminus of Stp1, Sip8 and Sip14 were not interacting with the C-terminus of Stp1 and the other interactors were interacting strongly with the C-terminus of Stp1 (Fig. 15). Whether the interaction between Sip6 and C-terminus of Stp1 or Sip8 & Sip14 and N-terminus of Stp1 reflect transient or weak interaction between $Stp1_{\Delta 136-432}$ and Sip6, Sip8 and Sip14 or they are not functional relevant still need to be tested biochemically. The differences observed suggested that N- and C-termini of Stp1 may play distinct functions. To investigate the relationship between different domains of Stp1, pGAD-$stp1_{\Delta 136-432}$, pGAD-$stp1_{29-135}$ and pGAD-$stp1_{433-515}$ were constructed. The interactions between different domains of Stp1 were tested using Y2H assays. The results showed that Stp1 was interacting with itself as well as $Stp1_{\Delta 136-432}$ while $Stp1_{\Delta 136-432}$ was not interacting with itself (Fig. 16). The C-terminus of Stp1 ($Stp1_{433-515}$) was interacting with itself weakly. The N-terminus of Stp1 ($Stp1_{29-135}$) showed no self-interaction and was unable to interact with the C-terminus (Fig. 16). This could indicate that N- and C-termini of Stp1 were not functioning in a complex.

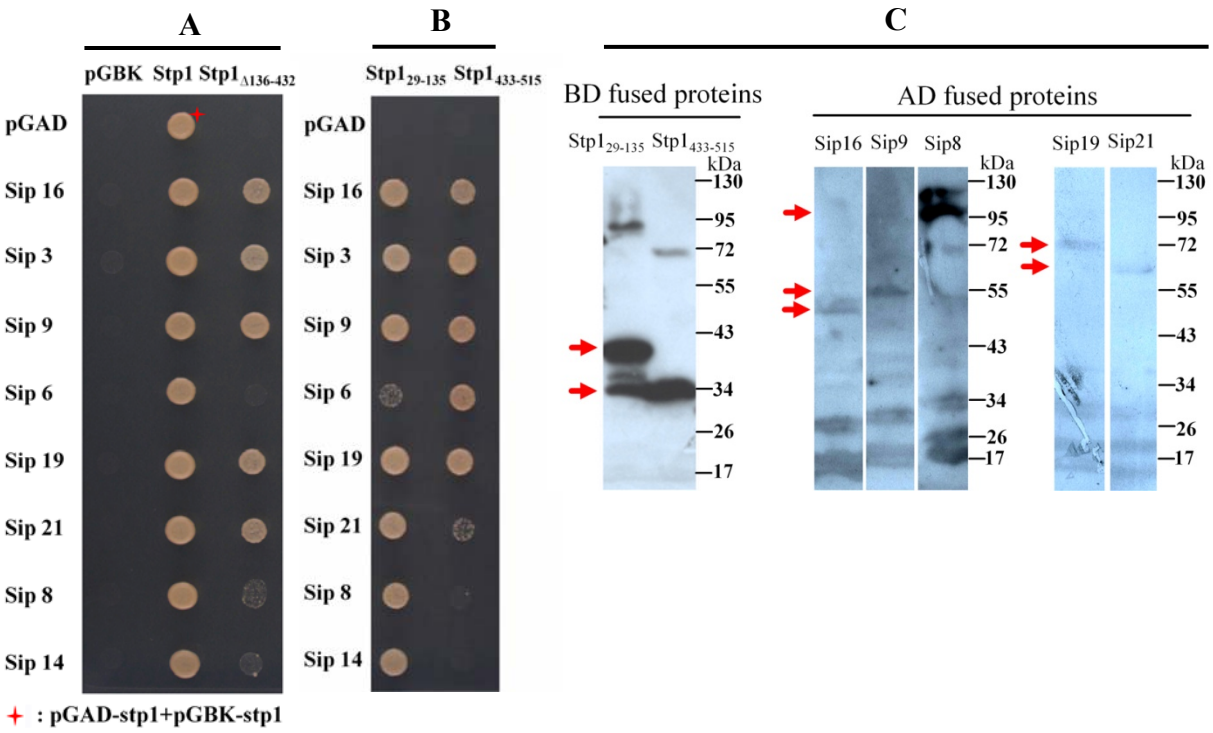

Fig. 15. Stp1 mutants were interacting with interactors isolated using $Stp1_{\Delta 136-432}$ as bait with different affinity. A, Full- length Sip6, Sip8 and Sip14 do not interact with $Stp1_{\Delta 136-432}$ in Y2H assays. B, N- and C-termini of Stp1 showed different patterns of interaction from that of $Stp1_{\Delta 136-432}$ and Stp1. The re-transformation and growth assay were performed as described in methods. C, Expression of indicated proteins in yeast detected by Western blotting. BD was detected using c-Myc antibody and AD was detected using HA antibody. The red arrows denote the signals of indicated proteins (BD-$Stp1_{29-135}$: 33.9 kDa, BD-$Stp_{433-515}$: 29.5 kDa. AD-Sip16: 54 kDa, AD-Sip9: 48.6 kDa, AD-Sip8: 95.1 kDa, AD-Sip19: 72.2 kDa, AD-Sip21: 60.3 kDa).

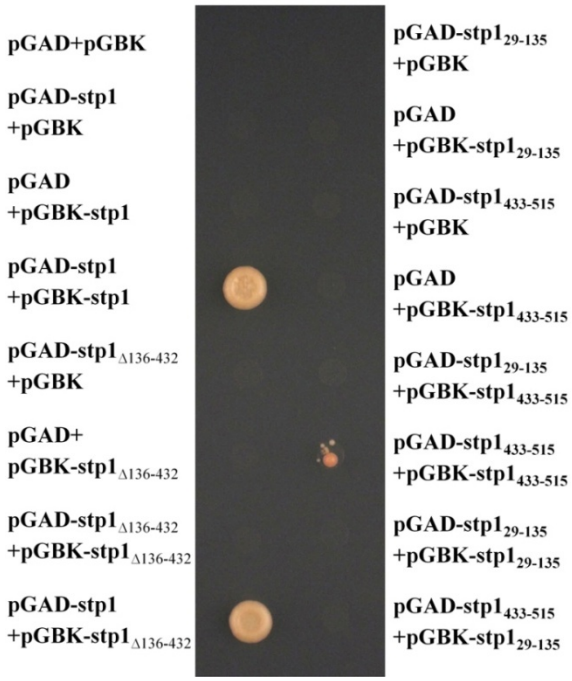

Fig. 16. Interaction between different domains of Stp1 tested by Y2H assays. The re-transformation and growth assays were performed as described in methods.

2.2.4 Stp1 can interact with several cysteine proteases of maize

One of the interaction partners of Stp1 is Sip3 encoding maize cysteine protease predicted to be secreted (Table. 1). Recently, Five distinct cysteine proteases (CP1-like A, CP1-like B (Sip3), CP2-like, XCP2 and CatB3-like) were identified from apoplastic fluid of *U.maydis* infected maize leaves (van der Linde *et al.*, 2012). The identification of Sip3 in apoplastic fluid verified that Sip3 was an extracellular cysteine protease of maize. In addition, another apoplastic maize cysteine protease, Mir3, was identified as interactor of the Tin2 effector (N. Neidig, personal communication). To determine whether Stp1$_{\Delta 136\text{-}432}$ was binding specifically to Sip3 or binding to all cysteine proteases identified, the interactions between Stp1$_{\Delta 136\text{-}432}$ and Sip3 (CP1-like B), Mir3 (CP1-like A), CP2-like, XCP2-like and CatB3-like were tested (respective prey plasmids were kindly provided by N. Neidig and A. Müller). The results showed that Stp1$_{\Delta 136\text{-}432}$ was interacting with all tested cysteine proteases with different affinity (Fig. 17). This indicated that the Stp1$_{\Delta 136\text{-}432}$ may be interacting with this class of cysteine proteases.

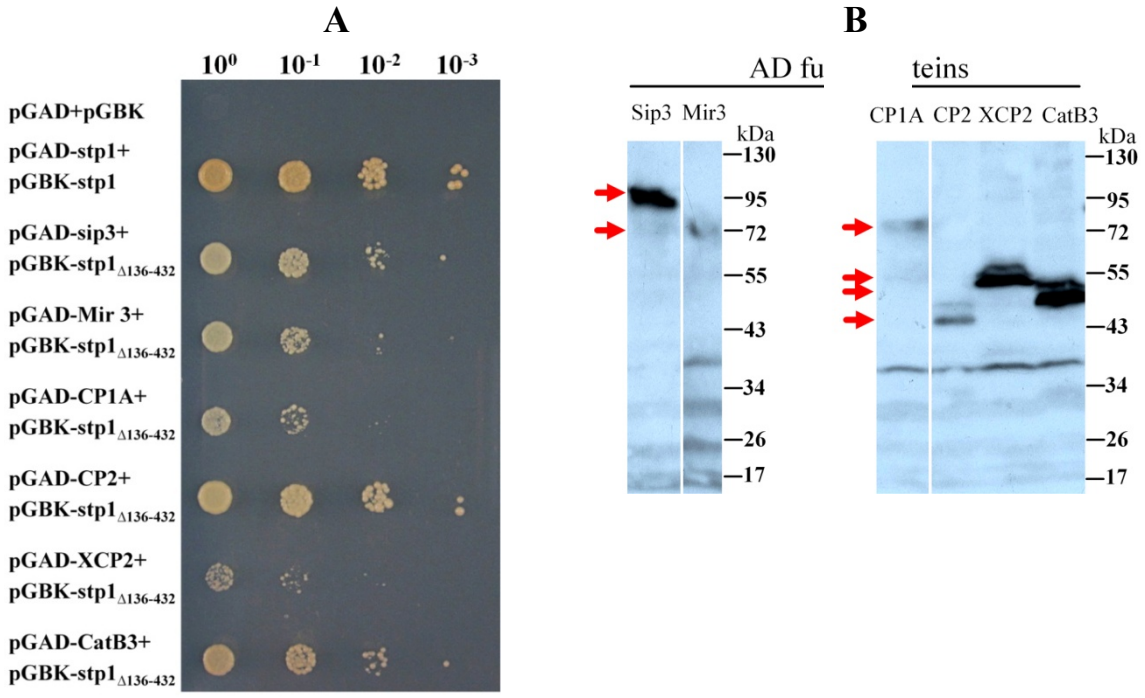

Fig. 17. Stp1$_{\Delta 136\text{-}432}$ interacts with a class of cysteine proteases. A, Interaction between Stp1$_{\Delta 136\text{-}432}$ and cysteine proteases. The re-transformation and growth assay were performed as described in methods. B, Expression of indicated proteins in yeast detected by Western blotting. BD was detected using c-Myc antibody and AD was detected using HA antibody. The red arrows denote the signals of indicated proteins (AD-Sip3: 72.7 kDa, AD-Mir3: 67.5 kDa, AD-CP1A: 56.7 kDa, AD-CP2: 44.1 kDa, AD-XCP2: 44 kDa, AD-CatB3: 47.8 kDa).

2.2.5 Comparison of the interactors with microarray data

10 interactors of Stp1 could be identified in the transcriptomes assessed by microarray (Table. 2) (Skibbe et al., 2010). When we adopt the same threshold with RNA-Seq analysis (Fold change=2, P-value=0.01, Table. 2), Sip4 and Sip17 were slightly up-regulated in seedling (1 dpi) while Sip8 and Sip17 were slightly down-regulated in adult leaves (Sip8-9 dpi, Sip 17-3 dpi) and Sip17 was obviously down-regulated in adult leaves (9 dpi). However, all the other interactors especially Sip3, Sip9, Sip16, Sip19 and Sip21 which were confirmed to interact with $Stp1_{\Delta 136-432}$ by full-length cDNA clones were not differentially expressed. In addition, full-length Sip8 was not interacting with $Stp1_{\Delta 136-432}$ while the interactions between Sip4, Sip17 and $Stp1_{\Delta 136-432}$ still need to be confirmed by cloning full-length genes. Therefore, most interactors isolated by Y2H are not differentially expressed significantly in microarray analysis.

Table. 2. Most of the inteactors isolated by Y2H are not identified among the differentially expressed genes in microarray analysis (Skibbe *et al.*, 2010)

	Adult leaf 3 dpi		Adult leaf 9 dpi		Seedling 1 dpi		Seedling 3 dpi	
	P-value	Foldch	P-value	Foldch	P-value	Foldch	P-value	Foldch
Sip3	0.168	0.80	0.004	0.58	0.926	1.02	0.046	0.71
Sip4	0.0607	0.64	0.405	1.24	0.0068	2.19	0.171	0.73
Sip8	0.00061	0.59	0.000089	0.42	0.105	1.23	0.0001	0.54
Sip9	0.484	0.95	0	1.62	0.814	0.98	0.092	0.87
Sip12	0.911	1.03	0.658	1.1	0.675	1.54	0.58	0.88
Sip14	0.312	0.81	0.67	1.09	0.025	1.66	0.245	0.78
Sip16	0.597	0.91	0.0046	0.56	0.027	1.52	0.541	0.90
Sip17	0.004	0.44	0	0.19	0.0012	2.01	0.049	0.60
Sip18	0.062	1.26	0.031	1.31	0.751	0.96	0.0002	1.74
Sip19	0.07	0.76	0.275	0.80	0.135	1.26	0.0052	0.62

Foldch: Fold change. The red fonts denote differential expression.

2.3 Purification of recombinant Stp1 protein

2.3.1 Purification of His-$Stp1_{\Delta 136-432}$

To analyze the structure of Stp1 and characterize the interaction between Stp1 and its interactors, $Stp1_{\Delta 136-432}$ was heterologously expressed in *E. coli* and purified. To this end, pRSET His TEV $Stp1_{\Delta 136-432}$ was constructed and transformed into *E. coli* BL21. Large

amounts of His-Stp1$_{\Delta 136\text{-}432}$ (24.4 kDa) could be expressed in BL21, but most of the protein was insoluble and ended up in the pellet faction (Fig. 18, Lane 2).

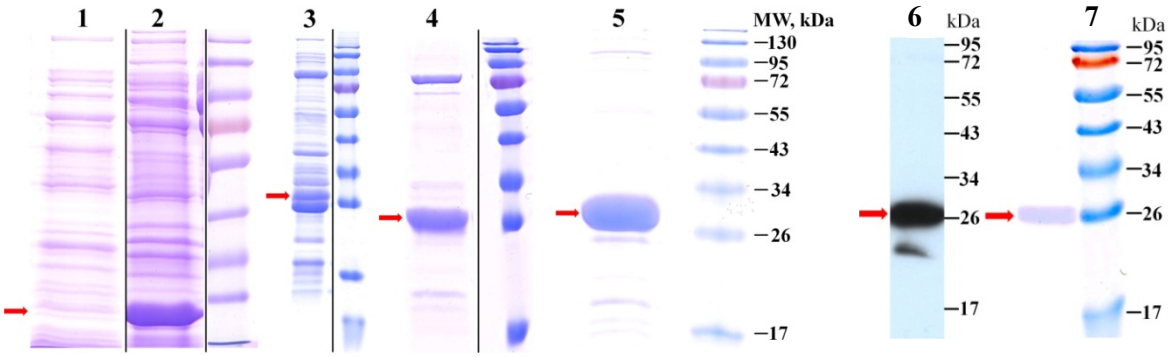

Fig. 18. Purificaiton of His- Stp1$_{\Delta 136\text{-}432}$. Lane 1, Supernatant of pRSET His TEV Stp1$_{\Delta 136\text{-}432}$; Lane 2, Pellet of pRSET His TEV Stp1$_{\Delta 136\text{-}432}$; Lane 3, His-Stp1$_{\Delta 136\text{-}432}$ purified through Ni-NTA-agarose; Lane 4, His-Stp1$_{\Delta 136\text{-}432}$ purified through MonoQ column; Lane 5, His-Stp1$_{\Delta 136\text{-}432}$ purified through Superdex 75 column; Lane 6, Western blotting after gel filtration, His-Stp1$_{\Delta 136\text{-}432}$ was detected using Stp1 antibody (Schipper, 2009); Lane 7, SDS-PAGE corresponding to the Western blotting. Pageruler: PageRuler™ Prestained Protein Ladder SM0671. The red arrows showed Stp1$_{\Delta 136\text{-}432}$. The differences in the migration rate were caused by the different concentration of SDS-PAGE gels.

To increase the amount of soluble protein, I altered the temperature, the IPTG concentration and added detergents like Triton X-100 (not shown). However, there was no significant improvement of amounts of Stp1 in the soluble fraction. To improve the solubility, SoluBL21™ strain (BioCat), Champion™ pET SUMO Expression System, GST-tag and codon optimized Stp1$_{\Delta 136\text{-}432}$ for *E. coli* (GENEART) were also tested, but again without obvious improvement. Therefore, His-Stp1$_{\Delta 136\text{-}432}$ expressed in *E. coli* BL21 was used for protein purification using Ni-NTA-agarose. After Ni-NTA-agarose purification, the abundance of His-Stp1$_{\Delta 136\text{-}432}$ was largely increased, but the purity of the protein was still low (Fig. 18, Lane 3). To improve the purification, a more specific tag, Strep-tag was fused to Stp1 and the protein was purified using Strep-Tactin Resins (IBA). Additionally, dissociation buffers containing ATP, K^+, and Mg^{2+} were also tested. However, the purity of the protein could not be improved significantly (data not shown). To purify Stp1$_{\Delta 136\text{-}432}$, I have chosen His-Stp1$_{\Delta 136\text{-}432}$ and scaled up the culture volume to at least 6 litters. The protein eluted from Ni-NTA-agarose was then applied to a MonoQ column. The purity after elution from the MonoQ column was greatly improved (Fig. 18, Lane 4). Although there were still some contaminating proteins, the protein purified from MonoQ was considered good enough for biochemical assays. However, to analyze the

structure of Stp1 by crystallography, the purity of His-Stp1$_{\Delta 136\text{-}432}$ from MonoQ needed to be improved. Thus, it was applied onto Superdex 75 column (GE Healthcare). The purity of Stp1$_{\Delta 136\text{-}432}$ after gel filtration was higher than 90 % analyzed by ImageQuant TL™ (TotalLab). After gel filtration, the bind of His-Stp1$_{\Delta 136\text{-}432}$ on SDA-PAGE (Fig. 18, Lane 5) was confirmed by Western blotting (Fig. 18, Lane 6 and 7). To get rid of His tag, His-Stp1$_{\Delta 136\text{-}432}$ was cleavage by TEV protease. The cleavage was not efficient (Fig. 19). Therefore, Stp1$_{\Delta 136\text{-}432}$ protein carry an N-terminal His-tag was used for subsequent experiments.

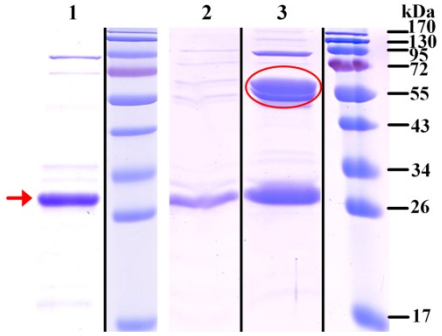

Fig. 19. The cleavage of His- Stp1$_{\Delta 136\text{-}432}$ by TEV protease decreased the homogeneity of the protein. Lane 1, His-Stp1$_{\Delta 136\text{-}432}$ purified through Superdex 75; Lane 2, Stp1$_{\Delta 136\text{-}432}$ cleavaged from Ni-NTA agarose; Lane 3, His-Stp1$_{\Delta 136\text{-}432}$ eluted from Ni-NTA agarose. Pageruler: PageRuler™ Prestained Protein Ladder SM0671. The red arrows showed His-Stp1$_{\Delta 136\text{-}432}$. The red cycle denotes TEV-protease with a HQ tag.

To analyze the purity and the confirmation features of His-Stp1$_{\Delta 136\text{-}432}$, besides SDS-PAGE visualization, gel filtration and limited proteolysis was used. Gel filtration showed that His-Stp1$_{\Delta 136\text{-}432}$ migrated in one main peak which also generated one single bind in SDS-PAGE (Fig. 20). The small peak running in front of the main peak, which is probably contaminating proteins or dimmers of His-Stp1$_{\Delta 136\text{-}432}$, could not be detected by SDS-PAGE (Fig. 20). This indicates that His-Stp1$_{\Delta 136\text{-}432}$ visualized on SDS-PAGE after gel filtration is pure protein (Fig. 18). The conformation features of His-Stp1$_{\Delta 136\text{-}432}$ were analyzed by limited proteolysis assays (Fontana *et al.*, 2004). The digestion by chymotrypsin showed that His-Stp1$_{\Delta 136\text{-}432}$ without denaturation by SDS was more resistance to protease than denatured protein (Fig. 21). In addition, the digestion of His-Stp1$_{\Delta 136\text{-}432}$ without denaturation is increasing with the increase of the concentration of chymotrypsin (Fig. 21). This indicates His-Stp1$_{\Delta 136\text{-}432}$ may have a correctly folded structure. In addition, His-Stp1$_{\Delta 136\text{-}432}$ could be concentrated to at least 20 mg per ml in low salt buffer. It could also be stored at room temperature for at least two weeks without obvious degradation (data not shown). Finally, 10 mg (measured by protein quantificaion assays according to Bradford

(Bradford, 1976)) His-Stp1$_{\Delta 136\text{-}432}$ was purified. Crystallography is in progress in collaboration with Michael Groll (TUM).

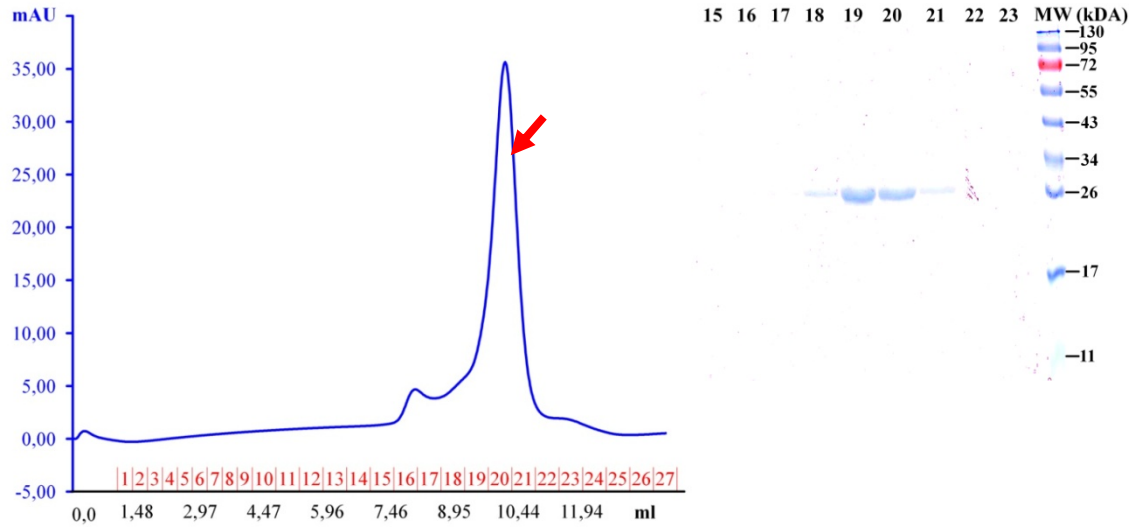

Fig. 20. Gel filtration assay of His-Stp1$_{\Delta 136\text{-}432}$. Left panel, gel filtration of His--Stp1$_{\Delta 136\text{-}432}$. Right panel, SDS-PAGE of the peaks in gel filtration. The lane numbers, 15-23 are corresponding to the fractions in the gel filtration chart. The red arrow shows the peak of His-Stp1$_{\Delta 136\text{-}432}$. X-axis, fractions and elution volume. Y-axis, UV abosrbance (mAU). Pageruler: PageRuler™ Prestained Protein Ladder SM0671.

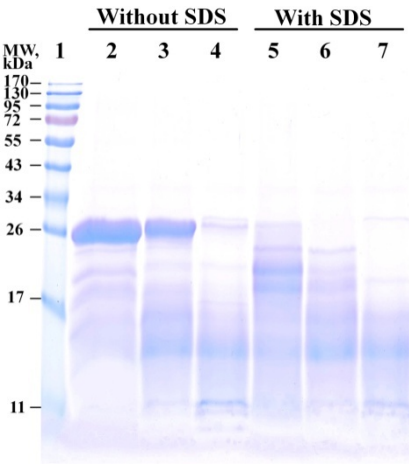

Fig. 21. Limited proteolysis assay of His-Stp1$_{\Delta 136\text{-}432}$. Lane 1, Pageruler; lane 2, His-Stp1$_{\Delta 136\text{-}432,}$ 1.6 µg/ml chymotrypsin; lane 3, His-Stp1$_{\Delta 136\text{-}432,}$ 8 µg/ml chymotrypsin; lane 4, His-Stp1$_{\Delta 136\text{-}432,}$ 40 µg/ml chymotrypsin; lane 5, His-Stp1$_{\Delta 136\text{-}432,}$ 1.6 µg/ml chymotrypsin plus 0.1 % SDS; lane 6, His-Stp1$_{\Delta 136\text{-}432,}$ 8 µg/ml chymotrypsin plus 0.1 % SDS; lane 7, His-Stp1$_{\Delta 136\text{-}432,}$ 40 µg/ml chymotrypsin plus 0.1 % SDS; His-Stp1$_{\Delta 136\text{-}432}$ was digested by different concentration of chymotrypsin for 30 min at 30 °C. Pageruler: PageRuler™ Prestained Protein Ladder SM0671.

2.3.2 Purification of His-Stp1$_{29\text{-}135}$, His-Stp1$_{433\text{-}515}$ and His-Aro7

Deletion analysis and Y2H assays suggested that N- and C-termini of Stp1 may play distinct functions during establishment of the biotrophic interaction between *U. maydis* and maize. To functionally analyze N- and C-termini of Stp1, both of them were also heterologously expressed in *E. coli*. To express N- and C-termini of Stp1, pRSET His TEV Stp1$_{29\text{-}135}$ and pRSET His TEV Stp1$_{433\text{-}515}$ were generated and transformed into *E. coli*

BL21. After induction, both His-Stp1$_{29\text{-}135}$ (14.8 kDa) and His-Stp1$_{433\text{-}515}$ (12.5 kDa) were well expressed as His-Stp$_{\Delta 136\text{-}432}$ but most of the protein was insoluble (data not shown). After optimization of expression conditions (See materials and methods), both His-Stp1$_{29\text{-}135}$ and His-Stp1$_{433\text{-}515}$ were purified employing Ni-NTA-agarose. This was followed by chromatography on a MonoQ column. The purity of His-Stp1$_{29\text{-}135}$ was still very low which precluded the following functional analysis of N-terminal domain of Stp1 (Fig. 22 B). Additionally, the purity of His-Stp1$_{29\text{-}135}$ after MonoQ purification was even lower than the purity after Ni-NTA purification which suggested that His-Stp1$_{29\text{-}135}$ was unstable (Fig. 22 A and B). His-Stp1$_{433\text{-}515}$ did not bind to the MonoQ column while most contaminating proteins remained bound to the column so that His-Stp1$_{433\text{-}515}$ could be efficiently separated from contaminant proteins. The flow through fraction of His-Stp1$_{433\text{-}515}$ from MonoQ column was collected and loaded on SDS-PAGE (Fig. 22 B). Besides Stp1 mutants, Aro7 the cytosolic chorismate mutase from *U. maydis* was also heterologously expressed and purified as a negative control. To express Aro7, pRSET His TEV Aro7 was generated and transformed into *E. coli* BL21. After Ni-NTA-agarose and MonoQ column purification, His-Aro7 was prepared for the following biochemical assays (Fig. 22 B).

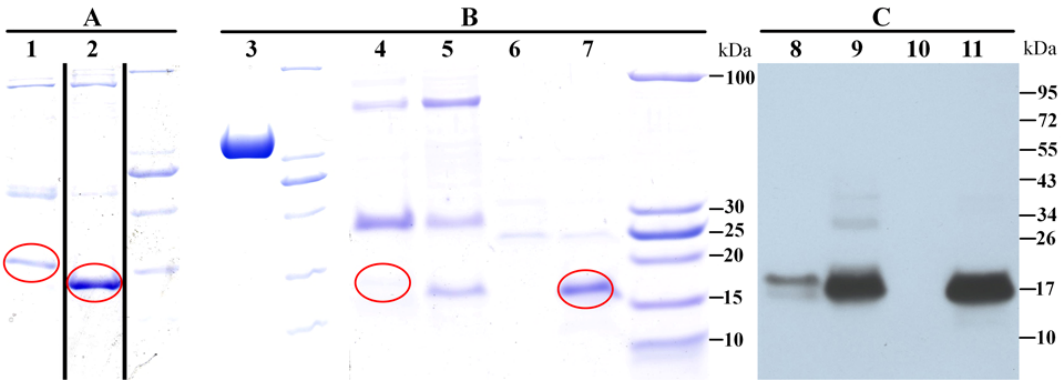

Fig. 22. Purificaiton of His-Stp1$_{29\text{-}135}$, His-Stp1$_{433\text{-}515}$ and His-Aro7. A, SDS-PAGE of His-Stp1$_{29\text{-}135}$ and His-Stp1$_{433\text{-}515}$ after Ni-NTA agarose purification. B, SDS-PAGE of His-Stp1$_{29\text{-}135}$, His-Stp1$_{433\text{-}515}$ and Aro7 after MonoQ purification. C, Western blotting of His-Stp1$_{29\text{-}135}$ and His-Stp1$_{433\text{-}515}$ after MonoQ purification. Lane 1, His-Stp1$_{29\text{-}135}$ purified by Ni-NTA agarose; Lane 2, His-Stp1$_{433\text{-}515}$ purified by Ni-NTA agarose; Lane 3, His-Aro7 purified by MonoQ; Lane 4, Main peak of His-Stp1$_{29\text{-}135}$ eluted from MonoQ column; Lane 5, Main peak of His-Stp1$_{433\text{-}515}$ eluted from MonoQ column; Lane 6, Flowthrough of Stp1$_{29\text{-}135}$ from MonoQ column; Lane 7, Flowthrough of His-Stp1$_{433\text{-}515}$ from MonoQ column; Lane 8-11 are corresponding western blotting to Lane 4-7. Pageruler, unstained Low Range Protein Ladder for A and B and PageRuler™ Prestained Protein Ladder SM0671 for C. The red cycles denote His-Stp1$_{29\text{-}135}$ and His-Stp1$_{433\text{-}515}$ on SDS-PAGE. The differences in the migration rate were caused by the different concentration of SDS-PAGE gels.

2.3.3 Purification of Strep-Sip3.

To study the interaction between Stp1 and Sip3 biochemically, $Sip3_{\Delta 351-469}$ (Sip3 without granulin domain) was heterologously expressed through agrobacterium mediated transient expression in tobacco. To express $Sip3_{\Delta 351-469}$ in tobacco, pBIN Strep $sip3_{\Delta 351-469}$ was generated, transformed into *A. tumefaciens* and the transformant was infiltrated into young leaves of *N. benthamiana*. Strep-$Sip3_{\Delta 351-469}$ was then purified employing IgG beads. The amount of Strep-$Sip3_{\Delta 351-469}$ purified from *N. benthamiana* was too low to be detected by SDS-PAGE (not shown). The enzymatic activity of Strep-$Sip3_{\Delta 351-469}$ could be detected using the fluorogenic substrate, Z-Phe-Arg-AMC (Fig. 23) which indicated that $Sip3_{\Delta 351-469}$ produced from transient expression in *N. benthamiana* could be used in the following biochemical assays.

2.4 The C-terminus of Stp1 inhibits the activity of the maize cysteine protease, Sip3

Stp1 is secreted into apoplast during biotrophic growth (Schipper, 2009) which suggests that Stp1 may influence the activity of the secreted maize cysteine protease, Sip3. Sip3 ($Sip3_{\Delta 351-469}$) was incubated with either $Stp1_{\Delta 136-432}$ or $Stp1_{433-515}$ and the protease activity was determined. E64, an irreversible inhibitor was used as positive control and Aro7 was used as negative control. $Stp1_{\Delta 136-432}$, $Stp1_{433-515}$ and E64 inhibited the activity of Sip3 while Aro7 showed little influence on the activity of Sip3 (Fig. 23). This suggested that the cysteine protease inhibitor function of Stp1 could reside in the C-terminal domain of Stp1. However, the possibility that the N-terminal domain of Stp1 may contribute to cysteine protease inhibition could not be ruled out from this assay.

To rule out the possibility that the inhibition of Sip3 was caused by substrate inhibition, $Stp1_{\Delta 136-432}$, $Stp1_{433-515}$ and Aro7 were visualized through SDS-PAGE after incubation with Sip3 using respective proteins without incubation with Sip3 as control. After 0.5 hour incubation, none of $Stp1_{\Delta 136-432}$, $Stp1_{433-515}$ and Aro7 showed obvious degradation (Fig. 24). After 24 hours incubation, no obvious degradation was observed for $Stp1_{\Delta 136-432}$ and Aro7, but $Stp1_{433-515}$ was heavily degraded (Fig. 24). However, the degradation of the control protein ($Stp1_{433-515}$ without incubation with Sip3) was even heavier than $Stp1_{433-515}$ incubated with Sip3 (Fig. 24). This suggested that $Stp1_{433-515}$ was not degraded by Sip3 and

Sip3 might stabilize Stp1$_{433-515}$. These results indicated that neither Stp1$_{\Delta136-432}$ nor Stp1$_{433-515}$ was the substrate of Sip3. In addition, without incubation with Sip3, Stp1$_{433-515}$ was heavily degraded while Stp1$_{\Delta136-432}$ was stable after 24 hours (Fig. 24). This suggests that N-terminus of Stp1 may be essential for the stability of C-terminus of Stp1.

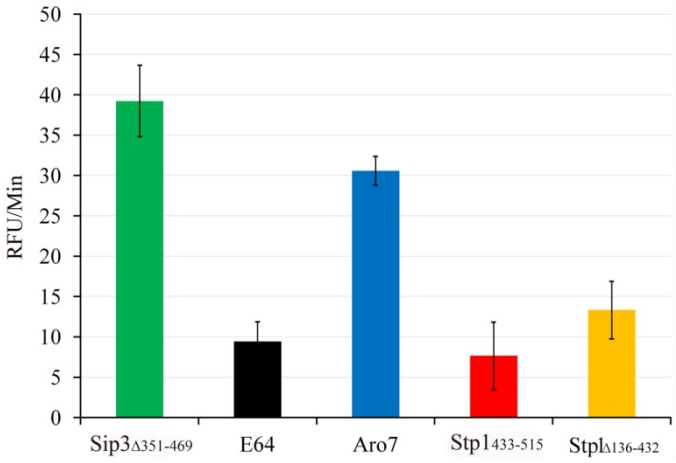

Fig. 23. Stp1 inhibits the activity of Sip3. 10 µM of cysteine protease inhibitor either proteins or E64 was used in the assay. The result was average of three repeats.

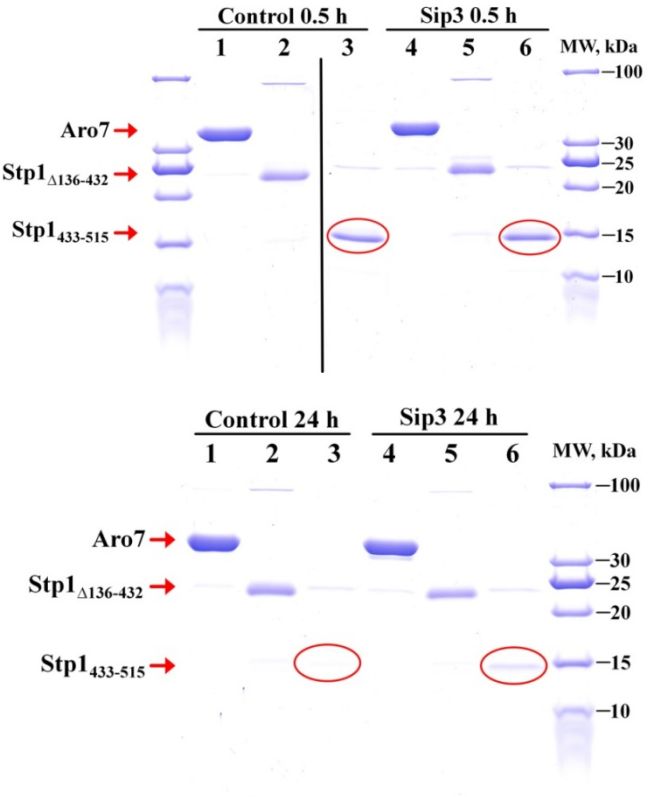

Fig. 24. None of Stp1$_{\Delta136-432}$, Stp1$_{433-515}$ and Aro7 was degraded by Sip3. Upper panel, SDS visualization of Stp1$_{\Delta136-432}$, Stp1$_{433-515}$ and Aro7 which were incubated with Sip3 for 0.5 hour. Lower panel, SDS visualization of Stp1$_{\Delta136-432}$, Stp1$_{433-515}$ and Aro7 which were incubated with Sip3 for 24 hours. Lane 1, His-Aro7 without incubation with Sip3; Lane 2, His-Stp1$_{\Delta136-432}$ without incubation with Sip3; Lane 3, His-Stp1$_{433-515}$ without incubation with Sip3; Lane 4, His-Aro7 incubated with Strep-Sip3; Lane 5, His-Stp1$_{\Delta136-432}$ incubated with Strep-Sip3; Lane 6, His-Stp1$_{433-515}$ incubated with Strep-Sip3; Pageruler, unstained Low Range Protein Ladder (Fisher Scientific). The red arrows showed His-Aro7 (36.1 kDa), His-Stp1$_{\Delta136-432}$ (24.4 kDa) and His-Stp1$_{433-515}$ (12.5 kDa). The red cycles denote His-Stp1$_{433-515}$.

2.5 Localization of Stp1 in infected plants

Transient expression through biolistic bombardment showed that Stp1 as well as C-terminal domain of Stp1 were localized in the nucleus of maize cells (Schipper, 2009). In addition,

Stp1 was secreted into apoplast during biotrophic growth (Schipper, 2009). However, translocation of Stp1 from fungal hyphae into plant cells was never visualized. To find out whether Stp1 can be translocated inside plant cells, a nuclear targeting assay using nuclear localization signal (NLS) was performed (Khang *et al.*, 2010). For this I constructed an *U. maydis* strain in which Stp1 was fused with mCherry and NLS and its expression was driven by the strong in planta induced *cmu1* promoter (Djamei et al., 2011). The plasmid p123pcmu-stp1-mcherry-HA-NLS was constructed and inserted into the *ip* locus of SG200Δstp1 to produce SG200Δstp1-stp1-mcherry-HA-NLS. As negative control, I constructed a strain SG200pcmu1-mcherry-HA-NLS expressing mCherry-HA-NLS under the *cmu1* promoter fused to the signal peptide of Stp1. Fluorescent signal of Stp1 fusion protein could be detected inside the plant nucleus (Fig. 25). However, the signal was very weak and could only be detected using high laser power.

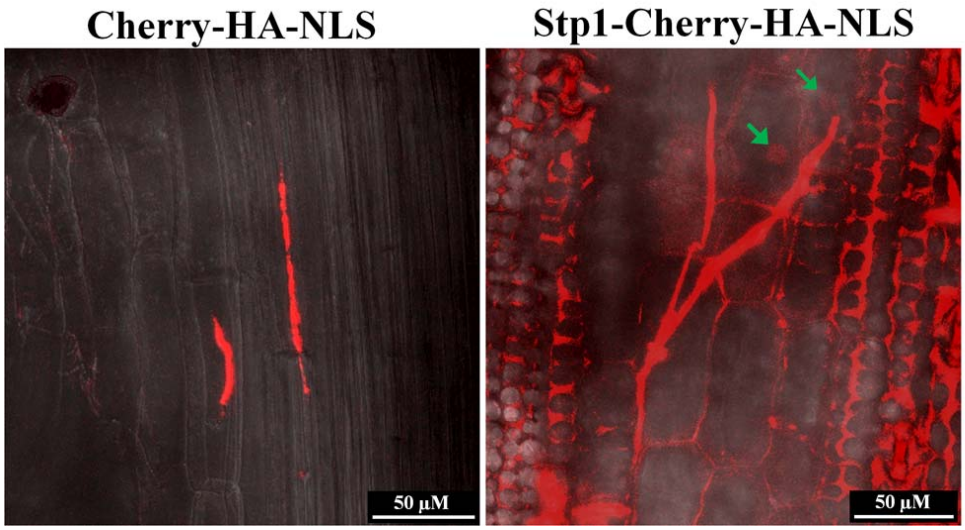

Fig. 25. Stp1-mCherry-HA-NLS may be translocated into plant cells. The maize leaves infected with SG200Δstp1-stp1-mcherry-HA-NLS and SG200pcmu1-mcherry-HA-NLS were taken three days after infection. The phenotype was observed using confocal microscopy. The figures are the overlay of bright field and mCherry channel. The green arrows show Stp1 fusion protein inside nuclei.

To substantiate the translocation of Stp1, SG200Δstp1-stp1-mcherry-HA-NLS infected maize leaves were stained using immunocytochemical techniques described by Sauer *et al.* (2006). As first antibody, a monoclonal anti-HA antibody produced in mouse (Sigma) was used, the secondary antibody was rabbit anti-mouse IgG (Life Technologies) and as third antibody, Cy3 conjugated goat anti-rabbit IgG (Millipore) was used. As negative controls,

SG200 was used to test the background of the staining method and SG200pcmu1-mcherry-HA-NLS was used as internal control. During confocal microscopy observation, beside DAPI channel for nuclear stain, Alexa fluor 633 channel was also observed as a control channel to detect autofluorescence. In SG200Δstp1-stp1-mcherry-HA-NLS infected maize leaves, fluorescent signals were observed in the nucleus as well as cytosol of the plant cell close to the hyphal tip where the secretion of effectors was robust (Fig. 26). Additionally, these patchy signals of Stp1-mCherry-HA-NLS are different from the evenly distributed autofluorescence of SG200 (Fig. 26). In SG200pcmu1-mcherry-HA-NLS infected maize leaves, fluorescent signals could also be detected in the nuclei of the plant cells. However, fungal hyphae were never observed adjacent to these nuclei. Additionally, the fluorescent signals are so dispersed that many nuclei in this experiment are producing fluorescent signals (Fig. 26), which reflects unspecific signals.

2.6 Differential expression analysis of *U. maydis* infected plants by RNA-Seq

Previous experiments had suggested that the N- and C- terminal domains of Stp1 could have distinct functions. To determine if *stp1* mutants expressing either N- or C- terminus of *stp1* could trigger distinct plant responses, RNA-Seq was performed to detect differentially expressed genes of *U. maydis* infected maize leaves.

2.6.1 Sequencing and mapping of reads to the maize genome

Plant samples infected with *U. maydis* (SG200, SG200Δstp1, SG200Δstp1-stp1$_{\Delta 40\text{-}136}$ and SG200Δstp1-stp1$_{\Delta 432\text{-}515}$) were collected at 12 hpi and 24 hpi. For each sample, three independent infections were performed and plant samples were kindly collected by Karin Münch. After extraction of total RNA and depletion of rRNA, samples were subjected to Illumina sequencing by the Max-Planck Genome-Centre-Cologne (Cologne, Germany). A 436.8 million 96-base reads RNA-Seq dataset was generated from Illumina sequencing (Table. 3). The sequencing data was then mapped to the genomic sequence of maize which consists of 39,656 genes (Filtered gene set of the release 5b (http://ftp.maizesequence.org)) using Clc genomics workbench 4. 373.0 million reads (85.4% of the total reads) could be mapped to the reference and 63.8 million reads (14.6% of the total reads) containing the *U. maydis* transcriptome could not be mapped to the reference (Table. 3). Specifically,

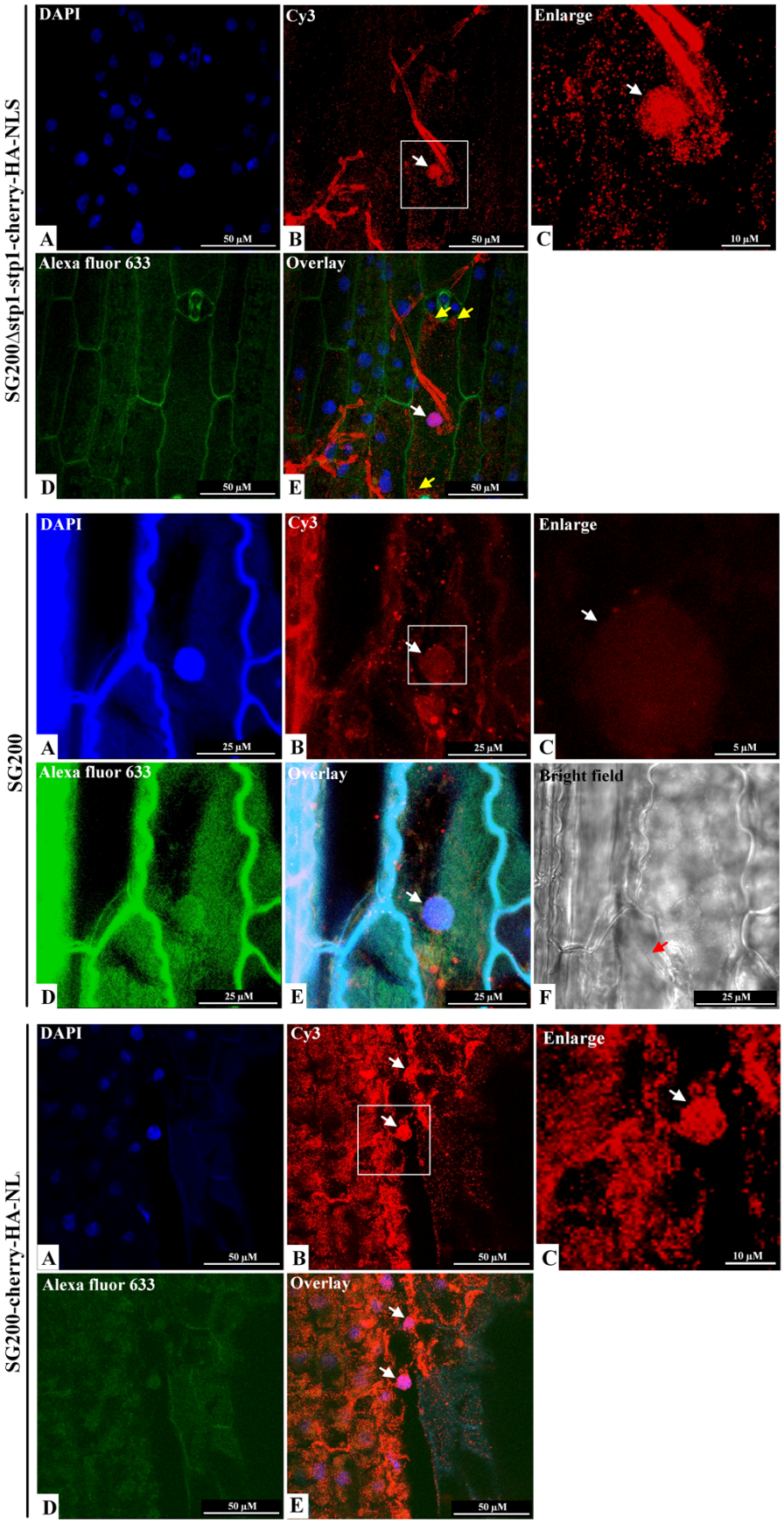
SG200Δstp1-stp1-cherry-HA-NLS
DAPI
Cy3
Enlarge
A
50 μM
B
50 μM
C
10 μM
Alexa fluor 633
Overlay
D
50 μM
E
50 μM
SG200
DAPI
Cy3
Enlarge
A
25 μM
B
25 μM
C
5 μM
Alexa fluor 633
Overlay
Bright field
D
25 μM
E
25 μM
F
25 μM
SG200-cherry-HA-NLS
DAPI
Cy3
Enlarge
A
50 μM
B
50 μM
C
10 μM
Alexa fluor 633
Overlay
D
50 μM
E
50 μM

Fig. 26. Immunostaining detected Stp1 fusion protein in the nucleus. A, DAPI channel to visualize the nucleus (blue); B, Cy3 channel to visualize Stp1-mcherry-HA-NLS signal (red); C, Enlargement of the area of white rectangular in B; D, Excitation at 633 nm as a control wavelength of autofuorescence (green); E, Merging of different channels. F, Bright field channel to visualize the hyphae of SG200. The white arrows show the nuclei. The yellow arrows denote cytosolic signals of Cy3 in SG200Δstp1-stp1-mcherry-HA-NLS infected plants. The maize leaves infected with indicated *U. maydis* strains were taken two days after infection.

26,944 to 34,268 (77.2% to 86.4% of all the genes in maize genome) distinct genes with at least one read were identified from individual samples (Table. 3).

2.6.2 Strategy for detection of differentially expressed genes

The Clc genomics workbench adopted the reads per kilobase per million mapped reads (RPKM) metric which normalizes a transcript read count by RNA length and total read number (Mortazavi *et al.*, 2008). This metric for normalization is too simple and may give rise to higher false positive rates and lower power to detect true expression differences (Robinson & Oshlack, 2010). Robinson and Smyth's EdgeR (R/Bioconductor packages, http://bioconductor.org), which is first proposed method based on negative binomial (NB) model, employs an exact test for the NB distribution based on the trimmed mean of M values (TMM) normalized data (Kvam *et al.*, 2012, Gao *et al.*, 2010). Hardcastle and Kelly's baySeq (R/Bioconductor packages, http://bioconductor.org) employs an empirical Bayesian analysis approach to detect differential expression (Hardcastle & Kelly, 2010). Multiple sample groups (more than two groups) comparison function was implemented in both methods, but this function has not yet been tested experimentally. In simulation tests, the false discovery rate of multiple sample groups comparison was considerably higher than pair-wise comparison (Hardcastle & Kelly, 2010, Robinson *et al.*, 2010). Both EdgeR and baySeq were used for pair-wise comparison of mapped genes in this study. Firstly, gene sets of SG200Δstp1, SG200Δstp1-stp1$_{\Delta 40\text{-}136}$ and SG200Δstp1-stp1$_{\Delta 432\text{-}515}$ infected plants were compared with gene sets of SG200 infected plants using both EdgeR and baySeq. Only the candidates which were classified to be differentially expressed genes by both methods were considered to be differentially expressed genes. Subsequently, the differentially expressed gene sets were compared to discover the differences between SG200Δstp1, SG200Δstp1-stp1$_{\Delta 40\text{-}136}$ and SG200Δstp1-stp1$_{\Delta 432\text{-}515}$. Meanwhile, gene ontology enrichment analysis of differentially expressed gene sets was performed to identify the enriched biological processes.

Table 3. Summary of samples mapped to reference

Samples*	Time	Total reads	Matched reads (Proportion in total reads)	Unmatched reads (Proportion in total reads)	Matched genes (Proportion in total genes)
SG200 R1	12 hpi	15056165	12938204 (85.9%)	2117961 (14.1%)	32583 (82.2%)
SG200 R2	12 hpi	16443430	13927677 (84.7%)	2515753 (15.3%)	32411 (81.7%)
SG200 R3	12 hpi	21140215	17725813 (83.8%)	3414402 (16.2%)	33090 (83.4%)
SG200Δstp1 R1	12 hpi	13261743	10732420 (80.9%)	2529323 (19.1%)	31476 (79.4%)
SG200Δstp1 R2	12 hpi	15778676	13633878 (86.4%)	2144798 (13.6%)	32196 (81.2%)
SG200Δstp1 R3	12 hpi	18178342	15349605 (84.4%)	2828737 (15.6%)	32552 (82.1%)
SG200Δstp1-stp1$_{\Delta 432\text{-}515}$ R1	12 hpi	17990021	15299374 (85.0%)	2690647 (15.0%)	33162 (83.6%)
SG200Δstp1-stp1$_{\Delta 432\text{-}515}$ R2	12 hpi	21330941	18021481 (84.5%)	3309460 (15.5%)	32620 (82.3%)
SG200Δstp1-stp1$_{\Delta 432\text{-}515}$ R3	12 hpi	20723065	17733613 (85.6%)	2989452 (14.4%)	33243 (83.8%)
SG200Δstp1-stp1$_{\Delta 40\text{-}136}$ R1	12 hpi	13037991	11311317 (86.8%)	1726674 (13.2%)	30619 (77.2%)
SG200Δstp1-stp1$_{\Delta 40\text{-}136}$ R2	12 hpi	15731348	13588764 (86.4%)	2142584 (13.6%)	31058 (78.3%)
SG200Δstp1-stp1$_{\Delta 40\text{-}136}$ R3	12 hpi	15676527	13672988 (87.2%)	2003539 (12.8%)	30346 (76.5%)
SG200 R1	24 hpi	17015081	14689755 (86.3%)	2325326 (13.7%)	31364 (79.1%)
SG200 R2	24 hpi	18827855	16527516 (87.8%)	2300339 (12.2%)	30202 (76.2%)
SG200 R3	24 hpi	20097898	17836964 (88.8%)	2260934 (11.2%)	30636 (77.3%)
SG200Δstp1 R1	24 hpi	20601786	17462086 (84.8%)	3139700 (15.2%)	32444 (81.8%)
SG200Δstp1 R2	24 hpi	18050529	15678870 (86.9%)	2371659 (13.1%)	31362 (79.1%)
SG200Δstp1 R3	24 hpi	23010721	19407234 (84.3%)	3603487 (15.7%)	32769 (82.6%)
SG200Δstp1-stp1$_{\Delta 432\text{-}515}$ R1	24 hpi	14028247	11841911 (84.4%)	2186336 (15.6%)	32170 (81.1%)
SG200Δstp1-stp1$_{\Delta 432\text{-}515}$ R2	24 hpi	15829361	13602005 (85.9%)	2227356 (14.1%)	33099 (83.5%)
SG200Δstp1-stp1$_{\Delta 432\text{-}515}$ R3	24 hpi	24880482	21017876 (84.5%)	3862606 (15.5%)	34268 (86.4%)
SG200Δstp1-stp1$_{\Delta 40\text{-}136}$ R1	24 hpi	16879123	14377147 (85.2%)	2501976 (14.8%)	33002 (83.2%)
SG200Δstp1-stp1$_{\Delta 40\text{-}136}$ R2	24 hpi	23423161	19885792 (84.9%)	3537369 (15.1%)	33381 (84.2%)
SG200Δstp1-stp1$_{\Delta 40\text{-}136}$ R3	24 hpi	19848841	16752063 (84.4%)	3096778 (15.6%)	34041 (85.8%)
Total		436841549	373014353 (85.4%)	63827196 (14.6%)	

*, The samples are maize plants infected with indicated *U. maydis* strains. R1, R2 and R3 indicate three biological replicates, corresponding to three independent infections.

2.6.3 SG200Δstp1-stp1$_{\Delta 40\text{-}136}$ triggered distinct plant responses from SG200Δstp1-stp1$_{\Delta 432\text{-}515}$

At 24 hpi, compared to SG200 infected plants, 130 genes were up-regulated and 52 genes were down-regulated in SG200Δstp1 infected plants while 78 genes were up-regulated and 48 genes were down-regulated in SG200Δstp1-stp1$_{\Delta 432\text{-}515}$ infected plants and 210 genes were up-regulated and 52 genes were down-regulated in SG200Δstp1-stp1$_{\Delta 40\text{-}136}$ infected plants. At 12 hpi, the difference between SG200 and *stp1* mutants was not as evident as for the 24 hpi time point (data not shown). Therefore, the following analysis focused on the dataset from 24 hpi. Clustering of all the differentially expressed genes in plant samples

infected with SG200Δstp1, SG200Δstp1-stp1$_{\Delta 432\text{-}515}$ and SG200Δstp1-stp1$_{\Delta 40\text{-}136}$ by transcript abundance showed that SG200Δstp1-stp1$_{\Delta 40\text{-}136}$ triggered distinct plant responses from SG200Δstp1 and SG200Δstp1-stp1$_{\Delta 432\text{-}515}$ (Fig. 27).

Comparison of differentially expressed gene sets of *stp1* mutants showed that there were 58 up-regulated genes and 30 down-regulated genes shared by plants infected with SG200Δstp1, SG200Δstp1-stp1$_{\Delta 432\text{-}515}$ and SG200Δstp1-stp1$_{\Delta 40\text{-}136}$ (Fig. 28 and Table. 4). Gene ontology enrichment analysis revealed that up-regulated genes are enriched in biological processes of cell wall organization or biogenesis, oxidation-reduction, protein modification, phosphorus metabolism, defense response to bacteria and fungi, respiratory gas exchange and nitrogen compound transport (See Supplementary Table. 2). Down-regulated genes are enriched in organic substance metabolism, small molecular metabolism, cell wall macromolecular metabolism, response to wounding and negative regulation of biosynthetic and macromolecular metabolism, etc. (See Supplementary Table. 2). The enrichment of cell wall organization or biogenesis process and protein modification process indicated the onset of a broad metabolic reprogramming of in infected tissue (Doehlemann *et al.*, 2008). Interestingly, response to wounding is down-regulated in all *stp1* mutants. During infection, SG200 proliferates profusely and may cause more damage to plants than SG200Δstp1, SG200Δstp1-stp1$_{\Delta 432\text{-}515}$ and SG200Δstp1-stp1$_{\Delta 40\text{-}136}$. Therefore, *stp1* mutants induced less plant responses to wounding than SG200.

Compared to SG200Δstp1 and SG200Δstp1-stp1$_{\Delta 432\text{-}515}$, there are 95 up-regulated genes and 6 down-regulated genes only identified in SG200Δstp1-stp1$_{\Delta 40\text{-}136}$ infected plants (Fig. 28 and Table. 5). Gene ontology enrichment analysis demonstrated that up-regulated genes are enriched in biological processes of phosphorus metabolism, cell wall organization or biogenesis, protein modification, cellular lipid metabolism, cell death and defense response to bacteria and fungi (See Supplementary Table. 2). Down-regulated genes have no enriched biological processes. There are 2 up-regulated genes and 8 down-regulated genes only identified in SG200Δstp1-stp1$_{\Delta 432\text{-}515}$ infected plants (Fig. 28 and Table. 6). Gene ontology enrichment analysis revealed that up-regulated genes have no enriched biological processes while down-regulated genes are enriched in cell wall organization or biogenesis process (See Supplementary Table. 2) which indicated metabolic reprogramming in

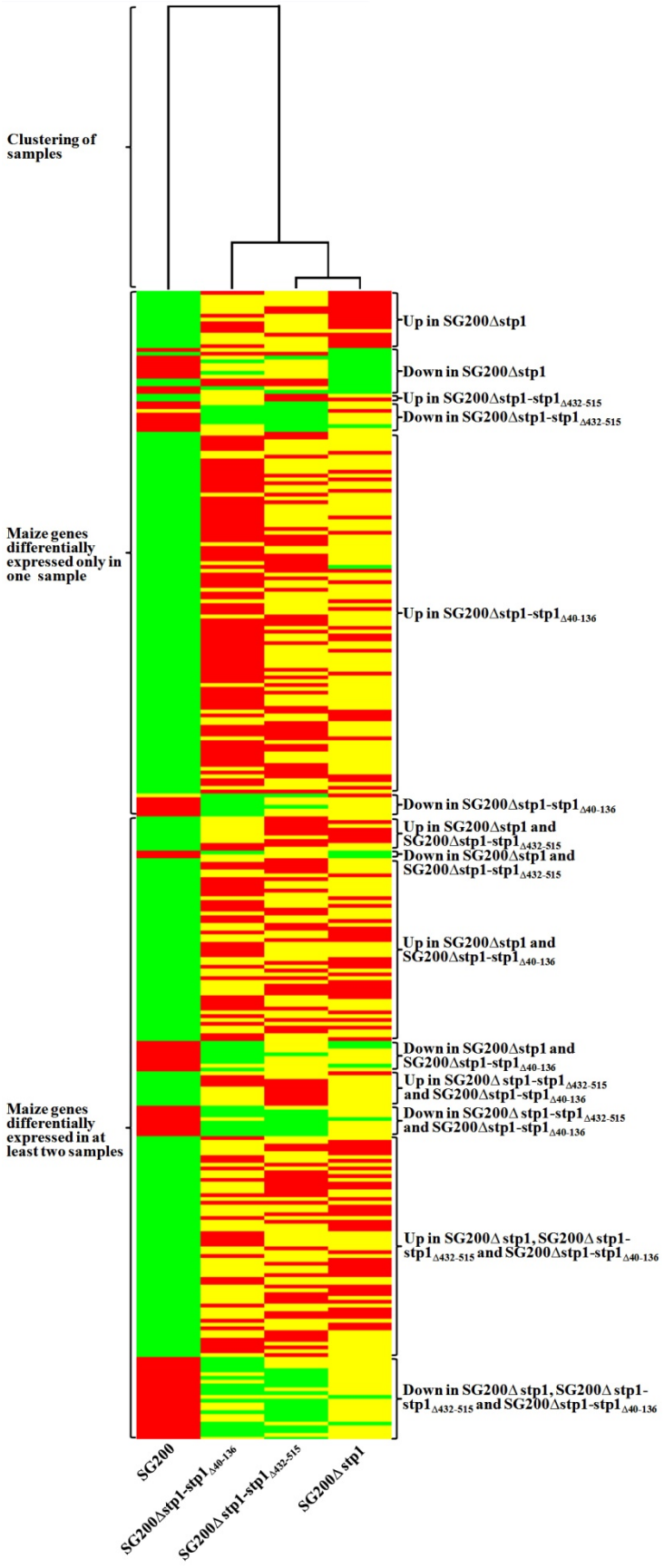

Fig. 27. SG200Δstp1-stp1$_{\Delta 40\text{-}136}$ triggered distinct plant responses from SG200Δstp1 and SG200Δstp1-stp1$_{\Delta 432\text{-}515}$. The abundance of genes from low to high is shown in colors from green to red. Different classes of maize genes differentially expressed in plants infected with indicated *U. maydis* strains are shown by the brace on the right.

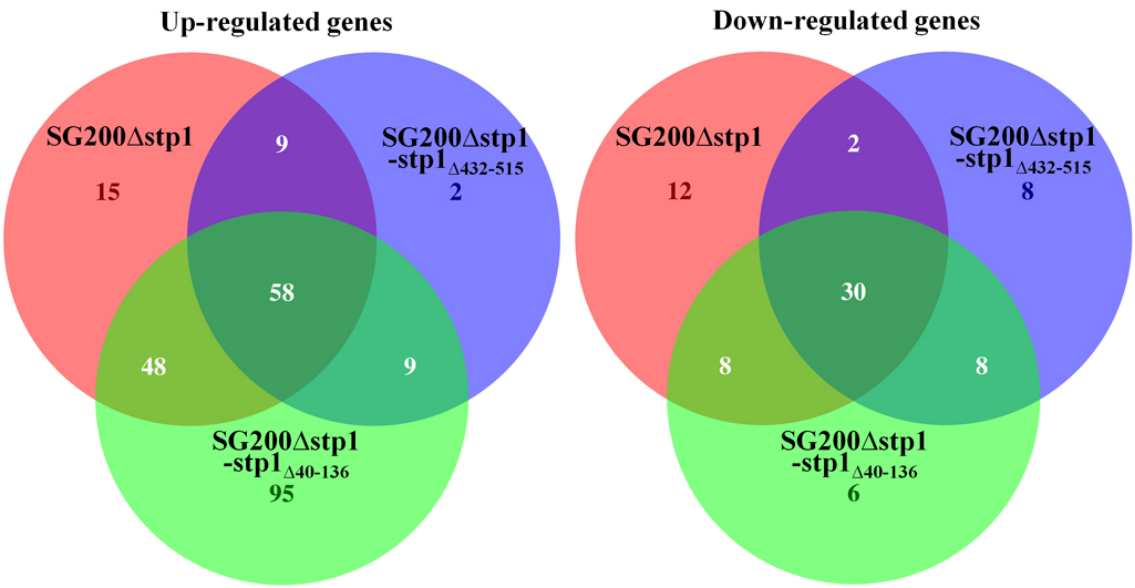

Fig. 28. Comparison of differentially expressed gene sets of plants infected with *stp1* mutants. The numbers in different areas refer to the numbers of differentially expressed genes of indicated strains.

infected tissue (Doehlemann et al., 2008). This process is also enriched in both up and down-regulated genes common to plants infected with SG200Δstp1, SG200Δstp1-stp1$_{\Delta 432\text{-}515}$ and SG200Δstp1-stp1$_{\Delta 40\text{-}136}$. There are 15 up-regulated genes and 12 down-regulated genes only identified in SG200Δstp1 infected plants (Fig. 28 and Table. 7). Gene ontology enrichment analysis showed that up-regulated genes are enriched in cell wall organization or biogenesis and phosphorus metabolic processes while down-regulated genes are enriched in negative regulation of primary metabolic, biosynthetic, and macromolecular metabolic processes (Table. 7)

There are 9 up-regulated genes and 2 down-regulated genes shared by SG200Δstp1 and SG200Δstp1-stp1$_{\Delta 432\text{-}515}$ infected plants (Fig. 28 and Table. 8). Gene ontology enrichment analysis demonstrated that phosphorus metabolism, cell wall organization or biogenesis and protein modification processes are enriched in up-regulated genes while there are no biological processes enriched in down-regulated genes (See Supplementary Table. 2). There are 48 up-regulated genes and 8 down-regulated genes shared by SG200Δstp1 and SG200Δstp1-stp1$_{\Delta 40\text{-}136}$ infected plants (Fig. 28 and Table. 9). Gene ontology enrichment analysis showed that up-regulated genes are enriched in phosphorus metabolism, protein modification, gamma-aminobutyric acid signaling pathway and anion transport processes

while there is no biological process enriched in the down-regulated genes (See Supplementary Table. 2). There are 9 up-regulated genes and 8 down-regulated genes shared by SG200Δstp1-stp1$_{\Delta 432\text{-}515}$ and SG200Δstp1-stp1$_{\Delta 40\text{-}136}$ infected plants (Fig. 28 and Table. 10). Gene ontology enrichment analysis revealed that up-regulated genes are enriched in phosphorus metabolic process while down-regulated genes are enriched in indole-containing compound metabolic process (See Supplementary Table. 2).

Table 4. Differentially expressed maize genes common to SG200Δstp1, SG200Δstp1-stp1$\Delta_{432\text{-}515}$ and SG200Δstp1-stp1$\Delta_{40\text{-}136}$ infected plants

Gene ID	GO descriptions
AC208897.3_FG004*	
GRMZM2G003970	
GRMZM2G004519	protein binding|zinc ion binding
GRMZM2G022699	
GRMZM2G026143	
GRMZM2G034611	protein kinase activity|protein serine/threonine kinase activity|ATP binding|protein amino acid phosphorylation
GRMZM2G036564	
GRMZM2G043857	
GRMZM2G056329	ATP binding
GRMZM2G063880	transcription factor activity|sequence-specific DNA binding|regulation of transcription
GRMZM2G065585	hydrolase activity, hydrolyzing O-glycosyl compounds|carbohydrate metabolic process|membrane
GRMZM2G067591	monooxygenase activity|iron ion binding|electron carrier activity|heme binding|oxidation reduction
GRMZM2G072406	
GRMZM2G074611	
GRMZM2G074743	mitochondrial envelope|respiratory gaseous exchange|oxidation reduction
GRMZM2G075884	protein kinase activity|protein serine/threonine kinase activity|binding|ATP binding|sugar binding|protein amino acid phosphorylation
GRMZM2G077914	protein kinase activity|protein serine/threonine kinase activity|ATP binding|protein amino acid phosphorylation
GRMZM2G079491	
GRMZM2G089506	aspartic-type endopeptidase activity|proteolysis
GRMZM2G099454	chitinase activity|carbohydrate metabolic process|chitin catabolic process|cell wall macromolecule catabolic process
GRMZM2G099467	iron ion binding|oxidoreductase activity|oxidation reduction
GRMZM2G113421	protein kinase activity|protein serine/threonine kinase activity|ATP binding|protein amino acid phosphorylation
GRMZM2G116629	
GRMZM2G117989	homoiothermy|defense response to bacterium|ice binding|response to freezing|defense response to fungus
GRMZM2G118800	aldehyde dehydrogenase [NAD(P)+] activity|cellular aldehyde metabolic process|metabolic process|oxidoreductase activity|oxidation reduction
GRMZM2G118809	monooxygenase activity|iron ion binding|electron carrier activity|heme binding|oxidation reduction
GRMZM2G119755	
GRMZM2G123107	hydrolase activity, hydrolyzing O-glycosyl compounds|carbohydrate metabolic process
GRMZM2G124175	oxidoreductase activity|oxidation reduction
GRMZM2G131099	
GRMZM2G135165	structural constituent of ribosome|intracellular|ribosome|translation|homoiothermy|ice binding|response to freezing
GRMZM2G145045	protein kinase activity|protein serine/threonine kinase activity|calcium ion binding|ATP binding|protein amino acid phosphorylation
GRMZM2G147752	monooxygenase activity|iron ion binding|electron carrier activity|heme binding|oxidation reduction

GRMZM2G153208	lipid metabolic process|phosphatidylglycerophosphatase activity|nutrient reservoir activity
GRMZM2G154870	monooxygenase activity|iron ion binding|electron carrier activity|heme binding|oxidation reduction
GRMZM2G160614	receptor activity|transporter activity|ion channel activity|extracellular-glutamate-gated ion channel activity|transport|ion transport|membrane|integral to membrane|substrate-specific transmembrane transporter activity|transmembrane transport
GRMZM2G160710	metal ion transport|metal ion binding
GRMZM2G161521	
GRMZM2G174449	
GRMZM2G176206	protein kinase activity|protein serine/threonine kinase activity|protein binding|ATP binding|protein amino acid phosphorylation
GRMZM2G176472	
GRMZM2G178645	nucleotide binding|ATP binding|nucleoside-triphosphatase activity
GRMZM2G180659	amino acid transport|membrane
GRMZM2G315726	integral to membrane
GRMZM2G337594	
GRMZM2G358153	hydrolase activity, hydrolyzing O-glycosyl compounds|chitinase activity|carbohydrate metabolic process|chitin catabolic process
GRMZM2G374309	protein kinase activity|protein serine/threonine kinase activity|ATP binding|protein amino acid phosphorylation
GRMZM2G402631	
GRMZM2G415529	nucleotide binding|ATP binding|membrane|ATPase activity|nucleoside-triphosphatase activity
GRMZM2G423202	
GRMZM2G426917	protein kinase activity|protein serine/threonine kinase activity|ATP binding|protein amino acid phosphorylation
GRMZM2G431039	hydrolase activity, hydrolyzing O-glycosyl compounds|carbohydrate metabolic process
GRMZM2G436448	protein kinase activity|protein serine/threonine kinase activity|ATP binding|protein amino acid phosphorylation
GRMZM2G453805	hydrolase activity, hydrolyzing O-glycosyl compounds|chitinase activity|carbohydrate metabolic process|chitin catabolic process
GRMZM2G465226	extracellular region
GRMZM2G475948	protein kinase activity|protein serine/threonine kinase activity|binding|ATP binding|protein amino acid phosphorylation
GRMZM5G868679	acid phosphatase activity|hydrolase activity|metal ion binding
GRMZM5G899851	catalytic activity|protein kinase activity|ATP binding|protein amino acid phosphorylation|electron carrier activity|oxidoreductase activity|metal ion binding|FAD binding|iron-sulfur cluster binding|oxidation reduction
AC196110.4_FG004	
AC206201.3_FG004	
GRMZM2G000326	serine-type endopeptidase inhibitor activity|response to wounding
GRMZM2G002178	monooxygenase activity|iron ion binding|electron carrier activity|heme binding
GRMZM2G005954	
GRMZM2G009232	monooxygenase activity|iron ion binding|electron carrier activity|heme binding|oxidation reduction
GRMZM2G039993	methyltransferase activity
GRMZM2G042789	serine-type endopeptidase inhibitor activity|response to wounding
GRMZM2G042895	nucleus|transcription regulator activity|regulation of transcription
GRMZM2G043336	carbon fixation|ribulose-bisphosphate carboxylase activity
GRMZM2G049211	
GRMZM2G049538	magnesium ion binding|metabolic process|lyase activity
GRMZM2G064360	chitinase activity|chitin catabolic process|chitin binding|cell wall macromolecule catabolic process
GRMZM2G094304	glutamine metabolic process|hydrolase activity
GRMZM2G096680	serine-type endopeptidase inhibitor activity|response to wounding
GRMZM2G103197	electron carrier activity|oxidoreductase activity
GRMZM2G108514	cellular amino acid and derivative metabolic process|carboxy-lyase activity|carboxylic acid metabolic process|pyridoxal phosphate binding
GRMZM2G119705	neuropeptide Y receptor activity|G-protein coupled receptor protein signaling pathway|integral to membrane|negative regulation of translation|rRNA N-glycosylase activity
GRMZM2G127336	magnesium ion binding|metabolic process|lyase activity
GRMZM2G159179	monooxygenase activity|iron ion binding|electron carrier activity|heme binding|oxidation reduction
GRMZM2G167698	monooxygenase activity|iron ion binding|electron carrier activity|heme binding|oxidation reduction

GRMZM2G174562	serine-type endopeptidase inhibitor activity|extracellular region
GRMZM2G312061	cysteine-type endopeptidase inhibitor activity
GRMZM2G329029	monooxygenase activity|iron ion binding|electron carrier activity|heme binding|oxidation reduction
GRMZM2G338160	
GRMZM2G353444	triglyceride lipase activity|lipid metabolic process
GRMZM2G359581	cysteine-type endopeptidase inhibitor activity
GRMZM2G565911	
GRMZM5G833406	lysosphingolipid and lysophosphatidic acid receptor activity|protein binding|G-protein coupled receptor protein signaling pathway|metabolic process|integral to membrane|hydrolase activity
GRMZM5G847669	serine-type endopeptidase inhibitor activity|extracellular region

*: The red font denotes up regulated genes. The black font denotes down regulated genes. See Supplementary Table. 1 for GO terms corresponding to the indicated genes. Gene ID: MaizeGDB, (Harris *et al.*, 2005)

Table 5. Differentially expressed maize genes identified only in SG200Δstp1-stp1$\Delta_{40\text{-}136}$ infected plants

Gene ID	GO descriptions
AC204515.4_FG006*	
AC214360.3_FG001	
AC225176.2_FG003	
GRMZM2G001332	
GRMZM2G005633	chitinase activity|carbohydrate metabolic process|chitin catabolic process|chitin binding|metabolic process|oxidoreductase activity|cell wall macromolecule catabolic process|oxidation reduction
GRMZM2G006894	catalytic activity|ATP binding|ATP biosynthetic process|cation transport|metabolic process|ATPase activity, coupled to transmembrane movement of ions, phosphorylative mechanism|membrane|integral to membrane|hydrolase activity, acting on acid anhydrides, catalyzing transmembrane movement of substances|ATPase activity
GRMZM2G009045	binding|transport|membrane|transmembrane transport
GRMZM2G014071	triglyceride lipase activity|lipid metabolic process
GRMZM2G014395	monooxygenase activity|iron ion binding|electron carrier activity|heme binding|oxidation reduction
GRMZM2G017164	protein kinase activity|protein serine/threonine kinase activity|ATP binding|sugar binding|protein amino acid phosphorylation
GRMZM2G018707	
GRMZM2G020508	
GRMZM2G021378	SNAP receptor activity|protein binding|intracellular protein transport|membrane|vesicle-mediated transport
GRMZM2G022972	
GRMZM2G028306	magnesium ion binding|metabolic process|lyase activity
GRMZM2G028713	nucleotide binding|protein binding|ATP binding|apoptosis|defense response|nucleoside-triphosphatase activity
GRMZM2G032602	nucleotide binding|protein binding|ATP binding|apoptosis|defense response|nucleoside-triphosphatase activity
GRMZM2G037209	
GRMZM2G039362	
GRMZM2G039639	
GRMZM2G044481	magnesium ion binding|metabolic process|lyase activity
GRMZM2G051921	chitinase activity|carbohydrate metabolic process|chitin catabolic process|chitin binding|cell wall macromolecule catabolic process
GRMZM2G052266	oxidoreductase activity
GRMZM2G059496	
GRMZM2G059740	protein kinase activity|protein serine/threonine kinase activity|ATP binding|protein amino acid phosphorylation
GRMZM2G064603	nucleotide binding|ATP binding|membrane|phosphotransferase activity, alcohol group as acceptor|ATPase activity|nucleoside-triphosphatase activity|homoiothermy|ice binding|response to freezing
GRMZM2G065655	protein kinase activity|protein serine/threonine kinase activity|ATP binding|protein amino acid phosphorylation
GRMZM2G069335	
GRMZM2G071436	
GRMZM2G072529	iron ion binding|oxidoreductase activity|oxidation reduction

GRMZM2G076394	
GRMZM2G080103	
GRMZM2G081127	DNA binding|nucleus
GRMZM2G082199	
GRMZM2G085974	
GRMZM2G086869	catalytic activity|metabolic process|hydrolase activity
GRMZM2G088819	calcium ion binding
GRMZM2G097706	metabolic process|oxidoreductase activity|oxidation reduction
GRMZM2G100475	
GRMZM2G101405	transcription factor activity|sequence-specific DNA binding|regulation of transcription
GRMZM2G106177	integral to membrane
GRMZM2G109056	iron ion binding|lipoxygenase activity|oxidoreductase activity, acting on single donors with incorporation of molecular oxygen, incorporation of two atoms of oxygen|metal ion binding|oxidation reduction
GRMZM2G113512	protein kinase activity|protein serine/threonine kinase activity|ATP binding|protein amino acid phosphorylation
GRMZM2G117942	defense response to bacterium|defense response to fungus
GRMZM2G117971	defense response to bacterium|defense response to fungus
GRMZM2G123119	DNA binding|transcription factor activity|regulation of transcription, DNA-dependent
GRMZM2G125762	protein kinase activity|protein serine/threonine kinase activity|ATP binding|protein amino acid phosphorylation
GRMZM2G125775	zinc ion binding
GRMZM2G126261	peroxidase activity|response to oxidative stress|heme binding|nutrient reservoir activity|oxidation reduction
GRMZM2G129189	chitinase activity|carbohydrate metabolic process|chitin catabolic process|chitin binding|cell wall macromolecule catabolic process
GRMZM2G129860	monooxygenase activity|iron ion binding|electron carrier activity|heme binding|oxidation reduction
GRMZM2G133430	
GRMZM2G135385	heme binding
GRMZM2G148087	transcription factor activity|sequence-specific DNA binding|regulation of transcription
GRMZM2G148904	metabolic process|methyltransferase activity
GRMZM2G151204	ubiquitin ligase complex|ubiquitin-protein ligase activity|binding|protein ubiquitination
GRMZM2G152739	triglyceride lipase activity|lipid metabolic process|oxidoreductase activity
GRMZM2G157218	
GRMZM2G158045	protein kinase activity|protein serine/threonine kinase activity|ATP binding|protein amino acid phosphorylation
GRMZM2G160739	nutrient reservoir activity
GRMZM2G162829	nucleic acid binding|endonuclease activity|protein kinase activity|protein serine/threonine kinase activity|protein binding|ATP binding|extrachromosomal circular DNA|protein amino acid phosphorylation|pathogenesis
GRMZM2G163054	transcription factor activity|sequence-specific DNA binding|regulation of transcription
GRMZM2G163307	
GRMZM2G164640	
GRMZM2G171400	
GRMZM2G173536	
GRMZM2G177883	protein kinase activity|protein serine/threonine kinase activity|protein binding|ATP binding|protein amino acid phosphorylation
GRMZM2G180080	nucleotide binding|ATP binding|nucleoside-triphosphatase activity
GRMZM2G181227	lysozyme activity|catalytic activity|metabolic process|cell wall macromolecule catabolic process
GRMZM2G314396	protein kinase activity|protein serine/threonine kinase activity|calcium ion binding|ATP binding|protein amino acid phosphorylation
GRMZM2G329002	
GRMZM2G333448	intracellular signaling pathway
GRMZM2G334181	
GRMZM2G334336	metabolic process|transferase activity, transferring hexosyl groups
GRMZM2G341499	G-protein coupled receptor activity|GABA-B receptor activity|ionotropic glutamate receptor activity|transporter activity|extracellular-glutamate-gated ion channel activity|transport|G-protein coupled receptor protein signaling pathway|membrane|integral to membrane|outer membrane-bounded periplasmic space
GRMZM2G372068	metabolic process|transferase activity, transferring hexosyl groups
GRMZM2G374827	catalytic activity|glucosylceramidase activity|sphingolipid metabolic process|glucosylceramide catabolic process|membrane|integral to membrane|homoiothermy|ice binding|response to freezing

GRMZM2G400470	protein kinase activity|protein serine/threonine kinase activity|ATP binding|protein amino acid phosphorylation
GRMZM2G410991	cell wall macromolecule catabolic process
GRMZM2G414252	nucleus|transcription regulator activity|regulation of transcription
GRMZM2G416632	glutathione transferase activity|cytoplasm|metabolic process
GRMZM2G433076	protein kinase activity|protein serine/threonine kinase activity|calcium ion binding|ATP binding|protein amino acid phosphorylation
GRMZM2G434363	protein kinase activity|protein serine/threonine kinase activity|ATP binding|protein amino acid phosphorylation
GRMZM2G439578	hydrolase activity|hydrolase activity, acting on carbon-nitrogen (but not peptide) bonds
GRMZM2G443843	protein kinase activity|protein serine/threonine kinase activity|binding|ATP binding|protein amino acid phosphorylation
GRMZM2G452121	protein kinase activity|protein serine/threonine kinase activity|binding|ATP binding|protein amino acid phosphorylation
GRMZM2G459663	calcium ion binding|homoiothermy|ice binding|response to freezing
GRMZM2G464157	hydrolase activity
GRMZM2G474546	protein kinase activity|protein serine/threonine kinase activity|ATP binding|protein amino acid phosphorylation
GRMZM2G493395	catalytic activity|metabolic process|1-deoxy-D-xylulose-5-phosphate synthase activity|terpenoid biosynthetic process
GRMZM5G838907	
GRMZM5G841893	monooxygenase activity|potassium ion transport|metabolic process|cation transmembrane transporter activity|oxidoreductase activity|oxidation reduction
GRMZM5G849600	galanin receptor activity|nucleus|G-protein coupled receptor protein signaling pathway|integral to membrane|transcription regulator activity|regulation of transcription
GRMZM5G863420	transcription factor activity|homoiothermy|sequence-specific DNA binding|regulation of transcription|ice binding|response to freezing
GRMZM5G892675	nucleotide binding|ATP binding|membrane|ATPase activity|nucleoside-triphosphatase activity
GRMZM2G012160	cysteine-type endopeptidase inhibitor activity
GRMZM2G075456	
GRMZM2G109252	
GRMZM2G111954	oxidoreductase activity|oxidation reduction
GRMZM2G470882	
GRMZM5G844309	

*: The red font denotes up regulated genes. The black font denotes down regulated genes. See Supplementary Table. 1 for GO terms corresponding to the indicated genes. Gene ID: MaizeGDB, (Harris et al., 2005)

Table 6. Differentially expressed maize genes identified only in SG200Δstp1-stp1$\Delta_{432\text{-}515}$ infected plants

Gene ID	GO descriptions
GRMZM2G011160*	
GRMZM2G422045	inositol or phosphatidylinositol phosphatase activity
GRMZM2G059693	triglyceride lipase activity|lipid metabolic process
GRMZM2G097297	methyltransferase activity|O-methyltransferase activity|protein dimerization activity
GRMZM2G109130	iron ion binding|lipoxygenase activity|oxidoreductase activity, acting on single donors with incorporation of molecular oxygen, incorporation of two atoms of oxygen|metal ion binding|oxidation reduction
GRMZM2G161905	
GRMZM2G165192	transferase activity, transferring acyl groups other than amino-acyl groups
GRMZM2G320117	
GRMZM2G389582	chitinase activity|chitin catabolic process|cell wall macromolecule catabolic process
GRMZM2G436020	

*: The red font denotes up regulated genes. The black font denotes down regulated genes. See Supplementary Table. 1 for GO terms corresponding to the indicated genes. Gene ID: MaizeGDB, (Harris et al., 2005)

Table 7. Differentially expressed maize genes identified only in SG200Δstp1 infected plants

Gene ID	GO descriptions
AC231745.1_FG003*	
GRMZM2G047791	
GRMZM2G056875	protein kinase activity|protein serine/threonine kinase activity|ATP binding|protein amino acid phosphorylation
GRMZM2G062974	chitinase activity|carbohydrate metabolic process|chitin catabolic process|chitin binding|cell wall macromolecule catabolic process
GRMZM2G092718	chromatin|DNA binding|nucleus|metal ion transport|metal ion binding
GRMZM2G096090	
GRMZM2G098102	cysteine-type endopeptidase activity|proteolysis|cysteine-type peptidase activity
GRMZM2G120016	metabolic process|transferase activity, transferring hexosyl groups
GRMZM2G136372	
GRMZM2G145461	chitinase activity|chitin catabolic process|chitin binding|cell wall macromolecule catabolic process
GRMZM2G154828	monooxygenase activity|iron ion binding|electron carrier activity|heme binding|oxidation reduction
GRMZM2G163494	
GRMZM2G313104	homoiothermy|ice binding|response to freezing
GRMZM2G427815	peroxidase activity|response to oxidative stress|heme binding|oxidation reduction
GRMZM2G449817	protein kinase activity|protein serine/threonine kinase activity|protein binding|ATP binding|protein amino acid phosphorylation
GRMZM2G006937	catalytic activity|intramolecular transferase activity
GRMZM2G047713	negative regulation of translation|rRNA N-glycosylase activity
GRMZM2G069736	
GRMZM2G071023	NAD+ kinase activity|metabolic process
GRMZM2G156861	iron ion binding|lipoxygenase activity|oxidoreductase activity, acting on single donors with incorporation of molecular oxygen, incorporation of two atoms of oxygen|metal ion binding|oxidation reduction
GRMZM2G158316	
GRMZM2G160990	dopamine receptor activity|G-protein coupled receptor protein signaling pathway|integral to membrane
GRMZM2G173596	
GRMZM2G173809	negative regulation of translation|rRNA N-glycosylase activity
GRMZM2G337387	
GRMZM2G528190	
GRMZM5G815098	serine-type endopeptidase inhibitor activity|extracellular region

*: The red font denotes up regulated genes. The black font denotes down regulated genes. See Supplementary Table. 1 for GO terms corresponding to the indicated genes. Gene ID: MaizeGDB, (Harris et al., 2005)

Table 8. Differentially expressed maize genes common to SG200Δstp1 and SG200Δstp1-stp1$\Delta_{432\text{-}515}$ infected plants

Gene ID	GO descriptions
GRMZM2G023827*	
GRMZM2G024024	protein kinase activity|protein serine/threonine kinase activity|ATP binding|protein amino acid phosphorylation|cell wall macromolecule catabolic process
GRMZM2G059214	protein kinase activity|protein serine/threonine kinase activity|protein binding|ATP binding|protein amino acid phosphorylation
GRMZM2G095126	hydrolase activity, hydrolyzing O-glycosyl compounds|protein binding|carbohydrate metabolic process|dicarboxylic acid transport|membrane|sodium:dicarboxylate symporter activity
GRMZM2G126975	extracellular region
GRMZM2G159908	protein kinase activity|protein serine/threonine kinase activity|ATP binding|protein amino acid phosphorylation
GRMZM2G177991	
GRMZM2G178753	protein kinase activity|protein serine/threonine kinase activity|protein binding|ATP binding|protein amino acid phosphorylation|phosphopantetheine binding

GRMZM2G316474	protein kinase activity|protein serine/threonine kinase activity|ATP binding|protein amino acid phosphorylation
GRMZM2G038153	magnesium ion binding|metabolic process|lyase activity
GRMZM2G371793	acid phosphatase activity

*: The red font denotes up regulated genes. The black font denotes down regulated genes. See Supplementary Table. 1 for GO terms corresponding to the indicated genes. Gene ID: MaizeGDB, (Harris et al., 2005)

Table 9. Differentially expressed maize genes common to SG200Δstp1 and SG200Δstp1-stp1$\Delta_{40\text{-}136}$ infected plants

Gene ID	GO descriptions
AC205012.3_FG002*	
AC214817.3_FG007	
GRMZM2G007477	protein kinase activity|protein serine/threonine kinase activity|ATP binding|protein amino acid phosphorylation
GRMZM2G026189	GTPase activity|ATP binding|GTP binding|apoptosis|protein complex|protein polymerization
GRMZM2G026203	protein kinase activity|protein serine/threonine kinase activity|ATP binding|protein amino acid phosphorylation
GRMZM2G032910	catalytic activity|aminopeptidase activity|proteolysis
GRMZM2G041356	catalytic activity|carbohydrate metabolic process|isomerase activity|carbohydrate binding
GRMZM2G050514	glutamate-ammonia ligase activity|phosphoglycerate kinase activity|glycolysis|glutamine biosynthetic process|nitrogen compound metabolic process
GRMZM2G057963	hydrolase activity
GRMZM2G061723	
GRMZM2G062600	hydrolase activity, hydrolyzing O-glycosyl compounds|carbohydrate metabolic process
GRMZM2G065696	
GRMZM2G077197	DNA binding|DNA topoisomerase (ATP-hydrolyzing) activity|protein binding|ATP binding|DNA topological change
GRMZM2G079219	protein kinase activity|protein serine/threonine kinase activity|ATP binding|protein amino acid phosphorylation
GRMZM2G079436	
GRMZM2G093072	protein kinase activity|protein serine/threonine kinase activity|ATP binding|protein amino acid phosphorylation
GRMZM2G098346	zinc ion binding|oxidoreductase activity|oxidation reduction
GRMZM2G104125	protein kinase activity|protein serine/threonine kinase activity|calcium ion binding|ATP binding|protein amino acid phosphorylation
GRMZM2G111657	exocyst|exocytosis
GRMZM2G112222	
GRMZM2G112456	transmembrane transport
GRMZM2G122654	monooxygenase activity|iron ion binding|electron carrier activity|heme binding|oxidation reduction
GRMZM2G124759	triglyceride lipase activity|lipid metabolic process
GRMZM2G126749	
GRMZM2G138770	nucleotide binding|ATP binding|nucleoside-triphosphatase activity
GRMZM2G140231	protein kinase activity|protein serine/threonine kinase activity|ATP binding|protein amino acid phosphorylation
GRMZM2G140721	protein kinase activity|protein serine/threonine kinase activity|ATP binding|protein amino acid phosphorylation
GRMZM2G140752	protein kinase activity|protein serine/threonine kinase activity|GABA-A receptor activity|ATP binding|protein amino acid phosphorylation|chloride transport|gamma-aminobutyric acid signaling pathway|integral to membrane
GRMZM2G145109	protein kinase activity|protein serine/threonine kinase activity|calcium ion binding|ATP binding|protein amino acid phosphorylation
GRMZM2G146108	
GRMZM2G151230	
GRMZM2G165987	
GRMZM2G175140	transport|ammonium transmembrane transporter activity|membrane|transmembrane transport
GRMZM2G175593	nucleotide binding|ATP binding|nucleoside-triphosphatase activity
GRMZM2G304897	protein kinase activity|protein serine/threonine kinase activity|calcium ion binding|ATP binding|sugar binding|protein amino acid phosphorylation
GRMZM2G326707	transporter activity|inorganic phosphate transmembrane transporter activity|transport|phosphate transport|integral to membrane|transmembrane transport

GRMZM2G355233	protein kinase activity|protein serine/threonine kinase activity|calcium ion binding|ATP binding|protein amino acid phosphorylation
GRMZM2G361256	nucleotide binding|ATP binding|transport|integral to membrane|ATPase activity|nucleoside-triphosphatase activity|ATPase activity, coupled to transmembrane movement of substances|transmembrane transport
GRMZM2G402977	
GRMZM2G431288	monooxygenase activity|iron ion binding|electron carrier activity|heme binding|oxidation reduction
GRMZM2G443829	protein kinase activity|protein serine/threonine kinase activity|binding|ATP binding|protein amino acid phosphorylation
GRMZM2G444560	nucleotide binding|ATP binding|nucleoside-triphosphatase activity
GRMZM2G452896	proteolysis|serine-type peptidase activity
GRMZM2G458095	nucleotide binding|ATP binding|nucleoside-triphosphatase activity
GRMZM2G472655	protein kinase activity|protein serine/threonine kinase activity|ATP binding|sugar binding|protein amino acid phosphorylation|G-protein coupled receptor protein signaling pathway|integral to membrane
GRMZM2G496370	protein kinase activity|protein serine/threonine kinase activity|ATP binding|protein amino acid phosphorylation
GRMZM5G879872	metal ion transport|metal ion binding
GRMZM5G897005	protein kinase activity|protein serine/threonine kinase activity|ATP binding|protein amino acid phosphorylation
GRMZM2G058149	triglyceride lipase activity|lipid metabolic process
GRMZM2G099678	
GRMZM2G110567	
GRMZM2G116614	
GRMZM2G118610	zinc ion binding|oxidoreductase activity|oxidation reduction
GRMZM2G136453	acid phosphatase activity|hydrolase activity|metal ion binding
GRMZM2G138710	
GRMZM2G496991	

*: The red font denotes up regulated genes. The black font denotes down regulated genes. See Supplementary Table. 1 for GO terms corresponding to the indicated genes. Gene ID: MaizeGDB, (Harris et al., 2005)

Table 10. Differentially expressed maize genes common to SG200Δstp1-stp1$\Delta_{432\text{-}515}$ and SG200Δstp1-stp1$\Delta_{40\text{-}136}$ infected plants

Gene ID	GO descriptions
GRMZM2G003411*	nucleotide binding|ATP binding|membrane|ATPase activity|nucleoside-triphosphatase activity
GRMZM2G055883	GTPase activity|GTP binding
GRMZM2G057116	transcription factor activity|sequence-specific DNA binding|regulation of transcription
GRMZM2G070312	
GRMZM2G109830	protein kinase activity|protein serine/threonine kinase activity|protein binding|ATP binding|protein amino acid phosphorylation
GRMZM2G117454	
GRMZM2G145075	protein kinase activity|protein serine/threonine kinase activity|calcium ion binding|ATP binding|protein amino acid phosphorylation
GRMZM5G846916	hydrolase activity, hydrolyzing O-glycosyl compounds|carbohydrate metabolic process
GRMZM5G893912	nucleotide binding|ATP binding|nucleoside-triphosphatase activity
GRMZM2G015892	catalytic activity|tryptophan synthase activity|tryptophan metabolic process|metabolic process
GRMZM2G036262	
GRMZM2G049695	nucleic acid binding|DNA binding|zinc ion binding|homoiothermy|ice binding|response to freezing
GRMZM2G079616	transferase activity, transferring acyl groups other than amino-acyl groups
GRMZM2G091540	protein binding|metabolic process|membrane|hydrolase activity|protein homooligomerization
GRMZM2G304474	
GRMZM2G389557	DNA binding|type I hypersensitivity|regulation of transcription
GRMZM2G700208	lipid metabolic process|hydrolase activity, acting on ester bonds

*: The red font denotes up regulated genes. The black font denotes down regulated genes. See Supplementary Table. 1 for GO terms corresponding to the indicated genes. Gene ID: MaizeGDB, (Harris et al., 2005)

The differentially regulated genes identified by RNA-Seq were compared with 37 genes involved in early defense response which were induced at 12 hpi in plants infected with SG200 but down-regulated at 24 hpi (Doehlemann et al., 2008). Among 37 early defense response genes, 22 were also identified by RNA-Seq analysis in plants infected with SG200Δstp1, SG200Δstp1-stp1$_{\Delta 432\text{-}515}$ and SG200Δstp1-stp1$_{\Delta 40\text{-}136}$ (Table. 11). 9 early defense response genes are common to plants infected with SG200Δstp1, SG200Δstp1-stp1$_{\Delta 432\text{-}515}$ and SG200Δstp1-stp1$_{\Delta 40\text{-}136}$ (Table. 11) indicating the plant defense response triggered by these strains. 7 genes are only identified in plants infected with SG200Δstp1-stp1$_{\Delta 40\text{-}136}$ (Table. 11) which indicated that SG200Δstp1 expressing C-terminus of Stp1 triggered stronger plant defense response than SG200Δstp1. 6 genes are identified only in plants infected with SG200Δstp1 or common to plants infected with SG200Δstp1 and SG200Δstp1-stp1$_{\Delta 432\text{-}515}$ but are absent in plants infected with SG200Δstp1-stp1$_{\Delta 40\text{-}136}$ (Table. 11) which indicated that SG200Δstp1 expressing N-terminus of Stp1 induce less plant defense response than SG200Δstp1.

Table 11. Differentially expressed maize genes involved in early plant defense response

Gene ID	Annotations	common to SG200Δstp1, SG200Δstp1-stp1$_{\Delta 432\text{-}515}$ and SG200Δstp1-stp1$_{\Delta 40\text{-}136}$	common to SG200Δstp1, and SG200Δstp1-stp1$_{\Delta 40\text{-}136}$	Only in SG200Δstp1-stp1$_{\Delta 40\text{-}136}$	Only in SG200Δstp1
GRMZM2G065585	1,3-β-glucanase	√			
GRMZM2G135385	Cytochrome b5			√	
GRMZM2G415529	ATPase activity	√			
GRMZM2G145461	chitinase activity				√
GRMZM2G067591	Cytochrome P450	√			
GRMZM2G118800	aldehyde dehydrogenase	√			
GRMZM2G065696	Nuclease sbcCD subunit		√		
GRMZM2G117989	Win1	√			
GRMZM2G092718	late blight resistance				√
GRMZM2G106177	Ergosterol biosynthetic protein			√	
GRMZM2G402977	Hypothetical protein		√		
GRMZM2G117971	Barwin like proteins			√	
GRMZM2G003970	hypothetical protein	√			
GRMZM2G109056	lipoxygenase			√	
GRMZM2G131099	hypothetical protein	√			
GRMZM2G044481	Copalyl Diphosphate Synthase			√	
GRMZM2G161521	hypothetical protein	√			

GRMZM2G026143	WIR1A protein	√			
GRMZM2G416632	glutathione transferase activity			√	
GRMZM2G072529	acc oxidase			√	
GRMZM2G032910	Epoxide hydrolase 2		√		
GRMZM2G136372	thaumatin-like protein				√

Gene ID: MaizeGDB, (Harris et al., 2005). See Supplementary Table. 3 for Affymetrix probe set of indicated genes.

3. Discussion

This study reveals that the N- and C-terminal conserved domains of Stp1 are essential for protein function while the variable domains are dispensable. The C-terminal domain of Stp1 (aa 433-515) can inhibit the activity of the maize extracellular cysteine protease Sip3, a protein identified as interactor of Stp1 in yeast two-hybrid assays. Based on the finding that Stp1 also interacts with several cytoplasmic plant proteins it is speculated that Stp1 may be an effector with both apoplastic and cytoplasmic functions. Moreover, RNA-Seq analysis indicates that the N- and C-terminal domains of Stp1 have distinct functions.

3.1 Domain structure of Stp1

Like most secreted effectors of *U. maydis*, the primary structure of Stp1 reveals no homology to any known functional main besides a signal peptide. Dissecting the domain structure of Stp1 is the basis for the following functional analysis.

3.1.1 The N- and C-terminal conserved domains of Stp1 are essential for protein function while the variable domains are dispensable.

Stp1 consists of a signal peptide, a N-terminal variable domain, a N-terminal conserved domain, a long glycine-rich variable domain in the middle part and a second conserved domain in the C-terminus (Fig. 29). The deletion analysis conducted in this study revealed that N- and C-terminal domains of Stp1 can be expressed separately but both are essential for the protein function. The N-terminal variable domain is dispensable (K. Schipper, personal communication). The glycine-rich variable domain in the middle part is also dispensable but may have minor virulence function. In the following, the putative functions of Stp1 as well as individual domains of it are discussed.

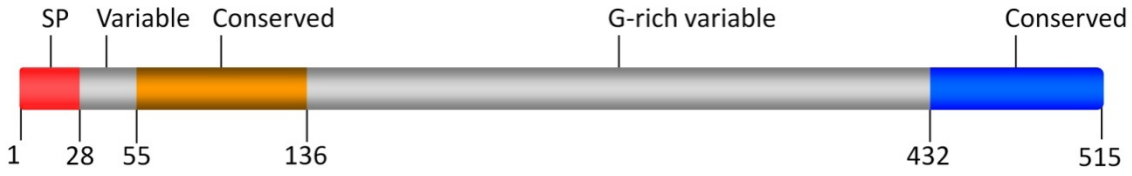

Fig. 29. Domain structure of Stp1. Red: signal peptide, grey: variable domains, orange: N-terminus, blue: C-terminus.

3.1.2 N- and C-terminal domains of Stp1 may be essential for the stability of each other

The N- and C-terminal domains of Stp1 could be separately expressed and no interaction between these two domains was observed in Y2H assays. This raises the question why N- and C-terminal domains of Stp1 are needed for the function of Stp1. During attempts to purify Stp1 and separate N- and C-terminal domains, the C-terminus of Stp1 was proved to be unstable at room temperature (Fig. 24), while the N-terminus of Stp1 was already degraded during the purification procedure at 4 ^{o}C (Fig. 22) making it difficult to obtain pure protein. However, Stp1$_{\Delta 136\text{-}432}$ in which N- and C-termini of Stp1 were fused was stable during purification procedure and subsequent biochemical assays (Fig. 24). The instability observed for the separated N- and C-terminal domains could suggest that N- and C-terminal domains of Stp1 may be mutually essential for the stability of each other. Mutual stabilization is not contradictory with the result that they can function when expressed separately. During establishment of the biotrophic interaction, Stp1 appears not to be needed in large amounts as the *stp1* promoter is relatively weak compared to strong promoters like the *cmu1* promoter which is up-regulated up to hundred thousand times compared to axenic culture during plant colonization (Schipper, 2009, Djamei et al., 2011). Moreover, the proposed mutual stabilization may not need a stable physical interaction which could explain why no interaction between these two domains could be detected. In addition, the short half life of N- and C-termini of Stp1 may be already enough for their function. However, it cannot be ruled out presently that the stability or even the interaction between N- and C-terminal domains will be affected by glycosylation. K. Schipper has shown that Stp1 is N-glycosylated and one N-glycosylation sites is predicted to reside in the C-terminal conserved domain (Schipper, 2009). It will therefore be necessary to investigate the stability and interaction after expressing these two domains in *U. maydis* by IP and Co-IP respectively.

3.2 The interaction partners of Stp1

By yeast two-hybrid analysis using Stp1$_{\Delta 136\text{-}432}$ as bait twelve interaction partners could be identified. This study complemented a study by K. Schipper (2009) who used full-length Stp1 as bait. Interestingly, a comparison of both studies revealed that several putative interactors, Sip10, Sip12, Sip29 and Sip31 showed interaction with full-length Stp1 but

failed to interact with $Stp1_{\Delta 136\text{-}432}$. This suggests that these proteins are unspecific interactors that contact Stp1 via the glycine-rich variable domain and allowed to discard these from further consideration. In the following, I will first discuss the putative apoplastic interactors of Stp1 and follow this up with a discussion of the cytoplasmic interactors.

3.2.1 The biological significance of the inhibition of Sip3 by the C-terminus of Stp1

Two apoplastic interactors, Sip1 and Sip3, were identified in this study. Sip1 is a beta-galactosidase. There is no conceivable evidence correlating it with either plant defense responses or the regulation of plant development and the interaction between Sip1 and Stp1 still needs to be confirmed by full-length cDNA clone. This leaves only the extracellular papain-like cysteine protease, Sip3 which was isolated as interactor of $Stp1_{\Delta 136\text{-}432}$ but was subsequently also shown to interact with full-length Stp1.

Cysteine proteases also referred to as thiol proteases, are comprised of 74 families (http://merops.sanger.ac.uk) that are encoded by viruses, bacteria, protozoa, plants, mammals and fungi (Otto & Schirmeister, 1997, Rawlings *et al.*, 2012). Plant cysteine proteases play an essential role in plant growth and development, senescence and programmed cell death, signaling pathways and the response to biotic and abiotic stresses (Leung-Toung *et al.*, 2002).

Sip3 belongs to C1A cysteine protease subfamily (http://merops.sanger.ac.uk). Both purified $Stp1_{\Delta 136\text{-}432}$ and $Stp1_{433\text{-}515}$ could inhibit the activity of Sip3 to a level comparable to E64, an irreversible cysteine protease inhibitor. Bioinformatic analysis demonstrated that Stp1 had no similarity to any known cysteine protease inhibitors like aprotinin, Avr2 and cystatin (Kunitz & Northrop, 1936, Rooney et al., 2005, Martinez *et al.*, 2009). This suggests that Stp1 could be a novel cysteine protease inhibitor. However, besides Stp1, the secreted effectors Pit2 and Tin3 could also interact with the C1A class of cysteine proteases (N. Neidig and A. Müller, personal communication). There is no conserved motif in Stp1, Pit2 and Tin3 and mutants in these three effector genes have very distinct phenotypes (N. Neidig, personal communication) (Schipper, 2009, Doehlemann et al., 2011) suggesting that these three effectors have non-redundant roles. The chance that all three secreted effectors possess distinct novel cysteine protease inhibitor motifs is very low. Therefore, Stp1 is probably inhibiting Sip3 unspecifically rather than functioning solely as a novel

cysteine protease inhibitor. Incubation of $Stp1_{\Delta 136\text{-}432}$ and $Stp1_{433\text{-}515}$ with Sip3 demonstrated that Stp1 is not a substrate of Sip3 and Sip3 may stabilize the C-terminus of Stp1 (Fig. 24). This could suggest a novel function for the interaction between Stp1 and Sip3 that needs to be substantiated by further experiments.

During the crosstalk between hosts and pathogens, secreted effectors functioning as cysteine protease inhibitor are playing distinct biological functions. *C. fulvum* secretes a protease inhibitor Avr2 that targets the tomato cysteine protease Rcr3, an apoplastic papain-like cysteine protease required specifically for Cf-2 mediated resistance (Song *et al.*, 2009, Dixon *et al.*, 2000). *P. infestans* secreted effector AVRblb2 suppresses plant defense responses by preventing the secretion of a plant papain-like protease C14 which positively contributes to immune responses against *P. infestans* (Bozkurt et al., 2011). To determine whether the C-terminus of Stp1 has the same function as Avr2 and AVRb1b2 or whether it has a novel function, it is necessary to generate stable RNAi lines. In Su1 maize RNAi lines, all members of this family of papain-like proteases could be silenced simultaneously. As the generation of stable transgenic maize plants takes about 18 months, Su1 lines are not yet available. To evaluate how important the inhibition of apoplastic cysteine protease is for the proliferation of *stp1* mutants in planta, maize plants were treated with E64 during infection with SG200Δstp1 expressing the N-terminus of Stp1 and the colonization was observed (data not shown). However, the colonization showed no differences with the control in which plants were infected with SG200Δstp1 expressing N-terminus of Stp1 in the absence of E64. This could suggest that the inhibition of cysteine proteases is either not the main function of the C-terminus of Stp1 or that the access of E64 to cysteine proteases is blocked by the hydrophobic surface of maize leaves and could not therefore inhibit respective cysteine preteases.

3.2.2 The cytoplasmic maize interaction partners of Stp1 shed light on a putative function of Stp1 in the plant cytosol

In this study, both cytoplasmic and apoplastic maize proteins were identified as interactors of Stp1 by Y2H assays. The interactions between Stp1 and the cytoplasmic interactors need to be analyzed biochemically particularly Sip9, Sip19, Sip16 and Sip21, which were verified with full-length cDNA clones.

Sip9 is predicted to be cell number regulator 8. CNR (cell number regulator) gene represents a gene family. For CNR1, it was shown that it could reduce overall plant size when ectopically overexpressed and increase organ size when its expression was suppressed (Guo *et al.*, 2010). It is conceivable that Stp1 could negatively regulate the activity of CNR protein and in this way contribute to higher cell numbers observed in infected tissue (Doehlemann et al., 2008). To test the influence of cell number regulator on pathogenicity, it will be interesting to analyze the development of *stp1* mutants in the CNR1 silenced maize line. However, due to patent restrictions it may be difficult to obtain Su1 lines (R. Kahmann, personal communication)

Sip19 is predicted to be serine/threonine-protein kinase. The Pto serine/threonine-protein kinase confers resistance to bacterial speck disease through recognition of a corresponding avirulence protein, AvrPto, from the pathogen *P. syringae* pv. tomato (Shan et al., 2008, Frederick *et al.*, 1998). To establish a connection between Sip19 and Stp1, Sip19 will be heterologously expressed and the influence of Stp1 on the protein kinase activity of Sip19 will be tested.

Sip16, a putative CCR4-NOT transcription complex subunit, and Sip21, a putative VIP2 protein, are predicted to be components of transcription complex. The CCR4-NOT complex is an evolutionary conserved protein complex and plays an important role in the control of transcription and mRNA decay as well as in defense against pathogens (Sarowar *et al.*, 2007). VIP2 from *Avena fatua* interacts specifically with *A. fatua* homologue of maize transcription factor VIVIPAROUS 1 (AfVP1) which has been implicated in controlling the maintenance of embryo dormancy in seeds (Jones *et al.*, 2000). The interaction between Stp1 and Sip16 & Sip21 may suppress plant defense response by influencing transcription of respective genes. Besides confirming the interaction between Stp1 and its putative interactors biochemically, the biological significance of these interactions could be determined by agrobacterium-mediated transient expression of these interactors in *N. benthamiana* to test if the expression of these interactors can induce plant defense responses which, by co-expression with Stp1 are then attenuated again.

3.3 Stp1, an effector with apoplastic and cytoplasmic functions?

To elucidate the function of secreted effectors, it is mandatory to establish where an effector localizes after secretion. There are several methods described for localization of secreted effectors such as heterologous localization in *M. oryzae*/onion pathosystem, root uptake assay and biolistic bombardment (Djamei et al., 2011, Kloppholz *et al.*, 2011, Kale et al., 2010). In addition, there are also *in situ* translocation assay systems established such as immunogold electron microscopy, nuclear targeting assay (employing nuclear localization signal fused proteins) and immunocytochemical technique (Djamei et al., 2011, Shimada *et al.*, 2009, Khang et al., 2010, Sauer et al., 2006). After transient expression in maize and *N. benthamiana* using biolistic bombardment, the C-terminus of Stp1 as well as full-length Stp1 was localized in the nucleus (Schipper, 2009). Although advances have been made in the localization assays, the uptake of Stp1 by plant cells has never been observed to date.

To detect the uptake of Stp1, nuclear targeting assay and immunocytochemical techniques were used in this study. The fluorescent signal of mCherry could be detected in the nuclei of SG200Δstp1-stp1-mcherry-HA-NLS infected maize but the signal was very weak and difficult to quantify because of high background fluorescence (Fig. 25). After immunocytochemical staining, the signal of Stp1-mCherry-HA-NLS in nuclei was strong and it could also be observed in the cytoplasm of the plant cell while the blank control (SG200) and the negative control (SG200pcmu1-mcherry-HA-NLS) produced no specific signal (Fig. 26). Together with the result that Stp1 was localized in the nucleus when transiently expressed in plant cells (Schipper, 2009), it revealed that Stp1 may suppress plant defense responses by affecting transcription of respective genes in the nucleus of plant cells. The fluorescence signals of Stp1-mCherry-HA-NLS may arise from both Cy3 and mCherry proteins because both the excitation and the emission spectra of Cy3 are close to mCherry and the mCherry tag may still retain its fluorescent properties after immunocytochemical staining procedure (Sauer et al., 2006). One advantage of the immunostain method is that the patchy signal of Cy3 can be easily discriminated from the evenly distributed autofluorescence. The background problems may be overcome using the recently established leaf sheath or silk infection (S. Tanaka and R. Kahmann, personal

communication) (Kankanala *et al.*, 2007). To substantiate the translocation, the localization of N- and C- terminal domains of Stp1 will also need to be analyzed.

In plants, secreted effectors can either be translocated into the host cell or targeted to the apoplast (Bozkurt et al., 2012). The preliminary localization assays indicated Stp1 was translocated in plant cells. Previous study using biolistic bombardment also suggested that Stp1 might function in plant cells. However, the identification of both apoplastic and cytoplasmic interactors and the inhibition of Sip3 which is an extracellular effector by the C-terminus of Stp1 suggested that Stp1 might also function in apoplast. Therefore, Stp1 may distinguish itself among others by functioning as an effector with both apoplastic and cytoplasmic functions. To substantiate this point the interaction between Stp1 and Sip3 without activation need to be tested. If Stp1 interacts with inactive Sip3, the interaction could also take place inside the plant cell like the inhibition of cysteine protease, C14 by AVRblb2 which blocks the secretion of C14 (Bozkurt et al., 2011).

3.4 Glycine-rich domain of Stp1 may promote fungal growth in vascular bundles.

The deletion of the long variable central domain of Stp1 did not attenuate the colonization of *U. maydis*. However this domain exists in all Stp1 orthologs with highly diverse sequence but similar in length (Fig. 1). Additionally, the middle parts of Stp1 orthologs from other smut fungi contain repeats which are not present in Stp1 of *U. maydis* (Fig. 30). Whether these species specific repeats are functionally relevant or not is not known yet. Additionally, this long variable domain is a glycine-rich region predicted to be unstructured. The proteins or protein segments lack secondary and/or tertiary structures are termed intrinsically disordered (or unstructured) proteins (IDPs/IUPs) (Galea *et al.*, 2008). It is now widely recognized that IDPs play broad biological roles in all kingdoms of life. Therefore, the possibility that the central domain of Stp1 might have a minor function in plant infection could not be rule out.

Although the deletion of the middle part of *stp1* did not influence the formation of tumors, SG200Δstp1 secreting the glycine-rich domain of Stp1 was detected more frequently in vascular bundles than SG200Δstp1 (Fig. 7). Growing inside vascular bundle is an essential stage for the infection of *Setosphaeria turcica* (Chung *et al.*, 2010). The transport of

conidia of *Verticillium* spp. in the sap stream of vascular tissues is also essential for the infection cycle (Fradin & Thomma, 2006). The growth of *U. maydis* in vascular bundle may not be important for infection in greenhouse condition where tumors are usually observed on the leaves but may be important in the field where tumors are mainly formed on the cob or tassel of maize plants. The colonization of vascular bundle by SG200Δstp1 expressing glycine-rich domain of Stp1 will be substantiated quantitatively by further confocal microscopy observation.

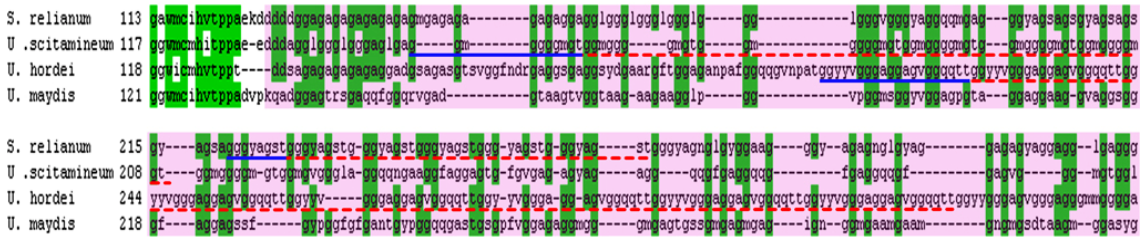

Fig. 30. Repeats in the central glycine-rich domain of Stp1 orthologs are absent in *U. maydis*. *S. relianum*: *Sporisorium reilianum* (Schirawski et al., 2010), *U. scitamineum*: *Ustilago scitamineum* (R. Kahmann, unpublished), *U. hordei*: *Ustilago hordei* (Laurie et al., 2012), *U. maydis*: *Ustilago maydis* (Kamper et al., 2006). Blue underline refers to repeats in indicated species. Red dash underline refers to repeat regions in indicated species. Green color denotes conserved amino acids. Pink color denotes variable domain.

3.5 The N- and C-terminal domains of Stp1 appear to have distinct functions

In infection with SG200Δstp1 expressing only the N- or C-terminal domains of Stp1, one would therefore have expected that only a subset of the genes down-regulated in wild type infection should be down-regulated when infections are carried out with SG200Δstp1-stp1$_{\Delta 432\text{-}515}$ and SG200Δstp1-stp1$_{\Delta 40\text{-}136}$ and added together this should be similar to the wild type.

RNA-Seq analysis indicated that 58 up-regulated genes are common to SG200Δstp1, SG200Δstp1-stp1$_{\Delta 40\text{-}136}$ and SG200Δstp1-stp1$_{\Delta 432\text{-}515}$ (Fig. 28). Besides the genes indicating metabolic reprogramming, genes involved in plant defense response were identified most likely representing those triggered by fungal PAMPs (Doehlemann et al., 2008). For example, 9 of these genes (Table. 11) are identified among the genes involved in early defense response (Doehlemann et al., 2008). These include among others GRMZM2G065585, a 1, 3-β-glucanase which can facilitate resistance of rice plants to fungi infection (Fujikawa *et al.*, 2012), GRMZM2G117989, a Win1 protein which can

increase the resistance response of Arabidopsis to effector protein, HopW1-1 of *P. syringae* (Lee *et al.*, 2008) and GRMZM2G026143, a WIR1A protein, a defense related protein of wheat (Bull *et al.*, 1992). The induction of these early defense response genes is in line with the phenotype of SG200Δstp1, SG200Δstp1-stp1$_{\Delta 40\text{-}136}$ and SG200Δstp1-stp1$_{\Delta 432\text{-}515}$ during infection which stopped after penetration.

3.5.1 Several early defense response genes were not induced by *stp1* mutants expressing the N-terminus of Stp1

The only biological process enriched in plants infected with SG200Δstp1-stp1$_{\Delta 432\text{-}515}$ is down-regulated cell wall organization or biogenesis process indicating metabolic reprogramming in infected tissue (Doehlemann et al., 2008). This is common to SG200Δstp1 and SG200Δstp1-stp1$_{\Delta 432\text{-}515}$ and SG200Δstp1-stp1$_{\Delta 40\text{-}136}$ and could not disclose specific function of the N-terminus of Stp1. Comparison with early defense genes (Doehlemann et al., 2008) indicated that 6 early defense genes are identified only in plants infected with SG200Δstp1 or common to plants infected with SG200Δstp1 and SG200Δstp1-stp1$_{\Delta 432\text{-}515}$ but are absent in plants infected with SG200Δstp1-stp1$_{\Delta 40\text{-}136}$ (Table. 11). These are for example, GRMZM2G145461, a chitinase which can enhance the resistance of tobacco plants to biotic and abiotic stress agents (de las Mercedes Dana *et al.*, 2006), GRMZM2G032910, a epoxide hydrolase 2 which participate in general defense systems of potato (Mowbray *et al.*, 2006) GRMZM2G092718, a late blight resistance protein (Doehlemann et al., 2008) and GRMZM2G136372, a thaumatin-like protein which enhanced the resistance of tobacco plants against fungal pathogen (Munis *et al.*, 2010). The absence of these early defense response genes suggests that less plant defense response is triggered by SG200Δstp1 expressing N-terminus of Stp1. However the data is not solid enough to conclude that N-terminus of Stp1 can partially suppress plant defense responses. It still needs to be substantiated by Q-PCR to verify the expression of these genes in plants infected with SG200Δstp1 and SG200Δstp1-stp1$_{\Delta 432\text{-}515}$ and SG200Δstp1-stp1$_{\Delta 40\text{-}136}$.

The putative role of the N-terminus of Stp1in suppressing plant defense response still needs to be verified. Beside this, the N-terminus of Stp1 might be needed for the uptake of the C-terminus of Stp1. As exemplified by oomycete secreted effectors Avr1b and AVR3a (Whisson et al., 2007, Dou *et al.*, 2008) and fungal effectors AvrL567 and AvrM (Kale et

al., 2010, Rafiqi *et al.*, 2010), the N-terminal domains of secreted effectors are frequently mediating the translocation of secreted effectors from pathogen to host. The translocation function of the N-terminus of Stp1 can be verified by localization assays of N- and C-terminal domains of Stp1. Additionally, as described above, the N-terminus of Stp1 may function to stabilize the C-terminus of Stp1. This needs to be addressed by future stability test and IP & Co-IP experiments.

3.5.2 *stp1* mutants expressing the C-terminus of Stp1 triggered stronger plant defense response than *stp1* mutants

Besides the maize genes that are common to plants infected with SG200Δstp1, SG200Δstp1-stp1$_{\Delta 40\text{-}136}$ and SG200Δstp1-stp1$_{\Delta 432\text{-}515}$ indicating metabolic reprogramming and plant defense response, 95 maize genes are up-regulated only in plants infected with SG200Δstp1-stp1$_{\Delta 40\text{-}136}$. In these genes, cell wall organization or biogenesis and protein modification processes are enriched which indicated further metabolic reprogramming. Interestingly, 7 early defense response genes (Table. 11) identified by microarray (Doehlemann et al., 2008) are only identified in this subset. For example, GRMZM2G117971, a Barwin like protein which may involve in a common defense mechanism in plants (Svensson *et al.*, 1992), GRMZM2G109056, a lipoxygenase which is a part of the early response of the rice plants to pathogenic attack (Peng *et al.*, 1994), GRMZM2G416632, a glutathione transferase which is speculated to involved in defense reactions against pathogens in wheat (Mauch & Dudler, 1993), GRMZM2G106177, an ergosterol biosynthetic protein which can elicit oxidative burst in tobacco cells (Kasparovsky *et al.*, 2004) and GRMZM2G044481, a Copalyl Diphosphate Synthase (AN2) which is induced in maize plants by *Fusarium* attack (Harris et al., 2005). This suggests that the scale of plant defense responses induced by SG200Δstp1-stp1$_{\Delta 40\text{-}136}$ is larger than SG200Δstp1 and SG200Δstp1-stp1$_{\Delta 432\text{-}515}$. Additionally, cell death process is only enriched in plants infected with SG200Δstp1-stp1$_{\Delta 40\text{-}136}$. Two genes associated with this cell death process are GRMZM2G028713 and GRMZM2G032602 which both involve in apoptosis (Supplementary Table. 1). Taken together, *stp1* mutant expressing the C-terminus of Stp1 triggered stronger plant defense response than *stp1* mutant.

The function of the C-terminus is still elusive beside the inhibition of cysteine protease, Sip3. The preliminary result of RNA-Seq analysis still needs to be verified by Q-PCR and the stronger plant defense response triggered by the C-terminus of Stp1 needs to be testified by microscopic observation and overexpression of the C-terminus of Stp1. One possible mechanism of the stronger plant defense response could be that the C-terminus of Stp1 could partially complement *stp1* mutant, thereafter, more biomass was produced and stronger plant defense response was induced. Another possibility is that the N-terminus of Stp1 might modify the C-terminus of Stp1 and when this modification is absent stronger plant defense response could be induced.

3.6 Working model of the function of Stp1

A working model is proposed based on current results (Fig. 31). After formation of the dikaryotic hyphae, Stp1 starts to be expressed and secreted in a glycosylated form to the apoplast of maize cells. In the apoplast, Stp1 can inhibit a class of papain-like cysteine proteases. Meanwhile, Stp1 may also be cleaved into separate N- and C- terminal domains in the apoplast. The inhibition of cysteine proteases may not be the only function of Stp1. Stp1 may be taken up by maize cells. In the plant cytosol, Stp1 may bind to and block the secretion of maize papain-like cysteine proteases. Moreover, Stp1 may also translocate to the nucleus of maize cells to suppress plant defense responses by affecting transcription of respective genes.

Several key challenges still need to be addressed to substantiate this preliminary model. First of all, the biological significance of the inhibition of cysteine proteases by Stp1 needs to be determined. Secondly, the interaction between Stp1 and the maize cytoplasmic interaction partners needs to be confirmed. Finally, the location of the full length Stp1 as well as N- and C-terminal domains during infection needs to be determined.

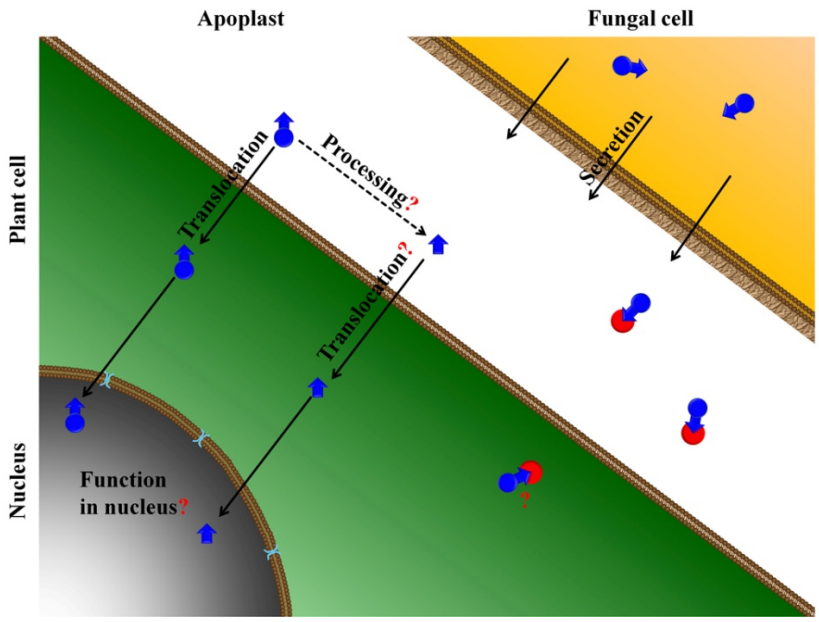

Fig. 31. Working model of the function of Stp1
: Stp1, : Sip3 and other maize secreted cysteine proteases.

4. Materials and methods

4.1 Materials and source of supplies

4.1.1 Chemicals and enzymes

All chemicals used in this study were obtained from Difco (Augsburg), Fisher Scientific (Schwerte), Fluka (Buchs), GE Healthcare (München), GERBU Biochemicals (Gaiberg), IBA **(**Göttingen**),** Life Technologies (Darmstadt), Merck (Darmstadt), Millipore (Schwalbach/Ts), NEB (Frankfurt am Main), PeptaNova (Sandhausen), QIAGEN (Hilden), Roche (Mannheim), Roth (Karlsruhe), Clontech (Saint-Germain-en-Laye) and Sigma-Aldrich (Deisenhofen).

All restriction enzymes, Taq DNA polymerase, T4 DNA ligase, T4 PNK was obtained from NEB (Frankfurt am Main). Phusion high-fidelity DNA polymerase was obtained from Finnzymes (Frankfurt am Main). KOD extreme polymerase was obtained from Merck (Darmstadt), Gateway clonase was obtained from Invitrogen (Karlsruhe), Prescission protease was obtained from GE Healthcare (München), TEV protease was obtained from Promega (Mannheim).

4.1.2 Buffers and solutions

Standard buffers and solutions are prepared according to Ausubel *et al*. (1987) and Sambrook *et al* (1989). Specific buffers and solutions are listed with the corresponding methods. All media, solutions and buffers were autoclaved for 5 min at 121 °C. Heat-sensitive solutions were filter-sterilized (pore size: 0.2 µm, Merck, Darmstadt).

4.1.3 Kits

The following kits were used following protocols recommended by the suppliers:

TOPO TA cloning kit (Invitrogen, Karlsruhe) for direct cloning of PCR products, Wizard SV gel and PCR clean-up system (Promega, Mannheim) for extraction and purification of DNA fragments, QIAquick plasmid purification kit (QIAGEN, Hilden) for plasmid isolation and purification, ECL Plus Western Blot detection reagent (GE Healthcare, München) was used for chemiluminescence detection. QuikChange Multi Site-Directed mutagenesis kit (Agilent Technologies, Böblingen) for site-directed mutagenesis of plasmid

DNA. ProLong® antifade kit (Life Technologies**,** Darmstadt) for protection of the dyes from fading during fluorescence microscopy.

4.2 Media

4.2.1 Media for *E. coli* and *A. tumefaciens*

E. coli and *A. tumefaciens* strains were grown in dYT liquid medium or YT solid medium supplemented with appropriate antibiotics (Ampicillin (Amp), 100 µg/ml; Kanamycin (Kan), 50 µg/ml; Rifampicin (Rif), 50 µg/ml). dYT glycerol medium was use for preparation of frozen stocks.

dYT liquid medium (Sambrook *et al*., 1989)	1.6 % (w/v) Trypton-Pepton 1.0 % (w/v) Yeast Extract 0.5 % (w/v) NaCl Add dH_2O and autoclave
YT solid medium	0.8 % (w/v) Trypton-Pepton 0.5 % (w/v) Yeast Extract 0.5 % (w/v) NaCl 1.3 % (w/v) Agar Add dH_2O and autoclave
dYT glycerol medium	1.6 % (w/v) Trypton-Pepton 1.0 % (w/v) Yeast Extract 0.5 % (w/v) NaCl 800 ml (v/v) 87 % Glycerol (f.c. 69.6 %) Add dH_2O and autoclave

4.2.2 Media for *U. maydis*

U. maydis strains were grown on potato-dextrose-agar (Difco), $YEPS_{light}$ liquid media or regeneration agar supplemented with carboxin (2 µg/ml). NSY-glycerol was used for preparation of frozen stocks.

Potato-Dextrose-Agar (PD)	2.4 % (w/v) Potato-Dextrose Broth 2 % (w/v) Bactoagar Add dH_2O and autoclave
$YEPS_{light}$ (modified from Tsukuda *et al.,* 1988)	1 % (w/v) Yeast-Extract 1 % (w/v) Pepton 1 % (w/v) Saccharose Add dH_2O and autoclave
NSY-glycerol	0.8 % (w/v) Nutrient Broth 0.1 % (w/v) Yeast-Extract 0.5 % (w/v) Saccharose 69.6 % (v/v) Glycerol Add dH_2O and autoclave
Regeneration Agar (Schulz et al., 1990)	1.5 % (w/v) Agar 1 M Sorbitol in YEPSL (described above) Add dH_2O and autoclave

4.2.3 Media for *S. cerevisiae*

Yeast strains were grown on YEPD-medium or SD-medium supplemented with appropriate nutrient (Table. 12).

YEPD-medium	2 % (w/v) Pepton (Difco) 1 % (w/v) Yeast extract 2 % (w/v) Agar 2 % (w/v) Glucose (after autoclave) 0,003 % (w/v) Adenine (after autoclave)
SD-medium	0,67 % (w/v) Yeast nitrogen base without amino acids 0.06 % (w/v) –Ade/-His/-Leu/-Trp

Do Supplement

2 % (w/v) Agar (for plate only)

2 % (w/v) Glucose (after autoclave)

Table 12. Nutrients supplemented in SD-medium

Nutrients	10×Concentration
L-Adenine hemi-sulfate salt	200 mg/L
L-Histidine HCl monohydrate	200 mg/L
L-Leucine	1000 mg/L
L-Tryptophan	200 mg/L

4.3 Strains

4.3.1 *Escherichia coli* strains

E. coli strains K-12 TOP10 ([F- *mcr*A Δ(*mrr-hsd*RMS-*mcr*BC) Φ80*lacZ*ΔM15 Δ*lac*O74 *rec*A1*ara*Δ139 Δ(*ara-leu*)7697 *gal*U *gal*K*rps*L (Str^R) *end*A1 *nup*G], Invitrogen, Karlsruhe) and K-12 DH5α ([F- Φ80d *lacZ* ΔM15 Δ(*lac*ZYA-*arg*F) U169 *deo*R *rec*A1 *end*A1 *hsd*R17(r$_{K^-}$, m$_{K^+}$) *pho*A *sup*E44 λ- *thi*-l *gyr*A96 *rel*A1], Gibco/BRL, Eggenstein) were used as host strains for plasmid constructions and amplifications. *E. coli* strains BL21 Rosetta (DE3)pLysS([F- *ompT hsdSB*(rB-mB-) *gal dcm* (DE3) pLacIRARE (Cam^R)], Novagen/Merck, Darmstadt) was used as host strains to produce recombinant proteins.

4.3.2 *Agrobacterium tumefaciens* strain

A. tumefaciens GV3101 stain is used for transient expression of protein in *Nicotiana benthamina*. *A. tumefaciens* GV3101 expressing p19 protein, a suppressor of gene silencing is used for co-infiltration of *N. benthamiana* with *A. tumefaciens* GV3101 expressing target proteins (Voinnet *et al.*, 2003).

4.3.3 *Ustilago maydis* strains

All *U. maydis* strains used in this study are listed in table. 13

Table 13. *U. maydis* strains used in this study

Strain	Genotype	Antibiotics	Reference
SG200	*a1mfa2bE1bW2*	Phleo	(Kamper et al., 2006)
SG200Δstp1	*a1mfa2bE1bW2 Δum02475::egfp*	Phleo, Hyg	(Schipper, 2009)
SG200Δstp1-stp1	*a1 mfa2 bE1 bW2 Δum02475*	Phleo, Hyg,	(Schipper, 2009)

	ip^r [Pstp1:stp1] ip^s	Cbx	
SG200Δstp1-stp1$_{\Delta 136-432}$	*a1 mfa2 bE1 bW2 Δum02475* *ip^r [Pstp1: stp1$_{\Delta 136-432}$] ip^s*	Phleo, Hyg, Cbx	This study
SG200Δstp1-stp1$_{\Delta 29-136/432-515}$	*a1 mfa2 bE1 bW2 Δum02475* *ip^r [Pstp1: stp1$_{\Delta 29-136/432-515}$] ip^s*	Phleo, Hyg, Cbx	This study
SG200Δstp1-stp1$_{\Delta 432-515}$	*a1 mfa2 bE1 bW2 Δum02475* *ip^r [Pstp1: stp1$_{\Delta 432-515}$] ip^s*	Phleo, Hyg, Cbx	(Schipper, 2009)
SG200Δstp1-stp1$_{\Delta 40-136}$	*a1 mfa2 bE1 bW2 Δum02475* *ip^r [Pstp1: stp1$_{\Delta 40-136}$] ip^s*	Phleo, Hyg, Cbx	(Schipper, 2009)
SG200Δstp1-stp1$_{\Delta 137-515}$+stp1$_{\Delta 37-431}$	*a1 mfa2 bE1 bW2 Δum02475* *ip^r [Pstp1: stp1$_{\Delta 137-515}$+ Pstp1: stp1$_{\Delta 37-431}$] ip^s*	Phleo, Hyg, Cbx	This study
SG200Δstp1-stp1$_{\Delta 136-432T452V}$	*a1 mfa2 bE1 bW2 Δum02475* *ip^r [Pstp1: stp1$_{\Delta 136-432T452V}$] ip^s*	Phleo, Hyg, Cbx	This study
SG200Δstp1-stp1$_{T452V}$	*a1 mfa2 bE1 bW2 Δum02475* *ip^r [Pstp1: stp1$_{T452V}$] ip^s*	Phleo, Hyg, Cbx	This study
SG200Δstp1-stp1$_{PPAA}$	*a1 mfa2 bE1 bW2 Δum02475* *ip^r [Pstp1: stp1$_{PPAA}$] ip^s*	Phleo, Hyg, Cbx	This study
SG200Δstp1-stp1$_{SRAA}$	*a1 mfa2 bE1 bW2 Δum02475* *ip^r [Pstp1: stp1$_{SRAA}$] ip^s*	Phleo, Hyg, Cbx	This study
SG200Δstp1-stp1$_{\Delta 433-454}$	*a1 mfa2 bE1 bW2 Δum02475* *ip^r [Pstp1: stp1$_{\Delta 433-454}$] ip^s*	Phleo, Hyg, Cbx	This study
SG200Δstp1-stp1$_{\Delta 455-476}$	*a1 mfa2 bE1 bW2 Δum02475* *ip^r [Pstp1: stp1$_{\Delta 455-476}$] ip^s*	Phleo, Hyg, Cbx	This study
SG200Δstp1-stp1$_{\Delta 477-494}$	*a1 mfa2 bE1 bW2 Δum02475* *ip^r [Pstp1: stp1$_{\Delta 477-494}$] ip^s*	Phleo, Hyg, Cbx	This study
SG200Δstp1-stp1$_{\Delta 495-515}$	*a1 mfa2 bE1 bW2 Δum02475* *ip^r [Pstp1: stp1$_{\Delta 495-515}$] ip^s*	Phleo, Hyg, Cbx	This study
SG200Δstp1-Uh-stp1	*a1 mfa2 bE1 bW2 Δum02475* *ip^r [Pstp1: Uh-stp1] ip^s*	Phleo, Hyg, Cbx	This study
SG200Δstp1-Us-stp1	*a1 mfa2 bE1 bW2 Δum02475* *ip^r [Pstp1: Us-stp1] ip^s*	Phleo, Hyg, Cbx	This study
SG200Δstp1-Stp1-cherry-HA-NLS	*a1 mfa2 bE1 bW2 Δum02475* *ip^r [Pcmu: stp1-cherry-HA-NLS] ip^s*	Phleo, Hyg, Cbx	This study
SG200Um05731-	*a1 mfa2 bE1 bW2 Δum02475*	Phleo, Hyg,	Armin Djamei (This lab)

cherry-HA-NLS	*ip^r [Pcmu: um05731-cherry-HA-NLS] ip^s*	Cbx	
SG200-cherry-HA-NLS	*a1 mfa2 bE1 bW2 Δum02475 ip^r [Pcmu: cherry-HA-NLS] ip^s*	Phleo, Hyg, Cbx	This study
SG200Δstp1-stp1$_{\Delta 136-432}$-HA-NLS	*a1 mfa2 bE1 bW2 Δum02475 ip^r [Pcmu: stp1$_{\Delta 136-432}$-HA-NLS] ip^s*	Phleo, Hyg, Cbx	This study
SG200-HA-NLS	*a1 mfa2 bE1 bW2 Δum02475 ip^r [Pcmu: HA-NLS] ip^s*	Phleo, Hyg, Cbx	This study

4.3.4 *Saccharomyces cerevisiae* strains

S. cerevisiae strain AH109 (*MATa, trp1-901, leu2-3, 112, ura3-52, his3-200, gal4Δ, gal80Δ, LYS2::GAL1UAS-GAL1TATA-HIS3, GAL2UAS-GAL2TATA-ADE2, RA3::MEL1UASMEL1TATA-lacZ, MEL1*, Clontech) was used as host strain for yeast two-hybrid assay.

4.4 Oligonucleotides

All oligonucleotides used in this study were ordered from Eurofins MWG Operon (Table. 14).

Table 14. Oligonucleotides used in this study

primer	Cleavage site*	Sequence
LL7		AACATGACCATGGCAGCCGCCCCTTCTCGTTAGGCG
LL8		ATGGCACCTCCTCCTGCCGCCTAGGCGCGGCCGCCC
LL15		ATGCGAGCCGACTTTTTATCC
LL21		ATGAGAGCCGTGCTCTCGCTCAAC
LL23	*Nco*I	CATGCCATGGCTGCACTGCAACCC
LL24	*Not*I	ATAAGAATGCGGCCGCTTTTCTGAGCTGCATAGCTTTCTG
LL25	*Sfi*I	CTCGGCCGGTGCGGCCGTGCTGATGTGCATCAATGGCGATCCTGCTG
LL30	*Nco*I	CATGCCATGGCAAGGTCAGGCTTAG
LL31	*Not*I	ATAAGAATGCGGCCGCTTCTAAGGTTTGGTGATGTTGAAG
LL32	*Nco*I	CATGCCATGGAAAGGTACAAATTGATACG
LL33	*Not*I	ATAAGAATGCGGCCGCTGAAGAAATTCACCTGCCG
LL56		ATGAGGGCCAAACTTTCGCTCAAC
LL61	*Bsp*HI	CAAGTCATGATAATGGGCCCTCCGCGGCCGG

LL62	*Not*I	ATAAGAATGCGGCCGCTGCAGCCGCACGGTCCCTCC
LL66	*Not*I	ATAAGAATGCGGCCGCTTGCGCTGCTCTTCATGCCATC
LL67	*Bsp*HI	CAAGTCATGATAGCGGACAGCATGTCGATCGTCTC
LL68		CAAGTTCAACACCATGACTGGTGTTCGCATCCGC
LL72		GGGATCCATCGAGCTCGAG
LL73		GGGAACATCAGCTGGGGG
LL74		GTGCTGATGTGCATCAATGG
LL75		CATATGAGCGTAATCTGGTACGTC
LL76		GGGATCCGTCGACCTGC
LL77		CATATGCAGGTCCTCCTCTG
LL78		GGCCTGAACGGCGACAAGTATCGGCAGG
LL79		TAGGCGCGGCCGCCCGGC
LL80		AAGCAAGCTGATGGAGGAGCAGGTACG
LL81		TTTCGGAGCATTTGCGTTTGAAGCGGG
LL87		GGCGCCGGCGCCCAGGAGGAT
LL88	*Not*I	ATAAGAATGCGGCCGCTCATCCGAGGGATGTGCAGTGGACGGAAGG
LL89		GGACAACATGTGTTTACGGAGC
LL90	*Not*I	ATAAGAATGCGGCCGCTCATCCGTGGCGAGTGCATTT
LL93		GGCGCCGGCGCCAACAAC
LL94	*Not*I	ATAAGAATGCGGCCGCTCATGCCACGCCCCATGGTCTGCTC
LL97		GTTCTGATGTGTATTAATGGTGATCCGGC
LL98		CGGAACATCTGCCGGAGGTGTAAC
LL112		CGTGTTCTCTGCTTTATTTTCTCGATAAAGTTGTGG
LL113	*Not*I	GCAGCCGGGCGGCCGCGCTTATTGCTTCGGAGGGGGG
LL114	*Not*I	GCAGCCGGGCGGCCGCGCCTAACGAGCAGGAGGAGGG
LL116		CGTAACCTAGAGCTCTTGCAGTTCG
LL117		AAGATCCGCTCGATCGCCACC
LL119		ACGAGAAGGAGGAGGTGCCATGGT
LL157		TAAAAGCTTGATCCGGCTGCTAACAAAG
LL158		GGATCCCTGAAAATACAGGTTTTCGGTC
LL159	*Bam*HI	CGGGATCCATGCACACGCTCGATATCCATTC
LL160	*Hin*dIII	TCCCAAGCTTCTAGCTTACAAACTTGTTGCTCTGC
LL175		GGCTGGGCCCATGGGCTGGAG
LL176	*Not* I	ATAAGAATGCGGCCGCTCAGAGGGTACGACGGCTCAACGGCGATAC
LL177		CACCCGCAGTTCGAAAAAGCGGACAGCATGTCGATCGTCTC
LL178	*Psp*OMI	GCTCCAGCCCATGGGCCCAGCCTGCTTTTTTGTACAAAGTTGGC
LL179		TTCCAGATTACGCTGGCGGCATGGACGAGCTGTACAAGTACCC

LL180	CATCGTATGGGTAGGTGGCGATCGAGCGGATCTTACGAGAAGG
LL181	CATCGTATGGGTAGGTGGCGATCGAGCGGATCTTGGCCTGAAC
oKS145 *Sfi*I	GAGGGCCGCACCGGCCCCGGGAACATCAGCTGGGGGAGTAACGTGGATGC

*, The cleavage sites of primers were underlined

4.5 Plasmids

4.5.1 Plasmids for generation of *U. maydis* mutants

p123_L-egfp, p123 (Aichinger *et al.*, 2003) derivative containing the carboxin resistance gene and an eGFP gene which is fused to the otef promoter and nos terminator.

p123-Pstp1-stp1, p123_L-egfp derivative incorporating stp1 and its native promoter(Schipper, 2009).

p123pstp1-stp1$_{\Delta 136\text{-}432}$, This plasmid was generated through inverse PCR using LL25 and oKS 145 as primers and p123-Pstp1-stp1 as template. The PCR product was digested by *Sfi*I and ligated to generate p123pstp1-stp1.

p123pstp1-Stp1$_{\Delta 29\text{-}136/432\text{-}515}$, The vector of this plasmids were obtained through inverse PCR employing LL78 and LL 79 as primers and p123-Pstp1-stp1 as template. The stp1$_{\Delta 29\text{-}136/432\text{-}515}$ fragment was amplified using LL80 and LL81 as primers and p123-Pstp1-stp1 as template. The fragments were treated with T4 PNK (NEB) and ligated to produce p123pstp1-Stp1$_{\Delta 29\text{-}136/432\text{-}515}$.

p123pstp1-stp1$_{\Delta 137\text{-}515}$+pstp1-stp1$_{\Delta 37\text{-}431}$, This plasmid was constructed by Michael Daume and Kerstin Schipper. It incorporates two gene fragments, encoding N- or C-termini of Stp1, which fused with promoter of stp1 separately.

p123pstp1-stp1$_{\Delta 136\text{-}432T452V}$, The point mutation was introduced through inverse PCR using QuikChange Multi Site-Directed Mutagenesis Kit using LL68 as primers and p123pstp1-stp1$_{\Delta 136}$-432 as a template. The PCR product was treated with T4 PNK and self-ligated to produce p123pstp1-stp1Δ136-432T452V.

p123pstp1-stp1$_{T452V}$, The point mutation was introduced through inverse PCR using QuikChange Multi Site-Directed Mutagenesis Kit using LL68 as primers and p123-Pstp1-stp1 as template. The PCR product was treated with T4 PNK and self-ligated to produce p123pstp1- stp1$_{\Delta 136\text{-}432T452V}$.

p123pstp1-stp1$_{PPAA}$, The point mutation was introduced through inverse PCR using QuikChange Multi Site-Directed Mutagenesis Kit using LL7 as primers and p123-Pstp1-stp1 as template. The PCR product was treated with T4 PNK and self-ligated to produce p123pstp1-stp1$_{PPAA}$.

p123pstp1-stp1$_{SRAA}$, The point mutation was introduced through inverse PCR using QuikChange Multi Site-Directed Mutagenesis Kit using LL8 as primers and p123-Pstp1-stp1 as template. The PCR product was treated with T4 PNK and self-ligated to produce p123pstp1-stp1$_{SRAA}$.

p123pstp1-stp1$_{\Delta 433\text{-}454}$, This plasmid was constructed by Kerstin Schipper. It incorporates C-terminus truncated Stp1.

p123pstp1-stp1$_{\Delta 455\text{-}476}$, This plasmid was constructed by Kerstin Schipper. It incorporates C-terminus truncated Stp1.

p123pstp1-stp1$_{\Delta 477\text{-}494}$, This plasmid was constructed by Kerstin Schipper. It incorporates C-terminus truncated Stp1.

p123pstp1-stp1$_{\Delta 495\text{-}515}$, This plasmid was constructed by Kerstin Schipper. It incorporates C-terminus truncated Stp1.

p123pstp1-Uh-stp1, The vector was amplified using LL25 and LL112 as primers and p123-Pstp1-stp1 as template. The Uh-stp1(*stp1* from *U. hordei*) was amplified using LL15 and LL113 as primers and genome DNA of *U. hordei* as template. Both

the fragment and the vector were treated with T4 PNK before digestion by *Not*I. Ligate the vector and the fragment to produce p123pstp1-Uh-stp1.

p123pstp1-Us-stp1, The vector was amplified using LL25 and LL112 as primers and p123-Pstp1-stp1 as template. The Us-stp1 (*stp1* from *U. scitaminum*) was amplified using LL56 and LL114 as primers and genome DNA of *U. scitaminum* as template. Both the fragment and the vector were treated with T4 PNK before digestion by *Not*I. The vector and the fragment was ligated to produce p123pstp1-Us-stp1.

p123pcmu-stp1-cherry-HA-NLS, Stp1 fragment was amplified using LL 21 and LL119 as primers and p123-Pstp1-stp1 as template. The vector containing mCherry, HA and NLS was amplified through inverse PCR using LL116 and LL117 as primers and p123-Um05731genomic-cherry (From Armin Djamei). The fragment and the vector were treated with T4 PNK and ligated to produce p123pcmu-Stp1-Cherry-HA-NLS.

P123pcmu-cherry-HA-NLS, The plasmid was constructed through inverse PCR using p123pcmu-Stp1-Cherry-HA-NLS as template and LL78 & LL117 as primers. The PCR product was treated with T4 PNK and self-ligated to produce P123pcmu-Cherry-HA-NLS.

P123pcmu-stp1$_{\Delta 136\text{-}432}$-HA-NLS, The vector was amplified using LL179 and oKS145 as primers and p123pcmu-Stp1-Cherry-HA-NLS as template. The *stp1* fragment was amplified using LL25 and LL180 as primers and p123pcmuStp1-Cherry-HA-NLS as template. Both the vector and the *stp1* fragment were digested by *Sfi*I and treated with T4 PNK. The vector and the *stp1* fragment were then ligated tp generate P123pcmu-stp1$_{\Delta 136\text{-}432}$-HA-NLS.

P123pcmu-HA-NLS, The plasmid was constructed through inverse PCR using LL179 and LL181 as primers and P123pcmu-Cherry-HA-NLS as template. The PCR product was treated with T4 PNK and self-ligated to produce P123pcmu-HA-NLS.

4.5.2 Plasmids for Y2H assays

pGADT7, AD/library cloning vector incorporating HA epitope and *LEU2* selection marker (Clontech).

pGBKT7, DNA/bait cloning vector incorporating c-Myc epitope and *TRP1* selection marker (Clontech).

pGAD-stp1, *stp1* inserted into pGADT7 vector (Schipper, 2009).

pGBK-stp1, *stp1* inserted into pGBKT7 vector(Schipper, 2009).

pGBK-stp1$_{\Delta 136\text{-}338}$, stp1$_{\Delta 136\text{-}338}$ inserted into pGBKT7 vector (Schipper, 2009).

pGAD-sip10, sip10 fragment inserted into pGAD vector(Schipper, 2009).

pAD, AD/library cloning vector incorporating HA epitope and *LEU2* selection marker (Stratagene, LaJolla/USA).

pAD-sip12, sip12 fragment inserted into pAD vector (Clontech).

pGAD-sip29, sip29 fragment inserted into pGAD vector (Schipper, 2009).

pGAD-sip31, sip31 fragment inserted into pGAD vector(Schipper, 2009).

pGBK-stp1$_{\Delta 136\text{-}432}$, This plasmid was generated through inverse PCR using LL25 and oKS 145 as primers and pGBK-stp1 as template. The PCR product was digested by *Sfi*I and ligated to generate pGBK-stp1$_{\Delta 136\text{-}432}$.

pGADGW, gateway destination vector modified from pGADT7 by Armin Djamei (this lab).

pGBKGW, gateway destination vector modified from pGBKT7 by Armin Djamei (this lab).

pEntry 4B Vcp1, gateway entry vector incorporating *Bsp*HI/*Nco*I and *Not*I cleavage sites modified from pENTR TOPO vector (invitrogen) by Armin Djamei (this lab).

pGAD-sip6, sip6 fragment was amplified using LL61 and LL62 as primers and cDNA of maize as template. Both sip6 fragment and pEntry 4B Vcp1 vector were digested by *Bsp*HI and *Not*I. The fragments was purified and ligated to generate pEntry-sip6. Sip6 fragment was transferted into pGADGW vector through an LR recombination reaction.

pGAD-sip8, sip8 fragment was amplified using LL23 and LL24 as primers and cDNA of maize as template. Both sip8 fragment and pEntry 4B Vcp1 vector were digested by *Nco*I and *Not*I. The fragments was purified and ligated to generate pEntry-sip8. sip8 fragment was transferted into pGADGW vector through an LR recombination reaction.

pGAD-sip9, sip9 fragment was amplified using LL93 and LL94 as primers and cDNA of maize as template. pEntry 4B Vcp1 vector was digested by *Nco*I and the gap was filled by DNA polymerase I large (Klenow) fragment. Both sip9 fragment and pEntry 4B Vcp1 fragment were digested by *Not*I. The fragments were purified and ligated to generate pEntry-sip9. Sip9 fragment was transferted into pGADGW vector through an LR recombination reaction.

pGAD-sip14, sip14 fragment was amplified using LL87 and LL88 as primers and cDNA of maize as template. pEntry 4B Vcp1 vector was digested by NcoI and the gap was filled by DNA polymerase I large (Klenow) fragment. Both sip14 fragment and pEntry 4B Vcp1 fragment were digested by *Not*I. The fragments were purified and ligated to generate pEntry-sip14. Sip14 fragment was transferted into pGADGW vector through an LR recombination reaction.

pGAD-sip16, sip16 fragment was amplified using LL30 and LL31 as primers and cDNA of maize as template. Both sip16 fragment and pEntry 4B Vcp1 vector were digested by *Nco*I and *Not*I. The fragments was purified and ligated to generate pEntry-sip16. Sip16 fragment was transferted into pGADGW vector through an LR recombination reaction.

pGAD-sip19, sip19 fragment was amplified using LL32 and LL33 as primers and cDNA of maize as template. Both sip19 fragment and pEntry 4B Vcp1 vector were digested by *Nco*I and *Not*I. The fragments was purified and ligated to generate pEntry-sip19. Sip19 fragment was transferted into pGADGW vector through an LR recombination reaction.

pGAD-sip21, sip21 fragment was amplified using LL89 and LL90 as primers and cDNA of maize as template. pEntry 4B Vcp1 vector was digested by NcoI and the gap was filled by DNA polymerase I large (Klenow) fragment. Both sip21 fragment and pEntry 4B Vcp1 fragment were digested by *Not*I. The fragments were purified and ligated to generate pEntry-sip21. Sip21 fragment was transferted into pGADGW vector through an LR recombination reaction.

pGAD-sip3, sip3 fragment was amplified using LL66 and LL67 as primers and cDNA of maize as template. Both sip3 fragment and pEntry 4B Vcp1 vector were digested by *Bsp*HI and *Not*I. The fragments was purified and ligated to generate pEntry-sip3. Sip3 fragment was transferted into pGADGW vector through an LR recombination reaction.

pGAD-stp1$_{\Delta 136\text{-}432}$, This plasmid was generated through inverse PCR using LL25 and oKS 145 as primers and pGAD-stp1 as template. The PCR product was digested by *Sfi*I and ligated to generate pGAD-stp1$_{\Delta 136\text{-}432}$.

pGBK-stp1$_{29\text{-}135}$, This plasmid was generated through inverse PCR using LL76 and LL77 as primers and pGBK-stp1 as template. The PCR product was treated with T4 PNK (NEB) and ligated to produce pGBK-stp1$_{29\text{-}135}$.

pGAD-stp1$_{29\text{-}135}$, This plasmid was generated through inverse PCR using LL72 and LL73 as primers and pGAD-stp1 as template. The PCR product was treated with T4 PNK (NEB) and ligated to produce pGAD-stp1$_{29\text{-}135}$.

pGBK-stp1$_{433\text{-}515}$, stp1$_{433\text{-}515}$ inserted into pGBKT7 vector (Schipper, 2009).

pGAD-stp1$_{433-515}$, This plasmid was generated through inverse PCR using LL74 and LL75 as primers and pGAD-stp1 as template. The PCR product was treated with T4 PNK (NEB) and ligated to produce pGAD-stp1$_{433-515}$.

pGAD-Mir3, Mir3 inserted into pGADT7 vector constructed by Nina Neidig (this lab).

pGAD-CP1A, CP1A inserted into pGADT7 vector (A. Müller this department, personal communication).

pGAD-CP2, CP2 inserted into pGADT7 vector (A. Müller, personal communication).

pGAD-XCP2, XCP2 inserted into pGADT7 vector (A. Müller, personal communication).

pGAD-CatB3, CatB3 inserted into pGADT7 vector (A. Müller, personal communication).

4.5.3 Plasmids for protein expression

pRSET His TEV, Expression vector for *E. coli* incorporating His-tag and TEV protease cleavage site(Schoepfer, 1993).

pBIN19AN-3CI-YFP, a plant binary vector derived from pBI121(Haseloff *et al.*, 1997, Jefferson *et al.*, 1987). Expression vector for agrobacterium mediated expression in tobacco, incorporating IgG-tag and prescission protease cleavage site(From Nina Neidig, this lab).

pMA Stp1$_{\Delta 136-432}$, Codon optimized Stp1$_{\Delta 136-432}$ for *E. coli* inserted in pMA vector(GENEART).

pBIN Strep sip3WG, pEntry strep sip3 was constructed through inverse PCR employing LL177 and LL178 as primers and pEntry-sip3 as template. The fragment was treated with T4 PNK (NEB) and ligated to produce pEntry strep sip3. Sip3WG fragment was amplified through PCR using LL175 and LL 176 as primers and pEntry strep sip3 as template. sip 3WG fragment and pBIN PP vector were digested by *Bsp*120I & *Not*I and ligated to produce pBIN strep sip3WG

pRSET His TEV Stp1$_{\Delta 136-432}$, Stp1$_{\Delta 136-432}$ fragment was obtained from pMA Stp1$_{\Delta 136-432}$ by digestion using *Bam*HI and *Hin*dIII. The vector was generated by digestion using *Bam*HI and *Hin*dIII. The fragment and the vector were ligated to produce pRSET His TEV Stp1$_{\Delta 136-432}$.

pRSET His TEV Stp1$_{29-135}$, This plasmid was generated through inverse PCR using pRSET His TEV Stp1$_{\Delta 136-432}$ as template and LL98 and LL157 as primers. The PCR product was treated with T4 PNK (NEB) and ligated to produce pRSET His TEV Stp1$_{29-135}$.

pRSET His TEV Stp1$_{433-515}$, This plasmid was generated through inverse PCR using pRSET His TEV Stp1$_{\Delta 136-432}$ as template and LL97 and LL158 as primers. The PCR product was treated with T4 PNK (NEB) and ligated to produce pRSET His TEV Stp1$_{433-515}$.

pRSET His TEV Aro7, Aro7 fragment was amplified from genomic DNA of SG200 using LL159 and LL160 as primers. Both the PCR product and pRSET His TEV were digested by *Bam*HI and *Hin*dIII. The purified and fragment and vector were ligated to generate pRSET His TEV Aro7.

4.6 Microbiological methods

4.6.1 *E. coli* and *A. tumefaciens* methods

Liquid cultures were incubated at 37 °C (*E. coli*) or 28 °C (*A. tumefaciens*) at 200 rpm. Solid media were incubated under aerobic condition at 37 °C (*E. coli*) or 28 °C (*A. tumefaciens*). To prepare frozen stocks, exponentially growing cultures were mixed with dYT glycerol medium at a 1:1 ratio and stored at -80 °C.

4.6.1.1 Preparation of chemical competent cells and transformation of *E. coli*

The chemical competent cells were prepared following the protocol of Hanahan (Hanahan, 1985). To transform the *E. coli*, an aliquot of competent cells was thawed on ice. Afterwards, 1-10 µl plasmid or ligation mixture was added, gently mixed and incubated on ice for 15-30 min. The mixture was then heat shocked at 42 °C for 1 min and immediately cooled on ice for 30 sec. For the recovery of the *E. coli* cells, 300 µl dYT medium was added and the cells were incubated at 600 rpm for 30-60 min at 37 °C. Finally, the entire *E. coli* cell suspension was plated on YT-agar containing appropriate antibiotics and incubated at 37 °C overnight.

4.6.1.2 Preparation of electro-competent cells and transformation of *A. tumefaciens*

Transformation by electroporation was used for *E. coli* as well as for *A. tumefaciens*. A fresh over night culture was diluted at a ratio 1:100 in 400ml dYT liquid medium and shaked at 200 rpm until OD600 ≈ 0.7. The cells were then cooled on ice for 15-30 min and centrifuged at 3000 rpm 15 min 4 °C. Afterwards, the pellet was washed by 200 ml distilled H_2O twice. Subsequently the pellet was washed by 10 ml 10 % glycerol and resuspended in 0.5-1.0 ml 10% glycerol. Finally, 50 µl of the competent cells were aliquoted into pre-chilled 1.5 ml microcentrifuge tubes for immediate use, or stored at -80 °C for later use.

For transformation, the electro-competent cells were thawed on ice. Up to 5 µl DNA was added, gently mixed and transferred into a pre-chilled 0.2 cm electroporation cuvette. The mixture was then placed into the holder on the gene pulser (*E. coli* pulser Bio-Rad) and the pulse was directly initiated (25 mF, 200 W, 2.0 kV for *E. coli* and 1.6 kV for *A. tumefaciens*). After discharge (hold the button for 4-5 sec), 1ml dYT liquid medium was pipetted into the transformation mixture. Subsequently, the mixture was transferred into a

1.5 ml microcentrifuge tube and the cells were incubated at 600 rpm for 30-60 min. Finally, the entire cell suspension was plated on YT-agar containing appropriate antibiotics.

4.6.1.3 TOPO TA cloning

DNA fragments were amplified through PCR using Taq polymerase. The PCR product was then ligated with the TOPO TA cloning vector following the standard protocol (Invitrogen) and transformed into *E. coli* cells as described above. The transformant with blue colony were selected. The plasmids were extracted using the QIAquick plasmid purification kit following the standard protocol and finally verified by restriction enzyme digestion.

4.6.1.4 Expression of His-Stp1$_{\Delta 136\text{-}432}$, His-Stp1$_{433\text{-}515}$ and His-Aro7 in *E. coli*

A pre-culture of *E. coli* BL21 cells containing plasmids encoding corresponding proteins were grown overnight. The culture was diluted at a ratio 1:100 in 400 ml dYT liquid medium containing appropriate antibiotics and grown until OD600≈1.0. The protein expression was induced by 0.5 mM IPTG. The temperature was then shifted to 20 °C and the induction was continued for ~ 20 hours.

4.6.1.5 *N. benthamiana* infiltration for protein expression

The pre-culture of *A. tumefaciens* strains containing p19 and the plasmids encoding corresponding proteins were grown overnight. The culture was diluted at a ratio 1: 20 in 50 ml dYT liquid medium containing appropriate antibiotics and grown until OD600≈1.0 (about 4 hours). The cells were harvested by centrifuging at 6000 rpm, 5min, and room temperature. Then, the cells were washed three times by MES buffer. Afterwards, the pellets were re-suspended in MES buffer supplemented with 150 µM acetosyringone and the cell density was adjusted to OD600≈1.0. The cells suspension of *A. tumefaciens* strains containing p19 and the plasmids encoding corresponding proteins were mixed for infiltration of *N. benthamiana*.

For infiltration, 2-3 weeks (after singling out of the seedlings) old *N. benthamiana* was used. The *A. tumefaciens* mixture was infiltrated into the back side of the young leaves using 1ml syringe without the needle. For each plant, two young leaves were infiltrated. The infiltrated leaves were harvested by immediate frozen in liquid nitrogen and stocked in -80 °C for protein purification.

MES	10 mM MES, pH 5.6
	10 mM $MgCl_2$
	Add dH_2O and autoclave

4.6.2 *U. maydis* methods

Liquid cultures were incubated at 28 °C at 200 rpm. Solid media were incubated under aerobic condition at 28 °C. The cell density of culture was determined using a Novosec II Photometer (Pharmacia Biotech) at an optical density of 600 nm (OD600). The corresponding culture medium was used as a reference. A culture density of OD600 ≈1.0 corresponds to about 1-5 $\times 10^7$ cells/ml. To prepare frozen stocks, exponentially growing cultures were mixed with NSY-glycerol at a 1:1 ratio and stored at -80 °C.

4.6.2.1 Protoplast preparation and transformation of *U. maydis*

Protoplast preparation and transformation of *U. maydis* was performed as described by Schulz (Schulz *et al.*, 1990). Pre-culture of *U. maydis* cells were grown in $YEPS_{light}$ medium for at least 8 hours. The culture was diluted in 50 ml $YEPS_{light}$ medium at a ratio 1:300 to 500 and grown over night to OD600 0.5-0.8. Cells were harvested by centrifugation at room temperature for 5 min at 3500 rpm, washed in 25 ml SCS, and re-suspended in 2 ml SCS containing 2.5 mg/ml Novozyme. Cells were incubated for 5-10 min at room temperature until about 50 % of the cells are beginning to protoplast, which was monitored under the microscope. Afterwards, *U. maydis* cells were washed three times with 20 ml SCS and centrifuged at 2300 rpm for 5 min at room temperature. This was followed by an additional wash with 20 ml STC and centrifuged at 2400 rpm for 5 min at room temperature. Finally, protoplast pellets were re-suspended in 0.5 ml of ice cold STC, and 70 µl of protoplasts were aliquoted into pre-chilled 1.5 ml microcentrifuge tubes for immediate use, or stored at -80 °C for later use.

For transformation of protoplasts, 30 min before transformation, bottom plate was prepared by pour 10ml Regeneration Agar medium containing 2× appropriate antibiotics into the plate. Then, a second layer of Regeneration Agar medium (10ml, no antibiotics) was poured onto the bottom plate before transformation. Afterwards, one aliquot of protoplast was thawed on ice, 1 µl heparin (1 mg/ml) and 1-10 µl of DNA (3-5 µg) was added to the protoplast and the mixture was incubated on ice for 10 min. 500 µl STC/PEG were then

added to the protoplasts, mixed gently, and incubated for another 15 min on ice. Finally, the transformation mixture was plated on regeneration agar plates. Transformants appeared after 4-7 days were singled out and grown on PD-agar plates containing no antibiotics. Single colonies were picked and correct transformants were determined by southern blotting.

SCS	20 mM Na-citrate, pH 5.8 1 M Sorbitol Add dH_2O and autoclave
STC	10 mM Tris-Cl, pH 7.5 100 mM CaCl2 1 M Sorbitol Add dH_2O and autoclave
STC/PEG	40 % (w/v) PEG (MW: 3350) Add STC and autoclave

4.6.2.2 Pathogenicity assays

Pathogenicity assays were performed as described by Kämper (2006). For maize (*Zea mays*) infections, pre-cultures of *U. maydis* strains were grown in $YEPS_{light}$ medium over night. The culture was diluted in 50 ml $YEPS_{light}$ medium to an OD600 of 0.4 and grew for about 1 hour 45 min to an OD600 ≈ 1.0. The cells were then harvested and resuspended in distilled water to an OD600 of 1.0 and injected into 7-day-old seedlings of the Early Golden Bantam (Olds Seeds, Madison, WI). Plants were kept in the greenhouse with a light-dark cycle of 16 (28 °C) and 8 hrs (20 °C). Disease symptoms were scored according to severity 12 days after infection (Kämper et al., 2006).

4.6.3 *S. cerevisiae* methods

Liquid cultures were incubated at 28 °C at 200 rpm. Solid media were incubated under aerobic condition at 28 °C. To prepare frozen stocks, exponentially growing cultures were mixed with NSY-glycerol at a 1:1 ratio and stored at -80 °C.

4.6.3.1 Preparation of compentent cells and transformation of *S. cerevisiae*

An overnight pre-culture of *S. cerevisiae* AH109 was diluted in 50ml YEPD medium at a ratio 1:50 and grew until OD600 ≈ 0.5-0.7 (4-6 hours). The cells were harvested by centrifuging at 2000 rpm/500 g, 3 min and room temperature. The pellet was then wash once by 15 ml sterile H_2O and once by 10 ml SORB. The cells were re-suspended in 400 µl SORB supplemented with 40 µl carrier DNA (10 mg/ml Herring sperm DNA, denatured at 100 °C for 10 min and cooled on ice, Invitrogen). 50 µl of cell suspension were aliquoted into pre-chilled 1.5 ml microcentrifuge tubes for immediate use, or stored at -80 °C for later use.

For yeast transformation, the protocol of Burke was followed (Burke *et al.*, 2000). An aliquot of competent cells was thawed. Subsequently, plasmid DNA (maximal 2µl plasmid DNA/10 µl competent cells) was added, gently mixed, then, 6 fold volume of the sterile PEG was added gently mixed and incubated at 30 °C for 30 min. The mixture was then heat shocked at 42 °C for 15 min and centrifuged at 2000 rpm, 3 min and room temperature. The cell pellet was then washed once with 1ml YEPD medium. For the recovery of the *S. cerevisiae* cells, the pellet was re-suspended in 1 ml YEPD medium and incubated at 500 rpm for 2-3 hours at 30 °C. Finally, the entire cell suspension was plated on SD medium plate.

SORB	10 mM Tris-HCl, pH 8.0
	100 mM lithium acetate
	1 M sorbitol
	1 mM EDTA
	Add dH_2O and autoclave
PEG	10 mM Tris-HCl, pH 8.0
	100 mM lithium acetate
	40 % PEG 3350
	1 mM EDTA
	Add dH_2O and autoclave

4.6.3.2 Yeast two-hybrid assay

The yeast two hybrid analysis was performed using the matchmarker GAL4 two hybrid system 3 (Clontech) following the manufacturer's instructions. Transformants were

spreaded on synthetic dropout medium plates without leucine and tryptophan. Growth assays were tested on synthetic dropout medium plates either without leucine, tryptophan or without Adenine, leucine, tryptophan and histidine.

4.6.3.3 Re-transformation and growth assay

The plasmids constructed on the backbone of either pGAD or pGBK were co-transformed into AH109. The transformants were grown in SD-Leu-Trp medium overnight. The cultures were adjusted to OD600≈ 1.0 and serial dilutions were spotted on the plates containing low stringency medium (-Leu-Trp) and the plates containing high stringency medium (-Leu-Trp-His-Ade) at the same time. The plates were incubated for three days before observation. The expression of genes was determined by Western blotting using HA antibody for activation domain and c-Myc antibody for DNA binding domain.

4.7 Molecular biological methods

Standard molecular biology methods are performed following protocols as described by Ausubel and Sambrook (Ausubel *et al.*, 1987, Sambrook *et al.*, 1989). The concentration of nucleic acids was determined by photometry (NanoDrop ND-1000 Spectrophotometer). The plasmid DNA purification was performed using QIAprep spin miniprep kit (QIAGEN) following the manufacturer's instructions. DNA fragment was purified using Wizard® SV Gel and PCR Clean-Up System (Promega) following the manufacturer' instructions. The preparation of genomic DNA from *U. maydis* was performed following the protocol of Hoffman and Winston (Hoffman & Winston, 1987).

4.7.1 Southern blotting

10 µl of genomic DNA was digested overnight with respective restriction enzymes (*Nde*I/*Bam*HI for cbx locus) in 20 µl volume. Digestions were separated on a 1× TAE 0.8 % agarose gel for about 4 hours at 90 V. The gels were soaked in 0.25 M HCl solution with shaking for 20-30 min until bromothymol blue turns yellow. HCl solution was then replaced by 0.4 M NaOH and incubated for 20-30 min with shaking until the color turns blue again. Subsequently, DNA was transferred from the gel to nylon membrane in 0.4 M NaOH for 2 hours (change the tissue every 30 min). The membrane was UV cross-linked at 1200 µJoules (100×) (UV Stratalinker 1800, Stratagene). Dig-labeling probe was generated

as described in the PCR DIG Labeling Mix protocol (Roche, Mannhein). The hybridization, wash and exposure steps were performed following the protocol of (Sambrook et al., 1989).

4.7.2 Western blotting

Proteins were separated by SDS-PAGE and transferred to a PVDF (polyvinylidene difluoride) membrane at 40-45 mA and 25 V for 1-2 hours. Afterwards, the membrane was blocked with TBST buffer containing 5 % non-fat dry milk at room temperature for at least one hour. The membrane was then incubated with respective primary antibody (Table. 15) diluted in TBST buffer containing 3 % non-fat dry milk for at least one hour. Subsequently, the membrane was washed three times with TBST buffer for 10 min. Then, the membrane was incubated with respective secondary antibody (Table. 15) diluted in TBST buffer containing 3 % non-fat dry milk for at least 1 hour. Subsequently, the membrane was washed three times with TBST buffer for 10 min. Chemiluminescent detection was performed using an ECL kit (Amersham Biosciences, cat. no. RPN-2106) following the manufacturer's instructions.

Table 15. Antibodies used in this study

Antibody	Source	Suppler	Working solution
α-c-myc	mouse	Sigma M5546	1:3,000
α -HA	mouse	Sigma H9658	1:3,000
α -BD	mouse	Santa Crutz biotechnology sc-510	1:2,000
α -AD	mouse	Santa Crutz biotechnology sc1663	1:2,000
Goat anti-Mouse IgG, Cy3 conjugate	Goat	Millipore AP124C	1: 300
Goat anti-Rabbit IgG, Cy3 conjugate	Goat	Millipore AP132C	1: 300
Rabbit anti-Mouse IgG	Rabbit	Life Technologies 61-6000	1: 500
α -mouse IgG, HRP-linked antibody	horse	Cell Signaling Technology #7076	1:10,000

TBST

50mM Tris-HCl, pH 7.4
150mM NaCl
0.1 % Tween-20
Add dH_2O and autoclave

4.7.3 Isolation of Plasmid DNA from *S. cerevisiae*

The yeast cells were collected by centrifugation. Then, 0.4 ml ustilago-lysis buffer, a spoon of glass beads and 0.4 ml phenol-chloroform was added subsequently into the tube. The mixture was vibrated for 1,500 rpm for 15-30 min and centrifuged at 13,000 rpm for 5 min. The upper layer was then transferred into a new 1.5 ml tube and 0.4 ml of chloroform was added. The mixture was vibrated for 10 min and centrifuged at 13,000 rpm for 5 min. Afterwards, the upper layer was transferred into a new 1.5 ml tube and 2.5×volume of 100 % ethanol was added into the new tube and mixed. After centrifugation, the pellet was washed once by 70 % ethanol and incubated at room temperature for 10 min for drying. The DNA was re-suspended in 30 µl of H_2O.

Ustilago-lysis	50 mM Tris-HCl, pH 7.5
	50 mM Na_2-EDTA
	1 % (w/v) SDS
	Add dH_2O

4.7.4 Protein extraction from *S. cerevisiae*

The yeast cells were harvested by centrifugation. Then, SDS-PAGE loading buffer supplemented with 100mM DTT was added and the mixture was incubated at 100 °C for 10 min. Then, the mixture was vortexed for 5 min. This was followed by incubation at 100 °C for 10 min again. Afterwards, the mixture was centrifuged for 5 min and the supernatant was transfered into a new tube for loading onto SDS-PAGE.

4×SDS-PAGE Loading	150 mM Tris-HCl, pH 7.0
	12 % SDS (w/v),
	6 % β-mercaptoethanol (v/v)
	0.05 % Coomassie blue G-250
	30 % glycerol (w/v)
	Add dH_2O

4.8 Biochemical methods

The concentration of proteins was determined using Roti®-Quant (Proteinbestimmung nach Bradford, Carl Roth) (Bradford, M., 1976, Anal. Biochem. 72, 248-254.) following the

manufaturer's instruction. Proteins was detected using SDS-PAGE Tris-Glycine gel system or Tricine gel system described by Hermann Schägger depending on the size of the proteins (Schagger, 2006).

4.8.1 Purification of GST-tagged protein

E. coli cells expressing recombinant protein were harvested by centrifugation at 8000 rpm for 8 min at 4 °C (could be stored at -20°C for later purification if necessary). The cells were dispersed in pre-chilled lysis buffer (PBS) at a ratio of 1 g/2-5 ml lysis buffer. After adding PMSF, the cells were sonicated (Duty cylcle 50 %, output 4, 0.5 min/ 1.5 min×6) and centrifuged for 30 min at 4 °C twice at 17,000 rpm. The supernatant was pipetted onto PBS equilibrated glutathione sepharose™ 4 fast flow resin (GE Healthcare, Uppsala). The tube was applied onto test tube rotator and incubated at 4 °C for 2 hours. The tube was centrifuged at 500 g for 5min at 4 °C to remove the supernatant and washed three times. To elute the protein from the resin, 1 CV (column volume) GST elution buffer was added and incubated for 20 min at room temperature. This step was repeat twice and the three elutes were pooled together.

100×PMSF stock solution (10 mM)	1.74 mg/ml PMSF Add isopropanol and store at -20 °C
10×PBS	17.8 g $Na_2HPO_4 \cdot 2H_2O$ pH 7.4 2.4 g $KHPO_4$ 2 g KCl 80 g NaCl Add dH_2O to 1L and autoclave
GST elution buffer	20 mM glutathione Add PBS and sterile filtered

4.8.2 Purification of Strep-tagged protein

E. coli cells were harvested and dispersed in pre-chilled buffer W at a ratio of 1 g/2-5 ml lysis buffer. Lysozyme, DNase I and Protease Inhibitor Cocktail (Roche Diagnostics) was added to the suspension and incubated for 30 min. The cells were broken using French

pressure cell press (SLM Aminco) at high ratio, 1000 psi. The lysate was centrifuged for 30 min at 4 °C twice at 17,000 rpm. The supernatant was then pipetted onto buffer W equilibrated column filled with Strep-Tactin Resins (IBA). The column was washed five times with buffer W. Finally, the protein was eluted by 6×0.5 CV buffer E. The resin was regenerated by wash with 3× 5 CV buffer R.

Buffer W (washing buffer)	100 mM Tris-HCl pH 8.0 150 mM NaCl 1 mM EDTA Add H_2O and autoclave
Buffer W (washing buffer)	100 mM Tris-HCl pH 8.0 150 mM NaCl 1 mM EDTA 2.5 mM desthiobiotin Add H_2O and autoclave
Buffer W (washing buffer)	100 mM Tris-HCl pH 8.0 150 mM NaCl 1 mM EDTA 1 mM HABA (hydroxy-azophenyl-benzoic acid) Add H_2O and autoclave

4.8.3 Purification of His-tagged protein

The cell lysate was prepared as describe in strep-tagged protein purification above. The supernatant was then pipetted onto his lysis buffer equilibrated column filled with Ni-NTA-agarose (Qiagen). The column was washed twice with his lysis buffer. Finally, the protein was eluted by 4 × 1.5 CV his elution buffer.

The protein purified from NTA-agarose was diluted 3-5 times and loaded onto MonoQ TM 5/50 GL column in AKTA FPLC System (GE Healthcare). After washing by 2 CV MonoQ start buffer, the protein was eluted by gradient elution with 25 CV from 0 % MonoQ elution buffer to 60 % MonoQ elution buffer. The column was cleaned by 5 CV MonoQ elution buffer and equilibrated by 5 CV MonoQ start buffer.

The protein purified from MonoQ column was concentrated on Amicon Ultra-4 3 kDa columns (Millipore) at 3000 g. The concentrated protein was loaded onto the Superdex^{TM} 75 10/300 GL (GE Healthcare) column and eluted using Gel filtration buffer at fraction size 0.5 ml and flow rate 0.5 ml/min.

His lysis	20 mM Tris-HCl pH 7.4 150 mM NaCl 20 mM Imidazole 1 mM EDTA Add H_2O and sterile filtered
His elution	20 mM Tris-HCl pH 7.4 150 mM NaCl 0.5 M Imidazole 1 mM EDTA Add H_2O and sterile filtered
MonoQ start	20 mM Tris-HCl pH 7.0 1 mM EDTA Add H_2O and sterile filtered
MonoQ elution	20 mM Tris-HCl pH 7.0 1 M NaCl 1 mM EDTA Add H_2O and sterile filtered
Gel filtration	15 mM Tris-HCl pH 7.0 5 mM NaCl Add H_2O and sterile filtered

4.8.4 Protein purification from *N. benthamiana*

Frozen tissue (about 4 leaves) was ground in liquid nitrogen, re-suspended in 6 ml BP buffer and centrifuged at 40,000g for 10 min at 4 °C. The supernatant was filtered through a filter pipette into a 15 ml tube with the IgG beads (Mouse IgG-Agarose, A0919, Sigma)

equilibrated with BP buffer without protease inhibitors. The mixture was incubate on a test tube rotator for 2 hours at 4 °C and centrifuged for 5 min at 1500 g. The supernatant was removed and 500 µl BP buffer was added into the tube and transferred into a 1.5 ml tube. The beads were then washed by 0.5 ml BP once and 1 ml BP2 twice. 50 µl BP2 containing the cleavage protease was added into the tube and incubated on a test tube rotator for at least 16 hours. Finally, the beads were span down and the supernatant containing the protein was transferred into a new tube.

BP	100 mM Tris-HCl pH 7.5
	100 mM NaCl
	5 mM EDTA
	5 mM EGTA
	10 mM NaF
	0.1 % Triton-X100
	1 mM β-mercaptoethanol
	10 % Glycerol
	0.1 mM $NaVO_3$
	10 mM β-GPh
	Protease inhibitors
	Add H_2O and sterile filtered
BP2	50 mM HEPES pH 7.0
	150 mM NaCl
	1 mM DTT
	0.1 % Triton-X100
	Add H_2O and sterile filtered
1000×Protease inhibitors	1 M Benzamidine in ethanol
	10 mg/ml Aprotinin in H_2O
	1 M 1-10 phenantroline in ethanol

4.8.5 Cysteine pretease activity and inhibition assay

The cyteine protease was activated by adding 10 mM DTT, adjusting pH to pH 4.0-4.5 with acetic acid and incubating at 30 °C for 1 hour. The enzymatic activity was tested in a 200 µl volume containing 100 µl NaPi buffer, cysteine protease, and 2 µM substrate (Z-Phe-Arg-AMC, PeptaNova). The progress of the reaction was monitored using fluorimeter (SAFIRE, Tecan).

NaPi Buffer	0.1 M Na phosphate pH 6.0
	Add H_2O and autoclave

4.9 Staining and microscopy observation

All the confocal images were taken using a TCS-SP5 confocal microscopy (Leica). WGA-AF488 was excited was at 488 nm and detected at 500-540 nm; Propidium Iodide was excited was at 561 nm and detected at 580-660 nm; Anniline blue was excited was at 405 nm and detected at 490-520 nm; DAPI was excited was at 405 nm and detected at 430-480 nm; Cy3 was excited was at 561 nm and detected at 573-610 nm; mCherry was excited was at 561 nm and detected at 573-610 nm.

4.9.1 WGA-AF488 / Propidium Iodide staining

Infected leaf tissue was harvested and cleared in ethanol overnight (or longer). The samples were then treated with 10 % KOH at 85 °C for 3-4 h. After washing with PBS for 2-4 times, the samples were incubated in staining solution for 30 min (vacuum infiltrate the samples three times for about 1-2 min) and destained in 1x PBS. Then, the samples were stored in dark at 4 °C until analysis. By this stain, fungal hyphae were stained with Fluorescein WGA (Vector Laboratories); Plant membranes were visualized using Propidium Iodide (Fluka).

Staining solution	20 µg/ml Propidium Iodide
	10 µg/ml WGA-AF
	0.02 % Tween-20
	PBS (pH 7.4)

4.9.2 Anniline blue / Propidium Iodide staining

Infected leaf tissue was harvested and rinsed twice with 50 % ethanol. The samples were then rinsed with 0.1 M Na_2HPO_4 buffer (pH≈9.0 without adjusting). Afterwards, incubate the samples in 20 µg/ml Propidium Iodide for 30 min and rinse the samples with 0.1 M Na_2HPO_4 buffer again. Subsequently, freshly prepared 0.05 % aniline blue (w/v in 0.1 M Na_2HPO_4 buffer) was added and incubated for 1 hour in dark. The sample was finally prepared on slides in 0.05 % aniline blue.

4.9.3 Chlorazol Black E staining

Infected leaf tissue was harvested and cleared in ethanol overnight (or longer). The samples were then treated with 10 % KOH at 85 °C for 3-4 h. After washing with dH_2O once, the samples was soak in chlorazol Black E staining solution (0.03 % Chlorazol black E in a 1:1:1 solution of dH_2O, lactic acid and glycerol) overnight at 60 °C. Afterwards, the samples were destained (or stored) for 3 days in 50 % glycerol.

5. References

Abramovitch, R. B. & G. B. Martin, (2005) AvrPtoB: a bacterial type III effector that both elicits and suppresses programmed cell death associated with plant immunity. *FEMS microbiology letters* 245: 1-8.

Aichinger, C., K. Hansson, H. Eichhorn, F. Lessing, G. Mannhaupt, W. Mewes & R. Kahmann, (2003) Identification of plant-regulated genes in Ustilago maydis by enhancer-trapping mutagenesis. *Mol Genet Genomics* 270: 303-314.

Ausubel, F. M., R., R. E. Brent, D. D. Kingston, J. G. Moore, J. A. S. Seidman & K. Struhl, (1987) Current Protocols in Molecular Biology. *Greene Publishing Associates/Wiley Interscience, New York.*

Banuett, F., (1992) Ustilago maydis, the delightful blight. *Trends Genet* 8: 174-180.

Basse, C. W. & G. Steinberg, (2004) Ustilago maydis, model system for analysis of the molecular basis of fungal pathogenicity. *Mol Plant Pathol* 5: 83-92.

Bennetzen, J. L. H., Sarah C. (Eds.), (2009) Handbook of Maize, Genetics and Genomics. XII, 800 p. 894 illus.

Benz, B. F., (2001) Archaeological evidence of teosinte domestication from Guila Naquitz, Oaxaca. *Proc Natl Acad Sci U S A* 98: 2104-2106.

Bhattacharjee, S., R. V. Stahelin, K. D. Speicher, D. W. Speicher & K. Haldar, (2012) Endoplasmic reticulum PI(3)P lipid binding targets malaria proteins to the host cell. *Cell* 148: 201-212.

Bolker, M., (2001) Ustilago maydis--a valuable model system for the study of fungal dimorphism and virulence. *Microbiology* 147: 1395-1401.

Bölker, M., Genin, S., Lehmler, C. and Kahmann, R, (1995) Genetic regulation of mating and dimorphism in Ustilago maydis. *Can. J. Bot* 73: 320-325

Bonas, U. & G. Van den Ackervaken, (1997) Recognition of bacterial avirulence proteins occurs inside the plant cell: a general phenomenon in resistance to bacterial diseases? *Plant J* 12: 1-7.

Bozkurt, T. O., S. Schornack, M. J. Banfield & S. Kamoun, (2012) Oomycetes, effectors, and all that jazz. *Curr Opin Plant Biol*.

Bozkurt, T. O., S. Schornack, J. Win, T. Shindo, M. Ilyas, R. Oliva, L. M. Cano, A. M. E. Jones, E. Huitema, R. A. L. van der Hoorn & S. Kamoun, (2011) Phytophthora infestans effector AVRblb2 prevents secretion of a plant immune protease at the haustorial interface. *Proc Natl Acad Sci U S A* 108: 20832-20837.

Bradford, M. M., (1976) A rapid and sensitive method for the quantitation of microgram quantities of protein utilizing the principle of protein-dye binding. *Anal Biochem* 72: 248-254.

Brefort, T., G. Doehlemann, A. Mendoza-Mendoza, S. Reissmann, A. Djamei & R. Kahmann, (2009) Ustilago maydis as a Pathogen. *Annu Rev Phytopathol* 47: 423-445.

Bull, J., F. Mauch, C. Hertig, G. Rebmann & R. Dudler, (1992) Sequence and Expression of a Wheat Gene That Encodes a Novel Protein Associated with Pathogen Defense. *Mol Plant Microbe In* 5: 516-519.

Burke, D., D. Dawson & T. Stearns, (2000) Methods in Yeast Genetics: A Cold Spring Harbor Laboratory Course Manual. *Cold Spring Harbor Laboratory Press, New York.*

Chisholm, S. T., G. Coaker, B. Day & B. J. Staskawicz, (2006) Host-microbe interactions: shaping the evolution of the plant immune response. *Cell* 124: 803-814.

Chung, C. L., J. M. Longfellow, E. K. Walsh, Z. Kerdieh, G. Van Esbroeck, P. Balint-Kurti & R. J. Nelson, (2010) Resistance loci affecting distinct stages of fungal pathogenesis: use of introgression lines for QTL mapping and characterization in the maize - Setosphaeria turcica pathosystem. *Bmc Plant Biol* 10.

Collier, S. M. & P. Moffett, (2009) NB-LRRs work a "bait and switch" on pathogens. *Trends in plant science* 14: 521-529.

Cornelis, G. R. & F. Van Gijsegem, (2000) Assembly and function of type III secretory systems. *Annual review of microbiology* 54: 735-774.

de Jonge, R., M. D. Bolton & B. P. Thomma, (2011) How filamentous pathogens co-opt plants: the ins and outs of fungal effectors. *Curr Opin Plant Biol* 14: 400-406.

de las Mercedes Dana, M., J. A. Pintor-Toro & B. Cubero, (2006) Transgenic tobacco plants overexpressing chitinases of fungal origin show enhanced resistance to biotic and abiotic stress agents. *Plant Physiol* 142: 722-730.

de Wit, P. J., (2007) How plants recognize pathogens and defend themselves. *Cellular and molecular life sciences : CMLS* 64: 2726-2732.

Dean, R., J. A. Van Kan, Z. A. Pretorius, K. E. Hammond-Kosack, A. Di Pietro, P. D. Spanu, J. J. Rudd, M. Dickman, R. Kahmann, J. Ellis & G. D. Foster, (2012) The Top 10 fungal pathogens in molecular plant pathology. *Mol Plant Pathol* 13: 414-430.

Dixon, M. S., C. Golstein, C. M. Thomas, E. A. van Der Biezen & J. D. Jones, (2000) Genetic complexity of pathogen perception by plants: the example of Rcr3, a tomato gene required specifically by Cf-2. *Proc Natl Acad Sci U S A* 97: 8807-8814.

Djamei, A., K. Schipper, F. Rabe, A. Ghosh, V. Vincon, J. Kahnt, S. Osorio, T. Tohge, A. R. Fernie, I. Feussner, K. Feussner, P. Meinicke, Y. D. Stierhof, H. Schwarz, B. Macek, M. Mann & R. Kahmann, (2011) Metabolic priming by a secreted fungal effector. *Nature* 478: 395-398.

Dodds, P. N. & J. P. Rathjen, (2010) Plant immunity: towards an integrated view of plant-pathogen interactions. *Nature reviews. Genetics* 11: 539-548.

Doehlemann, G., S. Reissmann, D. Assmann, M. Fleckenstein & R. Kahmann, (2011) Two linked genes encoding a secreted effector and a membrane protein are essential for Ustilago maydis-induced tumour formation. *Mol Microbiol* 81: 751-766.

Doehlemann, G., K. van der Linde, D. Assmann, D. Schwammbach, A. Hof, A. Mohanty, D. Jackson & R. Kahmann, (2009) Pep1, a secreted effector protein of Ustilago maydis, is required for successful invasion of plant cells. *PLoS Pathog* 5: e1000290.

Doehlemann, G., R. Wahl, R. J. Horst, L. M. Voll, B. Usadel, F. Poree, M. Stitt, J. Pons-Kuhnemann, U. Sonnewald, R. Kahmann & J. Kamper, (2008) Reprogramming a maize plant: transcriptional and metabolic changes induced by the fungal biotroph Ustilago maydis. *Plant J* 56: 181-195.

Dou, D., S. D. Kale, X. Wang, R. H. Jiang, N. A. Bruce, F. D. Arredondo, X. Zhang & B. M. Tyler, (2008) RXLR-mediated entry of Phytophthora sojae effector Avr1b into soybean cells does not require pathogen-encoded machinery. *Plant Cell* 20: 1930-1947.

Dubery, I. A., N. M. Sanabria & J. C. Huang, (2012) Nonself perception in plant innate immunity. *Adv Exp Med Biol* 738: 79-107.

Ellis, J. G., M. Rafiqi, P. Gan, A. Chakrabarti & P. N. Dodds, (2009) Recent progress in discovery and functional analysis of effector proteins of fungal and oomycete plant pathogens. *Curr Opin Plant Biol* 12: 399-405.

Feng, F. & J. M. Zhou, (2012) Plant-bacterial pathogen interactions mediated by type III effectors. *Curr Opin Plant Biol*.

Fontana, A., P. P. de Laureto, B. Spolaore, E. Frare, P. Picotti & M. Zambonin, (2004) Probing protein structure by limited proteolysis. *Acta Biochim Pol* 51: 299-321.

Food and Agriculture Organization of the United Nations, S. D., Statistics Division, (2010)

Fradin, E. F. & B. P. H. J. Thomma, (2006) Physiology and molecular aspects of Verticillium wilt diseases caused by V-dahliae and V-albo-atrum. *Molecular Plant Pathology* 7: 71-86.

Frederick, R. D., R. L. Thilmony, G. Sessa & G. B. Martin, (1998) Recognition specificity for the bacterial avirulence protein AvrPto is determined by Thr-204 in the activation loop of the tomato Pto kinase. *Mol Cell* 2: 241-245.

Fujikawa, T., A. Sakaguchi, Y. Nishizawa, Y. Kouzai, E. Minami, S. Yano, H. Koga, T. Meshi & M. Nishimura, (2012) Surface alpha-1,3-Glucan Facilitates Fungal Stealth Infection by Interfering with Innate Immunity in Plants. *PLoS Pathog* 8: e1002882.

Galea, C. A., Y. Wang, S. G. Sivakolundu & R. W. Kriwacki, (2008) Regulation of cell division by intrinsically unstructured proteins: intrinsic flexibility, modularity, and signaling conduits. *Biochemistry* 47: 7598-7609.

Gao, D., J. Kim, H. Kim, T. L. Phang, H. Selby, A. C. Tan & T. Tong, (2010) A survey of statistical software for analysing RNA-seq data. *Human genomics* 5: 56-60.

Guo, M., M. A. Rupe, J. A. Dieter, J. Zou, D. Spielbauer, K. E. Duncan, R. J. Howard, Z. Hou & C. R. Simmons, (2010) Cell Number Regulator1 affects plant and organ size in maize: implications for crop yield enhancement and heterosis. *Plant Cell* 22: 1057-1073.

Hanahan, D., (1985) In DNA Cloning - a Practical Approach. *(Glover, D.M., ed.). IRL Press, McLean, Virginia.* 1: 109.

Hann, D. R., S. Gimenez-Ibanez & J. P. Rathjen, (2010) Bacterial virulence effectors and their activities. *Curr Opin Plant Biol* 13: 388-393.

Hann, D. R. & J. P. Rathjen, (2010) The long and winding road: virulence effector proteins of plant pathogenic bacteria. *Cellular and molecular life sciences : CMLS* 67: 3425-3434.

Hardcastle, T. J. & K. A. Kelly, (2010) baySeq: empirical Bayesian methods for identifying differential expression in sequence count data. *BMC bioinformatics* 11: 422.

Harris, L. J., A. Saparno, A. Johnston, S. Prisic, M. Xu, S. Allard, A. Kathiresan, T. Ouellet & R. J. Peters, (2005) The maize An2 gene is induced by Fusarium attack and encodes an ent-copalyl diphosphate synthase. *Plant Molecular Biology* 59: 881-894.

Haseloff, J., K. R. Siemering, D. C. Prasher & S. Hodge, (1997) Removal of a cryptic intron and subcellular localization of green fluorescent protein are required to mark transgenic Arabidopsis plants brightly. *Proc Natl Acad Sci U S A* 94: 2122-2127.

Hemetsberger, C., C. Herrberger, B. Zechmann, M. Hillmer & G. Doehlemann, (2012) The Ustilago maydis effector Pep1 suppresses plant immunity by inhibition of host peroxidase activity. *PLoS Pathog* 8: e1002684.

Hoffman, C. S. & F. Winston, (1987) A ten-minute DNA preparation from yeast efficiently releases autonomous plasmids for transformation of Escherichia coli. *Gene* 57: 267-272.

Holliday, R., (2004) Early studies on recombination and DNA repair in Ustilago maydis. *DNA Repair (Amst)* 3: 671-682.

Jefferson, R. A., T. A. Kavanagh & M. W. Bevan, (1987) GUS fusions: beta-glucuronidase as a sensitive and versatile gene fusion marker in higher plants. *EMBO J* 6: 3901-3907.

Jones, H. D., S. Kurup, N. C. B. Peters & M. J. Holdsworth, (2000) Identification and analysis of proteins that interact with the Avena fatua homologue of the maize transcription factor VIVIPAROUS 1. *Plant Journal* 21: 133-142.

Jones, J. D. & J. L. Dangl, (2006) The plant immune system. *Nature* 444: 323-329.

Kahmann, R. S., G.; Basse, C.; Feldbrügge, M.; Kämper, J. , (2000) Ustilago maydis, the causative agent of corn smut disease. *Fungal pathology* 347-371

Kale, S. D., B. Gu, D. G. Capelluto, D. Dou, E. Feldman, A. Rumore, F. D. Arredondo, R. Hanlon, I. Fudal, T. Rouxel, C. B. Lawrence, W. Shan & B. M. Tyler, (2010) External lipid PI3P mediates entry of eukaryotic pathogen effectors into plant and animal host cells. *Cell* 142: 284-295.

Kamper, J., (2004) A PCR-based system for highly efficient generation of gene replacement mutants in Ustilago maydis. *Mol Genet Genomics* 271: 103-110.

Kamper, J., R. Kahmann, M. Bolker, L. J. Ma, T. Brefort, B. J. Saville, F. Banuett, J. W. Kronstad, S. E. Gold, O. Muller, M. H. Perlin, H. A. Wosten, R. de Vries, J. Ruiz-Herrera, C. G. Reynaga-Pena, K. Snetselaar, M. McCann, J. Perez-Martin, M. Feldbrugge, C. W. Basse, G. Steinberg, J. I. Ibeas, W. Holloman, P. Guzman, M. Farman, J. E. Stajich, R. Sentandreu, J. M. Gonzalez-Prieto, J. C. Kennell, L. Molina, J. Schirawski, A. Mendoza-Mendoza, D. Greilinger, K. Munch, N. Rossel, M. Scherer, M. Vranes, O. Ladendorf, V. Vincon, U. Fuchs, B. Sandrock, S. Meng, E. C. Ho, M. J. Cahill, K. J. Boyce, J. Klose, S. J. Klosterman, H. J. Deelstra, L. Ortiz-Castellanos, W. Li, P. Sanchez-Alonso, P. H. Schreier, I. Hauser-Hahn, M. Vaupel, E. Koopmann, G. Friedrich, H. Voss, T. Schluter, J. Margolis, D. Platt, C. Swimmer, A. Gnirke, F. Chen, V. Vysotskaia, G. Mannhaupt, U. Guldener, M. Munsterkotter, D. Haase, M. Oesterheld, H. W. Mewes, E. W. Mauceli, D. DeCaprio, C. M. Wade, J. Butler, S. Young, D. B. Jaffe, S. Calvo, C. Nusbaum, J. Galagan & B. W. Birren, (2006) Insights from the genome of the biotrophic fungal plant pathogen Ustilago maydis. *Nature* 444: 97-101.

Kankanala, P., K. Czymmek & B. Valent, (2007) Roles for rice membrane dynamics and plasmodesmata during biotrophic invasion by the blast fungus. *Plant Cell* 19: 706-724.

Kasparovsky, T., J. P. Blein & V. Mikes, (2004) Ergosterol elicits oxidative burst in tobacco cells via phospholipase A2 and protein kinase C signal pathway. *Plant physiology and biochemistry : PPB / Societe francaise de physiologie vegetale* 42: 429-435.

Kemen, E., A. C. Kemen, M. Rafiqi, U. Hempel, K. Mendgen, M. Hahn & R. T. Voegele, (2005) Identification of a protein from rust fungi transferred from haustoria into infected plant cells. *Molecular plant-microbe interactions : MPMI* 18: 1130-1139.

Khang, C. H., R. Berruyer, M. C. Giraldo, P. Kankanala, S. Y. Park, K. Czymmek, S. Kang & B. Valent, (2010) Translocation of Magnaporthe oryzae effectors into rice cells and their subsequent cell-to-cell movement. *Plant Cell* 22: 1388-1403.

Kloppholz, S., H. Kuhn & N. Requena, (2011) A secreted fungal effector of Glomus intraradices promotes symbiotic biotrophy. *Current biology : CB* 21: 1204-1209.

Koeck, M., A. R. Hardham & P. N. Dodds, (2011) The role of effectors of biotrophic and hemibiotrophic fungi in infection. *Cellular microbiology* 13: 1849-1857.

Kunitz, M. & J. H. Northrop, (1936) Isolation from Beef Pancreas of Crystalline Trypsinogen, Trypsin, a Trypsin Inhibitor, and an Inhibitor-Trypsin Compound. *The Journal of general physiology* 19: 991-1007.

Kunkel, B. N. & D. M. Brooks, (2002) Cross talk between signaling pathways in pathogen defense. *Curr Opin Plant Biol* 5: 325-331.

Kvam, V. M., P. Liu & Y. Si, (2012) A comparison of statistical methods for detecting differentially expressed genes from RNA-seq data. *American journal of botany* 99: 248-256.

Kvitko, B. H., D. H. Park, A. C. Velasquez, C. F. Wei, A. B. Russell, G. B. Martin, D. J. Schneider & A. Collmer, (2009) Deletions in the repertoire of Pseudomonas syringae pv. tomato DC3000 type III secretion effector genes reveal functional overlap among effectors. *PLoS Pathog* 5: e1000388.

Laurie, J. D., S. Ali, R. Linning, G. Mannhaupt, P. Wong, U. Guldener, M. Munsterkotter, R. Moore, R. Kahmann, G. Bakkeren & J. Schirawski, (2012) Genome comparison of barley and maize smut fungi reveals targeted loss of RNA silencing components and species-specific presence of transposable elements. *Plant Cell* 24: 1733-1745.

Lee, M. W., J. Jelenska & J. T. Greenberg, (2008) Arabidopsis proteins important for modulating defense responses to Pseudomonas syringae that secrete HopW1-1. *Plant Journal* 54: 452-465.

Leung-Toung, R., W. R. Li, T. F. Tam & K. Karimian, (2002) Thiol-dependent enzymes and their inhibitors: A review. *Curr Med Chem* 9: 979-1002.

Loubradou, G., A. Brachmann, M. Feldbrugge & R. Kahmann, (2001) A homologue of the transcriptional repressor Ssn6p antagonizes cAMP signalling in Ustilago maydis. *Mol Microbiol* 40: 719-730.

Martinez, M., I. Cambra, L. Carrillo, M. Diaz-Mendoza & I. Diaz, (2009) Characterization of the entire cystatin gene family in barley and their target cathepsin L-like cysteine-proteases, partners in the hordein mobilization during seed germination. *Plant Physiol* 151: 1531-1545.

Mauch, F. & R. Dudler, (1993) Differential induction of distinct glutathione-S-transferases of wheat by xenobiotics and by pathogen attack. *Plant Physiol* 102: 1193-1201.

Mortazavi, A., B. A. Williams, K. McCue, L. Schaeffer & B. Wold, (2008) Mapping and quantifying mammalian transcriptomes by RNA-Seq. *Nature methods* 5: 621-628.

Mowbray, S. L., L. T. Elfstrom, K. M. Ahlgren, C. E. Andersson & M. Widersten, (2006) X-ray structure of potato epoxide hydrolase sheds light on substrate specificity in plant enzymes. *Protein Sci* 15: 1628-1637.

Munis, M. F., L. Tu, F. Deng, J. Tan, L. Xu, S. Xu, L. Long & X. Zhang, (2010) A thaumatin-like protein gene involved in cotton fiber secondary cell wall development enhances resistance against Verticillium dahliae and other stresses in transgenic tobacco. *Biochem Biophys Res Commun* 393: 38-44.

Munkvold, K. R. & G. B. Martin, (2009) Advances in experimental methods for the elucidation of Pseudomonas syringae effector function with a focus on AvrPtoB. *Mol Plant Pathol* 10: 777-793.

Nunez-Corcuera, B., I. Serafimidis, E. Arias-Palomo, A. Rivera-Calzada & T. Suarez, (2008) A new protein carrying an NmrA-like domain is required for cell differentiation and development in Dictyostelium discoideum. *Dev Biol* 321: 331-342.

Otto, H. H. & T. Schirmeister, (1997) Cysteine proteases and their inhibitors. *Chem Rev* 97: 133-171.

Panstruga, R., J. E. Parker & P. Schulze-Lefert, (2009) SnapShot: Plant immune response pathways. *Cell* 136: 978 e971-973.

Peng, Y. L., Y. Shirano, H. Ohta, T. Hibino, K. Tanaka & D. Shibata, (1994) A Novel Lipoxygenase from Rice - Primary Structure and Specific Expression Upon Incompatible Infection with Rice Blast Fungus. *Journal of Biological Chemistry* 269: 3755-3761.

Perez-Martin, J., S. Castillo-Lluva, C. Sgarlata, I. Flor-Parra, N. Mielnichuk, J. Torreblanca & N. Carbo, (2006) Pathocycles: Ustilago maydis as a model to study the relationships between cell cycle and virulence in pathogenic fungi. *Mol Genet Genomics* 276: 211-229.

Pritchard, L. & P. Birch, (2011) A systems biology perspective on plant-microbe interactions: biochemical and structural targets of pathogen effectors. *Plant science : an international journal of experimental plant biology* 180: 584-603.

Rafiqi, M., J. G. Ellis, V. A. Ludowici, A. R. Hardham & P. N. Dodds, (2012) Challenges and progress towards understanding the role of effectors in plant-fungal interactions. *Curr Opin Plant Biol*.

Rafiqi, M., P. H. Gan, M. Ravensdale, G. J. Lawrence, J. G. Ellis, D. A. Jones, A. R. Hardham & P. N. Dodds, (2010) Internalization of flax rust avirulence proteins into flax and tobacco cells can occur in the absence of the pathogen. *Plant Cell* 22: 2017-2032.

Rawlings, N. D., A. J. Barrett & A. Bateman, (2012) MEROPS: the database of proteolytic enzymes, their substrates and inhibitors. *Nucleic Acids Research* 40: D343-D350.

Rehmany, A. P., A. Gordon, L. E. Rose, R. L. Allen, M. R. Armstrong, S. C. Whisson, S. Kamoun, B. M. Tyler, P. R. Birch & J. L. Beynon, (2005) Differential recognition of highly divergent downy mildew avirulence gene alleles by RPP1 resistance genes from two Arabidopsis lines. *Plant Cell* 17: 1839-1850.

Robinson, M. D., D. J. McCarthy & G. K. Smyth, (2010) edgeR: a Bioconductor package for differential expression analysis of digital gene expression data. *Bioinformatics* 26: 139-140.

Robinson, M. D. & A. Oshlack, (2010) A scaling normalization method for differential expression analysis of RNA-seq data. *Genome Biol* 11: R25.

Rooney, H. C., J. W. Van't Klooster, R. A. van der Hoorn, M. H. Joosten, J. D. Jones & P. J. de Wit, (2005) Cladosporium Avr2 inhibits tomato Rcr3 protease required for Cf-2-dependent disease resistance. *Science* 308: 1783-1786.

Rose, J. K., K. S. Ham, A. G. Darvill & P. Albersheim, (2002) Molecular cloning and characterization of glucanase inhibitor proteins: coevolution of a counterdefense mechanism by plant pathogens. *Plant Cell* 14: 1329-1345.

Sambrook, J., E. F. Fritsch & T. Maniatis., (1989) Molecular cloning: a laboratory

manual. *Cold Spring Harbor Laboratory Press, New York, USA*.
Sarowar, S., H. W. Oh, H. S. Cho, K. H. Baek, E. S. Seong, Y. H. Joung, G. J. Choi, S. Lee & D. Choi, (2007) Capsicum annuum CCR4-associated factor CaCAF1 is necessary for plant development and defence response. *Plant J* 51: 792-802.
Sauer, M., T. Paciorek, E. Benkova & J. Friml, (2006) Immunocytochemical techniques for whole-mount in situ protein localization in plants. *Nat Protoc* 1: 98-103.
Schagger, H., (2006) Tricine-SDS-PAGE. *Nat Protoc* 1: 16-22.
Schipper, K., (2009) Charakterisierung eines Ustilago maydis Genclusters, das für drei neuartige sekretierte Effektoren kodiert. *PhD thesis*.
Schirawski, J., G. Mannhaupt, K. Munch, T. Brefort, K. Schipper, G. Doehlemann, M. Di Stasio, N. Rossel, A. Mendoza-Mendoza, D. Pester, O. Muller, B. Winterberg, E. Meyer, H. Ghareeb, T. Wollenberg, M. Munsterkotter, P. Wong, M. Walter, E. Stukenbrock, U. Guldener & R. Kahmann, (2010) Pathogenicity determinants in smut fungi revealed by genome comparison. *Science* 330: 1546-1548.
Schnable, P. S., D. Ware, R. S. Fulton, J. C. Stein, F. Wei, S. Pasternak, C. Liang, J. Zhang, L. Fulton, T. A. Graves, P. Minx, A. D. Reily, L. Courtney, S. S. Kruchowski, C. Tomlinson, C. Strong, K. Delehaunty, C. Fronick, B. Courtney, S. M. Rock, E. Belter, F. Du, K. Kim, R. M. Abbott, M. Cotton, A. Levy, P. Marchetto, K. Ochoa, S. M. Jackson, B. Gillam, W. Chen, L. Yan, J. Higginbotham, M. Cardenas, J. Waligorski, E. Applebaum, L. Phelps, J. Falcone, K. Kanchi, T. Thane, A. Scimone, N. Thane, J. Henke, T. Wang, J. Ruppert, N. Shah, K. Rotter, J. Hodges, E. Ingenthron, M. Cordes, S. Kohlberg, J. Sgro, B. Delgado, K. Mead, A. Chinwalla, S. Leonard, K. Crouse, K. Collura, D. Kudrna, J. Currie, R. He, A. Angelova, S. Rajasekar, T. Mueller, R. Lomeli, G. Scara, A. Ko, K. Delaney, M. Wissotski, G. Lopez, D. Campos, M. Braidotti, E. Ashley, W. Golser, H. Kim, S. Lee, J. Lin, Z. Dujmic, W. Kim, J. Talag, A. Zuccolo, C. Fan, A. Sebastian, M. Kramer, L. Spiegel, L. Nascimento, T. Zutavern, B. Miller, C. Ambroise, S. Muller, W. Spooner, A. Narechania, L. Ren, S. Wei, S. Kumari, B. Faga, M. J. Levy, L. McMahan, P. Van Buren, M. W. Vaughn, et al., (2009) The B73 maize genome: complexity, diversity, and dynamics. *Science* 326: 1112-1115.
Schoepfer, R., (1993) The pRSET family of T7 promoter expression vectors for Escherichia coli. *Gene* 124: 83-85.
Schulz, B., F. Banuett, M. Dahl, R. Schlesinger, W. Schafer, T. Martin, I. Herskowitz & R. Kahmann, (1990) The b alleles of U. maydis, whose combinations program pathogenic development, code for polypeptides containing a homeodomain-related motif. *Cell* 60: 295-306.
Shan, L., P. He, J. Li, A. Heese, S. C. Peck, T. Nurnberger, G. B. Martin & J. Sheen, (2008) Bacterial effectors target the common signaling partner BAK1 to disrupt multiple MAMP receptor-signaling complexes and impede plant immunity. *Cell host & microbe* 4: 17-27.
Shimada, Y., S. Ichinose, A. Sadr, M. F. Burrow & J. Tagami, (2009) Localization of matrix metalloproteinases (MMPs-2, 8, 9 and 20) in normal and carious dentine. *Australian dental journal* 54: 347-354.
Skibbe, D. S., G. Doehlemann, J. Fernandes & V. Walbot, (2010) Maize tumors caused by Ustilago maydis require organ-specific genes in host and pathogen. *Science* 328: 89-92.

Song, J., J. Win, M. Tian, S. Schornack, F. Kaschani, M. Ilyas, R. A. van der Hoorn & S. Kamoun, (2009) Apoplastic effectors secreted by two unrelated eukaryotic plant pathogens target the tomato defense protease Rcr3. *Proc Natl Acad Sci U S A* 106: 1654-1659.

Staskawicz, B., (2009) First insights into the genes that control plant-bacterial interactions. *Mol Plant Pathol* 10: 719-720.

Stassen, J. H. & G. Van den Ackerveken, (2011) How do oomycete effectors interfere with plant life? *Curr Opin Plant Biol* 14: 407-414.

Stergiopoulos, I. & P. J. de Wit, (2009) Fungal effector proteins. *Annu Rev Phytopathol* 47: 233-263.

Svensson, B., I. Svendsen, P. Hojrup, P. Roepstorff, S. Ludvigsen & F. M. Poulsen, (1992) Primary structure of barwin: a barley seed protein closely related to the C-terminal domain of proteins encoded by wound-induced plant genes. *Biochemistry* 31: 8767-8770.

Takken, F. & M. Rep, (2010) The arms race between tomato and Fusarium oxysporum. *Mol Plant Pathol* 11: 309-314.

Takken, F. L. W. & M. H. A. J. Joosten, (2000) Plant resistance genes: their structure, function and evolution. *Eur J Plant Pathol* 106: 699-713.

Tian, M., E. Huitema, L. Da Cunha, T. Torto-Alalibo & S. Kamoun, (2004) A Kazal-like extracellular serine protease inhibitor from Phytophthora infestans targets the tomato pathogenesis-related protease P69B. *J Biol Chem* 279: 26370-26377.

Tian, M., J. Win, J. Song, R. van der Hoorn, E. van der Knaap & S. Kamoun, (2007) A Phytophthora infestans cystatin-like protein targets a novel tomato papain-like apoplastic protease. *Plant Physiol* 143: 364-377.

van den Burg, H. A., N. Westerink, K. J. Francoijs, R. Roth, E. Woestenenk, S. Boeren, P. J. de Wit, M. H. Joosten & J. Vervoort, (2003) Natural disulfide bond-disrupted mutants of AVR4 of the tomato pathogen Cladosporium fulvum are sensitive to proteolysis, circumvent Cf-4-mediated resistance, but retain their chitin binding ability. *J Biol Chem* 278: 27340-27346.

van der Hoorn, R. A. & S. Kamoun, (2008) From Guard to Decoy: a new model for perception of plant pathogen effectors. *Plant Cell* 20: 2009-2017.

van der Linde, K., C. Hemetsberger, C. Kastner, F. Kaschani, R. A. van der Hoorn, J. Kumlehn & G. Doehlemann, (2012) A maize cystatin suppresses host immunity by inhibiting apoplastic cysteine proteases. *Plant Cell* 24: 1285-1300.

Voinnet, O., S. Rivas, P. Mestre & D. Baulcombe, (2003) An enhanced transient expression system in plants based on suppression of gene silencing by the p19 protein of tomato bushy stunt virus. *Plant J* 33: 949-956.

Vollmeister, E., K. Schipper, S. Baumann, C. Haag, T. Pohlmann, J. Stock & M. Feldbrugge, (2012) Fungal development of the plant pathogen Ustilago maydis. *FEMS Microbiol Rev* 36: 59-77.

Whisson, S. C., P. C. Boevink, L. Moleleki, A. O. Avrova, J. G. Morales, E. M. Gilroy, M. R. Armstrong, S. Grouffaud, P. van West, S. Chapman, I. Hein, I. K. Toth, L. Pritchard & P. R. Birch, (2007) A translocation signal for delivery of oomycete effector proteins into host plant cells. *Nature* 450: 115-118.

Zipfel, C., (2008) Pattern-recognition receptors in plant innate immunity. *Current opinion in immunology* 20: 10-16.

Supplementary data

The data CD contains the following files:

Supplementary Table. 1, Differentially expressed maize genes.xlsx

Supplementary Table. 2, Enriched biological processes.xlsx

Supplementary Table. 3, Early defense response genes.xlsx

Acknowledgements

With great pleasure, I would like to express my sincere gratitude to all who contribute to this thesis.

First and foremost I thank my thesis supervisor, Prof. Dr. Regine Kahmann for offering me such a challenging and promising project. A warm reception in a snowing day on 2009 started her three and a half years' encouragement, trust, guidance and thoughtful support. This enable me to overcome all the hardness and frustrations and learn not only science itself but also the dedication, insistence, and important of precise and scientific ethics. In particular, I would like to thank her insightful guidance during my writing. I am deeply greetful to my advisory and thesis committee members, Prof. Dr. Michael Bölker, Prof. Dr. Martin Thanbichler, Prof. Dr. Alfred Batschauer and Dr. Seigo Shima for their time and constructive suggestions.

My deep and sincere thanks go to current and former colleagues from Kahmann lab and department of orgnismic interactions for the precious suggestions, encouragement and help. Special thanks to Dr. Armin Djamei, Dr. Stefanie Reißmann, Dr. Julien Yann Dutheil, Dr. Kerstin Schipper, Dr. Christian Herrberger for their help in data process and interpretation, discussion, encouragement and valuable suggestions. I am sincerely greatful to Karin Münch, Nicole Rössel, Volker Vincon for encouragement and assistance in the lab, Rolf Rösser for computational support, Stefan Schmidt, Anita Boos, Ria Faber, Vera Matschiske-Peters, Claudia Schäfer for their assitance and generous help. I thank our collaborators Prof. Dr. Michael Groll (TUM), Prof. L. Søgaard-Andersen (MPI) and Dr. Bruno Huettel (MPGC) and IMPRS-Mic Marburg for all the support to promote the development of this project. I would like to extend my thanks to Mr. Christian Bengelsdorff, Susanne Rommel and Simone Hain for taking care of all the documents. I would like to thank the financial support through SFB593 and Synmikro.

Finally, I am indebted to my family. I would like to express my heatily thankful to my parents, Liang Yingchun and Zhou Ping and my parents-in-law, Wang Mingliang and Zeng Xianping for their everlasting love and support; my wife, Li Fujin for her love, encouragement and care of my life and my son, Liang Yiheng who was born during my writing and provided us with plenty of joys and moral support.

Curriculum Vitae

Personal information

Name	Liang Liang
Date of birth	Dec 1979
Place of birth	Hebei, P. R. China

Education

Jan 2009-Jun 2012	Philipps-Universität Marburg Max-Planck-Institute for Terrestrial Microbiology Marburg/Lahn, Germany PhD thesis: The role of Stp1, a secreted effector, in the biotrophic interaction of *Ustilago maydis* and its host plant maize
Jul 2005–Jan 2008	Institute of Microbiology, Chinese Academy of Sciences Beijing, P. R. China Master of Science. Master thesis: The function of *iunH* and *gerA* in spore germination of *Bacillus thuringiensis*
Sep. 2004-Jul. 2005	Graduate school of Chinese Academy of Sciences Beijing, P. R. China
Sep. 2000-Jun. 2004	Hebei University Baoding, P. R. China. Bachelor of Science